



Unraveling the “Eaglebine”: A Sequence Stratigraphic Framework for the Eagle Ford Group in the East Texas Basin

A. D. Donovan, P. Johnson, S. R. Gifford, M. J. Meyer, S. Dangtran, and M. Pope

*Department of Geology and Geophysics, Texas A&M University,
3115 TAMU, College Station, Texas 77843–3115, U.S.A.*

ABSTRACT

A major stratigraphic problem presently exists in the southern East Texas Basin. Geoscientists working in the subsurface in this region are no longer sure, as to what strata, between the Buda Formation and Austin Group, are equivalent to the Woodbine and Eagle Ford groups, as defined along the outcrop belt. As a result, this stratal succession is now commonly just referred to as the “Eaglebine.” To resolve this dilemma, a regional grid of well-log cross-sections, tied to petrophysical and geochemical data from (1) two shallow subsurface government research cores and (2) a deeper subsurface industry core, was used to unravel the “Eaglebine.” This research revealed that the “Eaglebine” in the southern East Texas Basin actually consists of a vertical succession four petrophysically and geochemically distinct unconformity-bounded sequences (sequences 1 to 4, from the base up), all of which (1) have a sharp basal contact and (2) display underlying stratal terminations, on the grid of regional well-log cross-sections. The lowermost “sequence 1,” which is interpreted as the False Buda, is a moderate gamma ray (GR)/resistivity unit, that is rich in Ca, but poor in total organic content (TOC), Al, and Ti. “Sequence 2,” which is interpreted as the Pepper Formation (Woodbine Group), is a low-resistivity unit, that is poor in Ca and TOC, but rich in Al and Ti. “Sequence 3,” which is interpreted as the Lower Eagle Ford Formation (LEF), is a high-resistivity/GR unit, that overall is enriched in Ca and TOC, but poor in Al and Ti. The uppermost unit, “Sequence 4,” which is interpreted as the Lower Member of the Upper Eagle Ford Formation (UEF), is primarily a low-resistivity unit, that is rich in Al and Ti, but overall poor in Ca and TOC. In general, across the study area, Ca- and TOC-rich, high-resistivity LEF mudstones separate more Al-rich, as well as Ca- and TOC-poor strata, of both the Woodbine Group/Freestone delta (below) from the UEF/Harris delta (above).

INTRODUCTION

During the Late Cretaceous, present-day Texas was located at the southern gateway of the Cretaceous Western Interior Seaway positioned at the transition from a foreland basin to the west, and a tiered passive continental margin to the east (Fig. 1). The Late Cretaceous was also a time of global greenhouse conditions marked by expanding epicontinental seaways (Fig. 2), and episodes of ocean anoxia, reflected by the deposition of organic-rich source rocks (Kauffman, 1995). During this time, the Woodbine, Eagle Ford, and Austin groups were sequentially deposited across Texas (Fig. 3).

During the early Cenomanian (Fig. 2A), seas began to transgress the North American craton from the Gulf of Mexico to the

south, and the Arctic Ocean from the north. According to Kauffman (1995) by the earliest Turonian (Fig. 2B), when interpreted peak global greenhouse conditions occurred, (1) eustatic sea-level was elevated nearly 1000 ft (300 m) above its present positions, (2) atmospheric CO₂ was at least four times above present levels, (3) warm, more-equable climates, reflecting low thermal gradients, existed from the pole to the equator, as well as from top to bottoms in the world’s oceans, and (4) the Cretaceous Western Interior Seaway covered the craton from the Gulf of Mexico to the South to the Arctic Ocean to the north.

Associated with the overall sea-level rise is the Ocean Anoxic Event 2 (OAE2), also referred to as the Cenomanian/Turonian Boundary Event (Pearce et al., 2009). The OAE2 (Fig. 3) is an approximate 750,000 yr long period in the earth’s history marked by the punctuated extinction of over a quarter of the of marine invertebrates, that existed prior to this event (Forkner et al., 2021).

Geochemically, the OAE2 is characterized by a globally recognized positive carbon isotope ($\delta^{13}\text{C}$) excursion reflecting widespread removal of ¹²C-enriched organic matter in marine sediments and denoting one of the major global perturbations in the carbon cycle of the earth’s paleo-oceans. The OAE2, with its

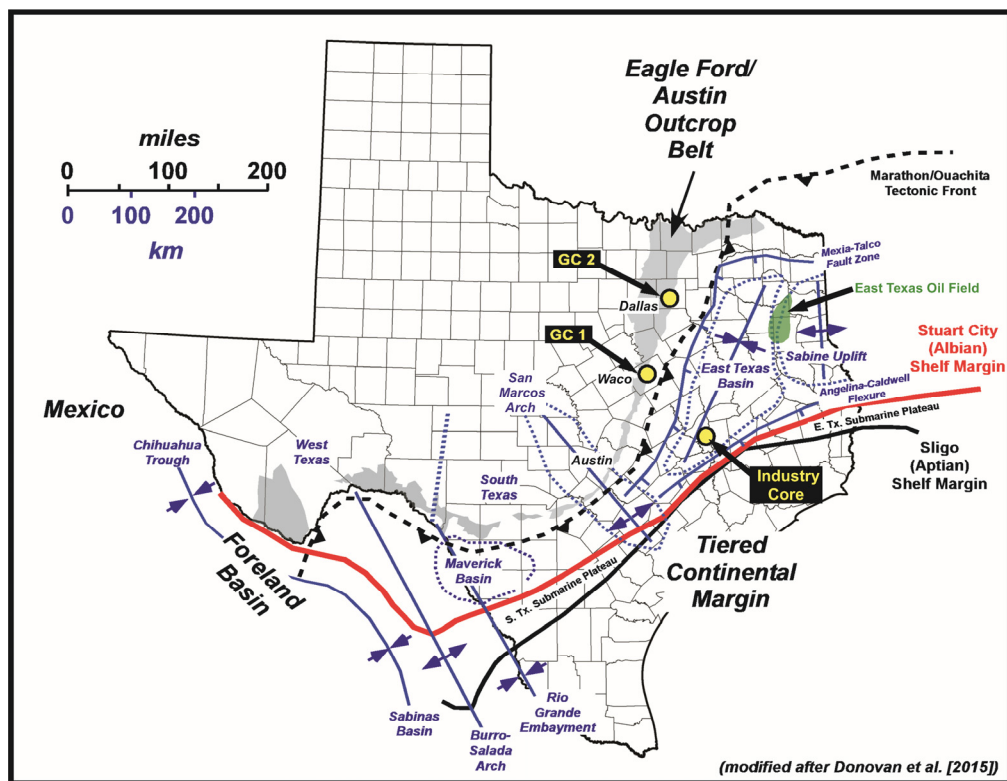


Figure 1. The East Texas Basin is bounded by the Sabine Uplift to the east of the Marathon/Ouachita Tectonic front to the north and west, the Stuart City Shelf Margin to the south, and the San Marcos Arch to the southwest. Please note the (1) Eagle Ford/Austin outcrop belt, (2) location of the USGS GC-1 and GC-2, as well as the industry core, used in this study; and (3) East Texas Field on the west flank of the Sabine Uplift.

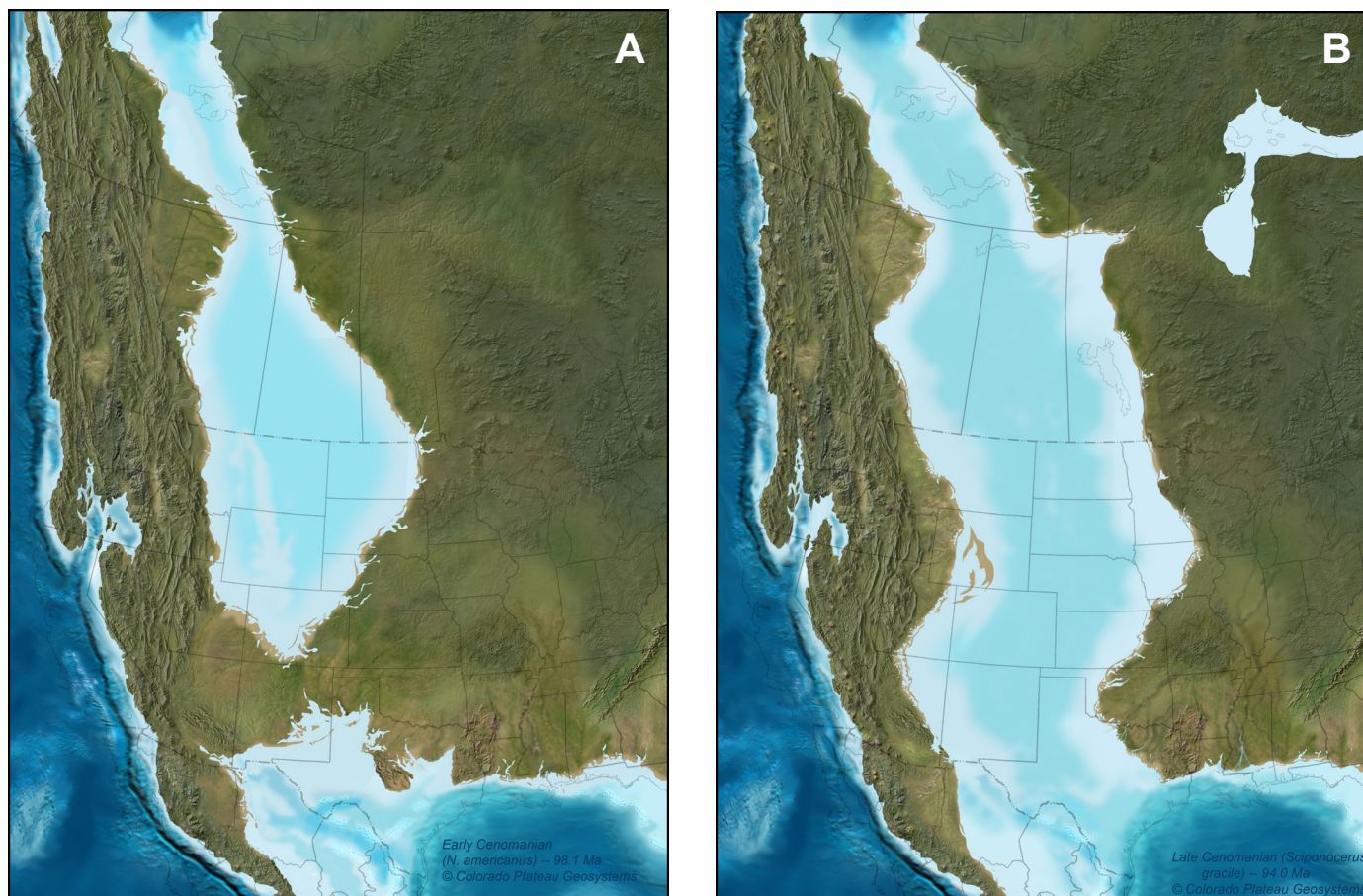


Figure 2. Paleogeographic maps for the (A) early Cenomanian (Woodbine) and (B) latest Cenomanian (basal UEF) for the Western U.S., illustrating the spreading and final connection of the Tethyan and Boreal seas which formed the Cretaceous Western Interior Seaway in the latest Cenomanian. The red circle on these maps highlights the location of Texas. Maps courtesy of Colorado Plateau Geosystems.

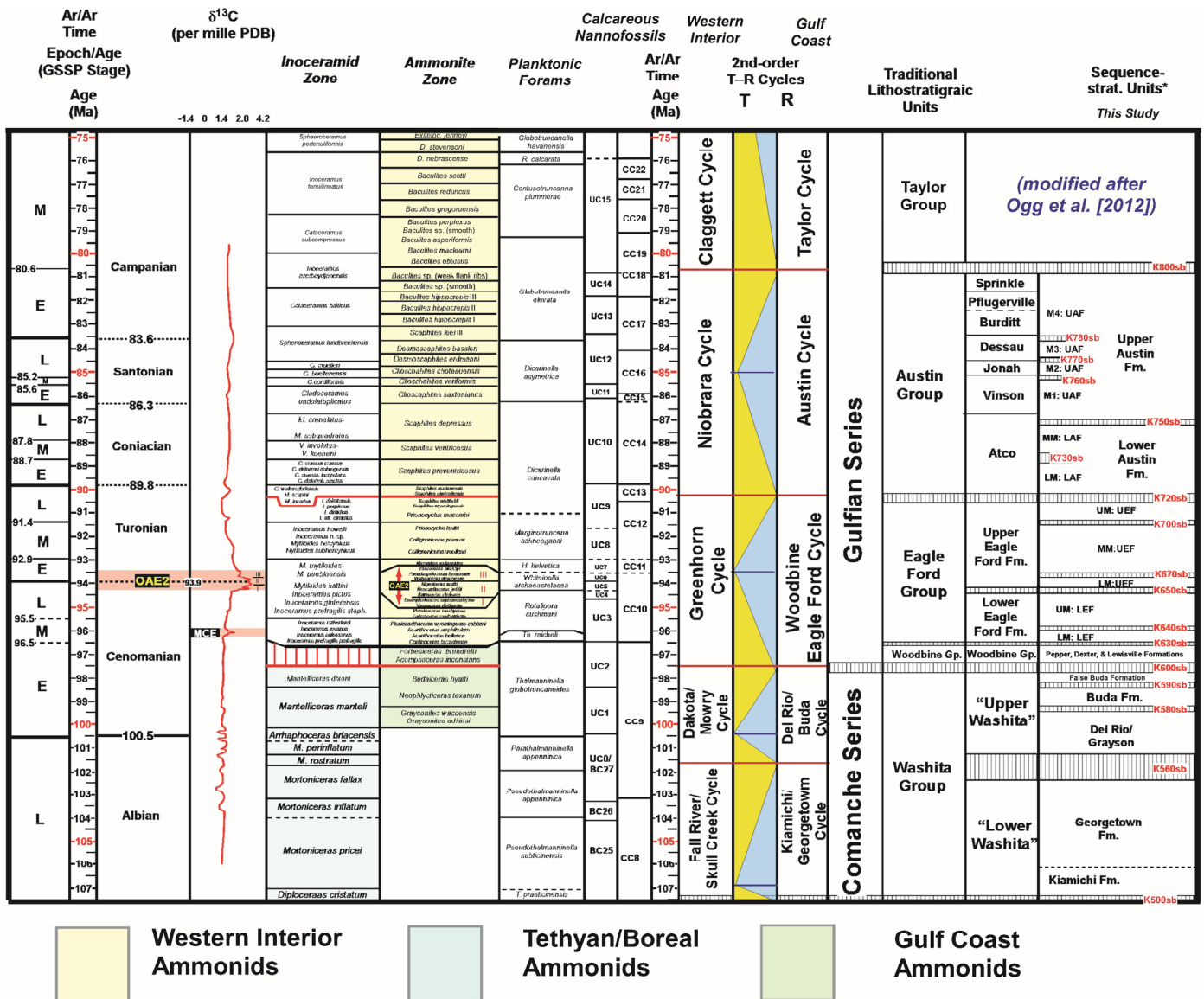


Figure 3. Generalized stratigraphic column for the Upper Cretaceous in Texas illustrating the ages, stage boundaries, macrofaunal zones, mega-cycles, $\delta^{13}\text{C}$ global isotope profile from the 2012 Geologic Time Scale (Ogg and Hinnov, 2012). Please note the (1) relative positions of the Washita, Woodbine, Eagle Ford, and Austin groups, (2) onset the Western Interior ammonite zones (base yellow) at the base of the middle Cenomanian Eagle Ford Group, (3) positive $\delta^{13}\text{C}$ excursion associated with the OAE2 (red), which coincides with the base of the UEF, and (4) the surface naming convention used in this study, where the base of the Woodbine Group is the K600sb, the base Eagle Ford Group is the K630sb, and the base Austin Group is the K720sb. Click [here](#) for a high-resolution, large-format version of this image.

distinctive positive $\delta^{13}\text{C}$ signature, provides a useful chronostratigraphic maker suitable for regional and inter-regional correlations within Late Cretaceous successions around the globe.

Bed-by-bed stratigraphic and palaeontologic studies by Cobban and Scott (1972), and later Cobban (1985, 1993), at the base Turonian stratotype near Pueblo, Colorado, documented abrupt changes in the ammonite assemblages within the 20 ft (6 m) OAE2 interval in this section (Fig. 4). At this locality, Cobban (1985, 1993) noted the loss of typical latest Cenomanian ammonites at six discrete levels within the lower 13.1 ft (4 m) of the OAE2, spanning the biozones of *Sciponoceras gracile* (*Vascoceras diartanum* and *Euophaloceras septemseriatum* sub-zones) and, overlying (younger) *Neocardioceras* (*Euophaloceras navahopiensis*, *Neocardioceras juddi*, and *Nigericeras scotti* subzones). Cobban (1985, 1993), as well as Kennedy and Cobban (1990), defined the base of the Turonian (Fig. 4), at the start of

the *Watinoceras* biozone (*W. devonense* subzone), and within the overlying 6.6 ft (2 m) earliest Turonian portion of the OAE2 at this locality, Cobban (1985, 1993) noted the loss of typical earliest Turonian ammonites at three discrete levels spanning the *Watinoceras* biozone (*Watinoceras devonense*, *Pseudaspidoceras flexuosum*, and *Vascoceras birchbi* subzones).

In this paper, the *Sciponoceras gracile*, *Neocardioceras*, and *Watinoceras* ammonite zones within the OAE2, will be respectively referred to as zones I, II, and III from the base up (Fig. 4). In terms of the $\delta^{13}\text{C}$ curve and the ammonite zones, the basal zone I consists of the initial $\delta^{13}\text{C}$ increase and then a decrease; the middle zone II, consist of the main blocky part of the $\delta^{13}\text{C}$ excursion, while the uppermost zone III, consists of a funnel-shaped drop off at the top of the excursion. In terms of the OAE2 interval in the East Texas Basin, which is the geographic focus of this study, the lowermost *Sciponoceras gracile* ammo-

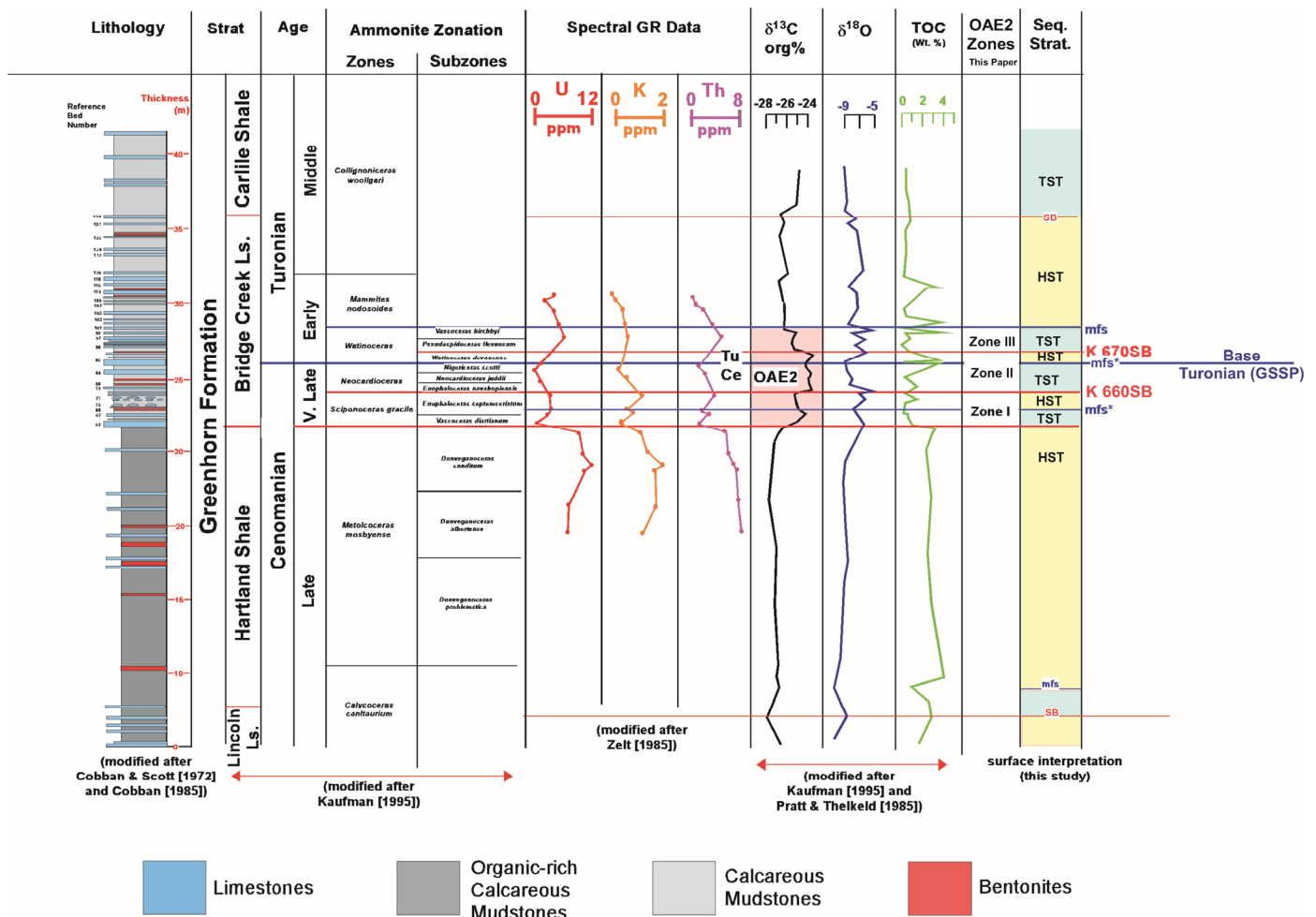


Figure 4. Measured section with geochemical and ammonite data of the base Turonian GSSP in Rock Canyon, near Pueblo, Colorado. Please note the (1) base of the Bridge Creek Limestone, which corresponds to the onset of the positive $\delta^{13}\text{C}$ signature of the OAE2, (2) drop in U and TOC content at the base of the OAE2, and (3) OAE2 zones I to III, and their associated $\delta^{13}\text{C}$ signatures and ammonite zones and subzones. Click [here](#) for a high-resolution, large-format version of this image.

nite zone (zone I), is a very important part of the stratigraphic story in the Dallas, Texas area, that is discussed later in this paper.

The East Texas Basin (Fig. 1), which is the focus of this paper, is one of the many Mesozoic sedimentary basins that developed along the southern margin of the North American craton during the Triassic opening of the Gulf of Mexico (Jackson and Seni, 1983). It is bounded by the Sabine Uplift to the east, the Mexia-Talco Fault Zone to the north and west, the San Marcos Arch to the southwest, and the Angelia-Caldwell Flexure to the south (Fig. 1). Within the East Texas Basin, Jurassic Louann Salt was deposited unconformably on Paleozoic basement rocks, and Triassic rift-valley fill (Jackson and Seni, 1983). Subsequent salt diapirism produced by loading from (1) deposition of a Lower Cretaceous carbonate wedge, (2) progradation of thick Upper Cretaceous siliciclastic units, to (3) uplift, erosion, and tilting of the basin occurred, forming simple salt-cored anticlines (Jackson and Seni, 1983). Adding to the structural complexity, key basement features, such as the San Marcos Arch and Sabine Uplift, were intermittently active in the Late Cretaceous, due to Laramide tectonics (Jackson and Laubach, 1991). This far-field Laramide compressional deformation, and associated uplift and erosion, played a major role in setting up many of the sub-unconformity traps in the East Texas Basin, like the super-giant East Texas Field (Jackson and Laubach, 1991).

The Cretaceous succession within the East Texas Basin, one of the most prolific hydrocarbon-bearing intervals and provenances in the United States, for within this time and space occurs the supergiant East Texas Field. In this field, fluvial-deltaic strata of the Woodbine Group are the conventional reservoirs, the Eagle Ford Group is the source rocks, and the Austin Group serves as the seal and trap (Halbouty, 1991). Toward the end of the 20th century, however, production in the East Texas Basin began to switch toward unconventional reservoirs. This started with the Austin Chalk. In the mid 1980s, Sun Exploration and Production Company successfully utilized modern horizontal drilling techniques to exploit the fractured Austin Chalk Play (Zuckerman, 2013). More recently, industry has utilized horizontal wells, and fracking to unlock Upper Cretaceous source rock and tight rock plays within the Woodbine and Eagle Ford groups in the southern East Texas Basin (Hentz et al., 2014).

Recent work by Hentz et al. (2014) in the southern East Texas Basin, has highlighted a major stratigraphic problem (Fig. 5) in the southern East Texas Basin. Geoscientists working in the subsurface are no longer sure, as to what is coeval to the early Cenomanian Woodbine Group, or to the middle Cenomanian to late Turonian Eagle Ford Group, as defined and mapped along the outcrop belt on the western flank of the basin. As a result, strata between the Buda and Austin in the southern East Texas Basin are now commonly referred to as the “Eaglebine.” To add further

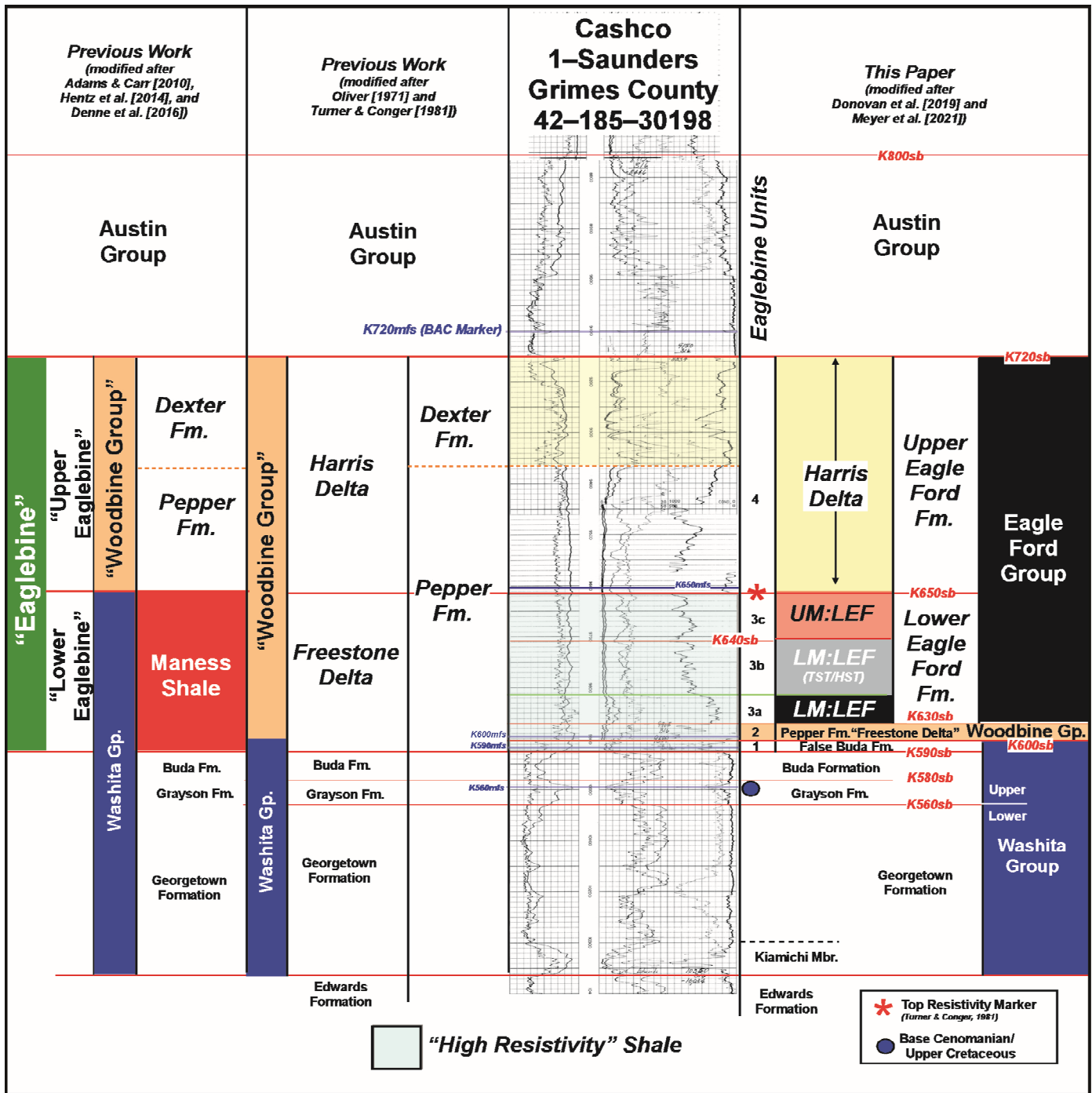


Figure 5. Type well in the southern East Texas Basin illustrates the various interpretations for the “Eaglebine” succession in the southern East Texas Basin. In previous studies, the Lower Eaglebine “resistivity zone” (colored blue) within the East Texas Basin have been assigned to either the (1) basal portions of the Pepper Shale (Woodbine Group) or (2) Maness Shale of the Washita Group. In this study, these strata were assigned to the False Buda Formation (unit 1), the Pepper Shale (unit 2), and the LEF (unit 2). Please note the “classic top resistivity marker” of **Turner and Conger (1981, 1984)**, which they used to define the base of the Woodbine “Harris delta,” as well as the top of the Woodbine “Freestone delta. In this study, this surface was interpreted as the K650sb, at the base of the UEF. Click [here](#) for a high-resolution, large-format version of this image.

complexity to the issue, a major juxtaposition in the stratigraphic position of high-resistivity, organic-rich source rock facies also occurs between the outcrop belt and the southern East Texas Basin. As illustrated on **Figure 5**, previous researchers assigned and interpreted organic-rich “Eaglebine resistivity zone” in the southern East Texas Basin to either the (1) basal portions of the Pepper (Shale) Formation, interpreted as coeval to the Woodbine Free-

stone delta (**Oliver, 1971; Turner and Conger, 1981, 1984**) or (2) Maness Shale of the Washita Group, which predates the Woodbine Group (**Adams and Carr, 2010; Hentz et al., 2014; Denne et al., 2016**). Along the outcrop belt to the northwest, similar organic-rich, high-resistivity mudstones occur at the base of the Eagle Ford Group (**Figs. 6 and 7**), where they overlie Al-rich, but total organic content (TOC)- and Ca-poor mudstones of the

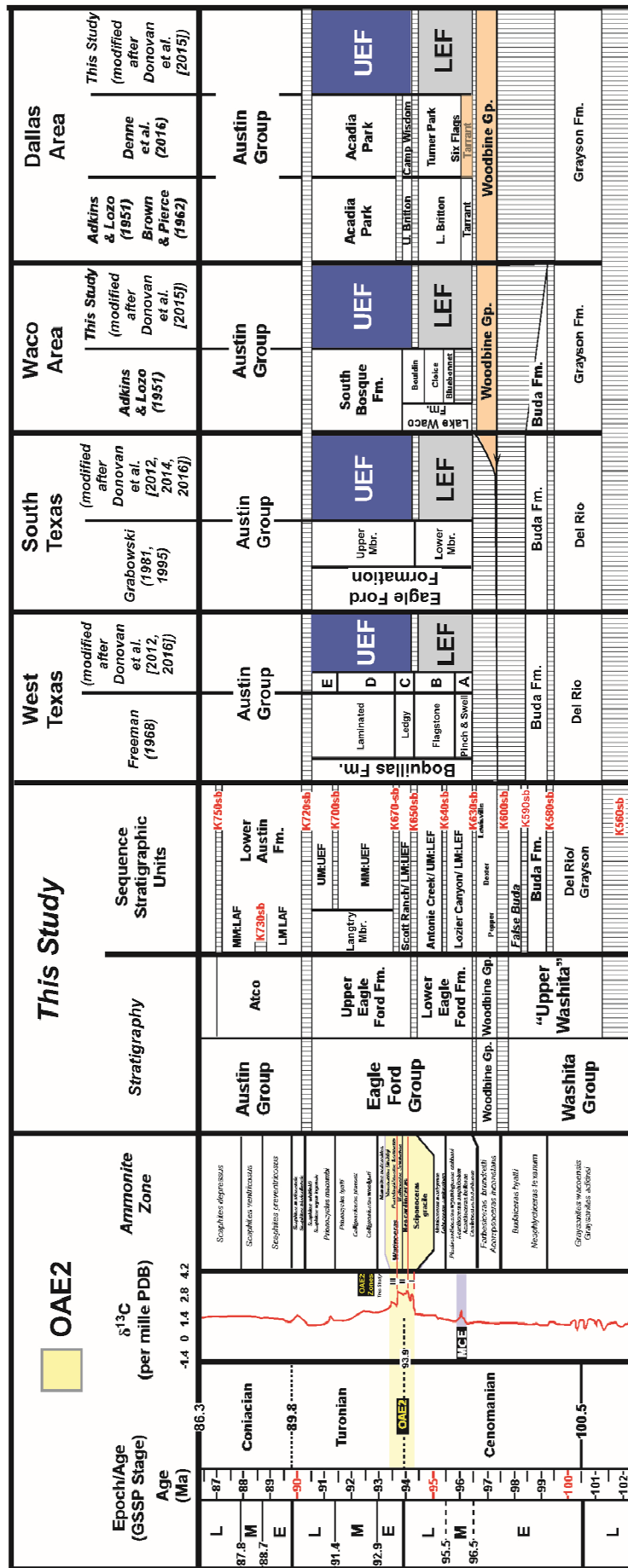


Figure 6. Chart summarizing the provincial outcrop nomenclatures in West Texas, South Texas, and the Waco and Dallas areas in the East Texas Basin. The sequence stratigraphic framework used in this, and previous works, provides a Rosetta Stone to compare, and correlate, among these units across the Texas. Please note the occurrence of the OAE2 at the base of the UEF across the study area. Click [here](#) for a high-resolution, large-format version of this image.

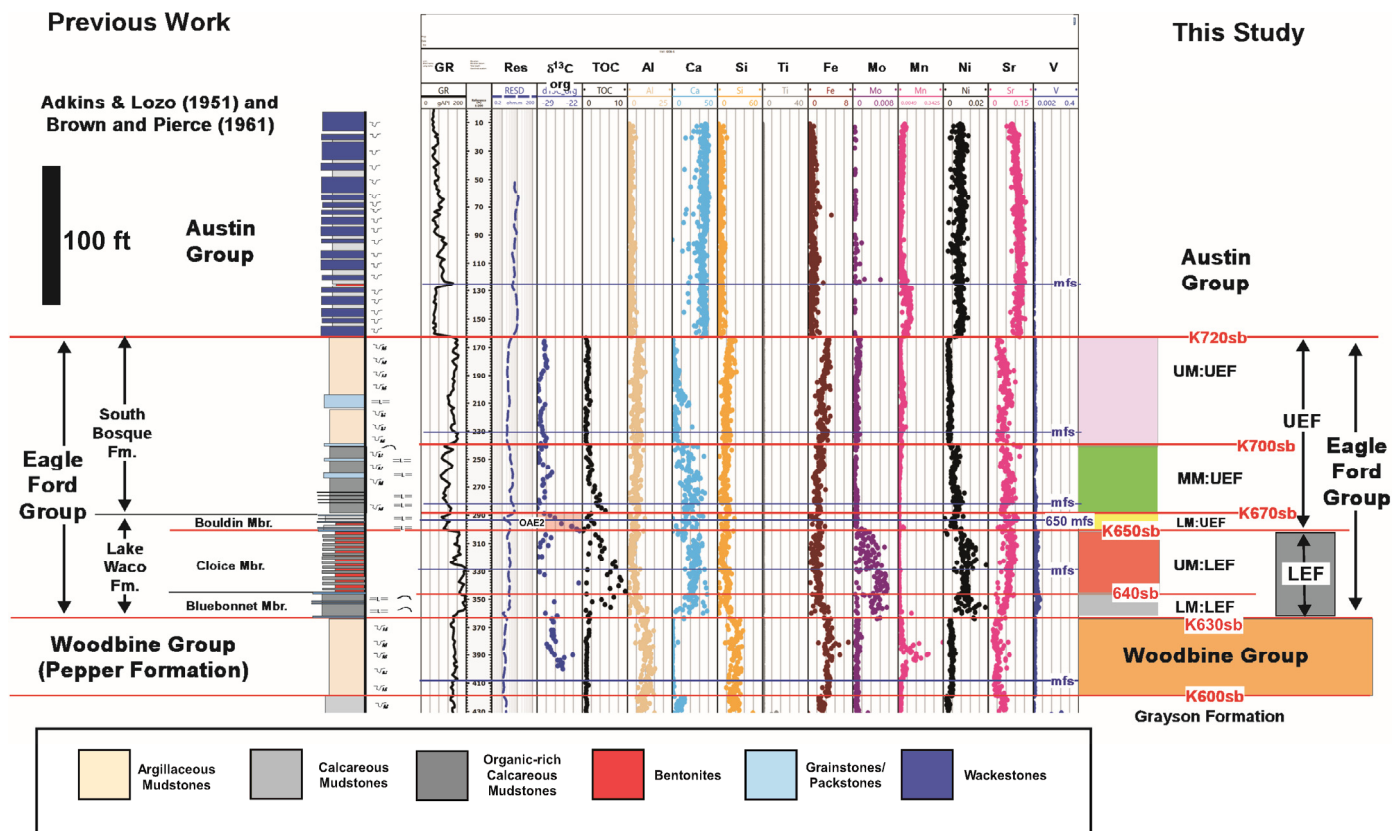


Figure 7. Core description, petrophysical, and geochemical data of the USGS GC-1 core, located near Waco Texas. Please note the (1) Al-rich and TOC- and Ca-poor deposits of the Pepper Shale (Woodbine Group), (2) TOC- and Ca-rich and Al-poor LEF, (3) thin (10 ft [3 m] thick) positive $\delta^{13}\text{C}$ excursion, interpreted as the OAE2 at the base of the UEF, (4) Ca- and TOC-enriched MM:UEF marked by the K670sb at its base and K700sb at its top, (5) Al-rich and Ca-poor UM:UEF, (6) Ca-rich and Al-poor Austin Chalk, and (7) classic provincial lithostratigraphy and the sequence based framework used in this study. Click [here](#) for a high-resolution, large-format version of this image.

Woodbine Group (Donovan et al., 2015). Resolving the stratigraphic inconsistencies between the outcrop belt, and the subsurface in the East Texas Basin is the focus of this paper.

CRETACEOUS STRATIGRAPHIC OVERVIEW

In the late 19th and early 20th century, outcrops of the Cretaceous System across Texas were classically divided into what were originally interpreted as a “Lower Cretaceous” Comanche Series, and an “Upper Cretaceous” Gulfian Series (Adkins, 1932). However, with the adoption of the International Time Scale over the last 50 yr (Ogg and Hinnov, 2012), the relative placement of the base Cenomanian changed, and the classic base Gulfian (Woodbine) now occurs within the early Cenomanian, near the base of the Grayson Formation (Fig. 3).

Within the classic Gulf Coast Comanche Series (Fig. 3), the Trinity, Fredericksburg, and Washita groups were defined from the base up (Adkins, 1932). In the Gulfian Series (Fig. 3), the unconformity-bounded Woodbine, Eagle Ford, Austin, Taylor, and Navarro groups were defined (Adkins, 1932). In the East Texas Basin, the Washita Group, at the top of the Comanche Series, commonly is subdivided into three Formations, which from the base up are the Georgetown, Grayson, and Buda Formations (Fig. 3). In this study, the Kiamichi Shale, which traditionally is placed at the top of the underlying Fredericksburg Group (Adkins, 1932) is included as the basal member of the Georgetown Formation within the Washita Group (Fig. 3). Lastly, a calcareous mudstone, informally termed the False Buda Formation and Woodbine groups, is interpreted as the unconformity-bounded False Buda Formation in this study (Fig. 3).

In terms of the classic Gulfian Series, Hill (1887) originally referred to the sandstone-prone strata, at the base of his “Gulfian Series,” as the Timber Creek Group, a name he subsequently changed to the Woodbine Group (Hill, 1902), when the type locality for this unit was defined near the town of Woodbine, Texas in eastern Cooke County, approximately 60 mi north of Dallas, Texas (Fig. 8). In the Dallas area, Adkins (1932) subdivided the Woodbine into its now classic 3-fold lithostratigraphic subdivision, which consists of (1) a basal (mudstone-prone) Pepper Formation, (2) a middle (sandstone-prone) Dexter Formation, and (3) an upper, more mudstone-prone, Lewisville Formation. This tripartite framework was utilized in many subsequent Woodbine subsurface studies in the East Texas Basin, such as in the work of Oliver (1971).

Besides defining the Woodbine Group, Hill (1887) also defined the Eagle Ford, as the mudstone-prone strata situated between Timber Creek/Woodbine (below) and Austin (above). The type locality was the town of Eagle Ford, located on the south bank of the Trinity River in western Dallas County (Fig. 8). Adkins (1932) elevated the Eagle Ford to group level, and based on biostratigraphic input from W. L. Moremon, divided the Eagle Ford Group in the Dallas area into three formations, which he named the Tarrant, Britton, and Arcadia Park from the base up (Fig. 6). The basal Tarrant Formation is a thin (15–20 ft [4.6–6.1 m]) fossiliferous unit containing interbedded limestones, sandstones and mudstones. The Tarrant Formation is important because its basal beds contains the ammonite *Colineoceras tarrant-*

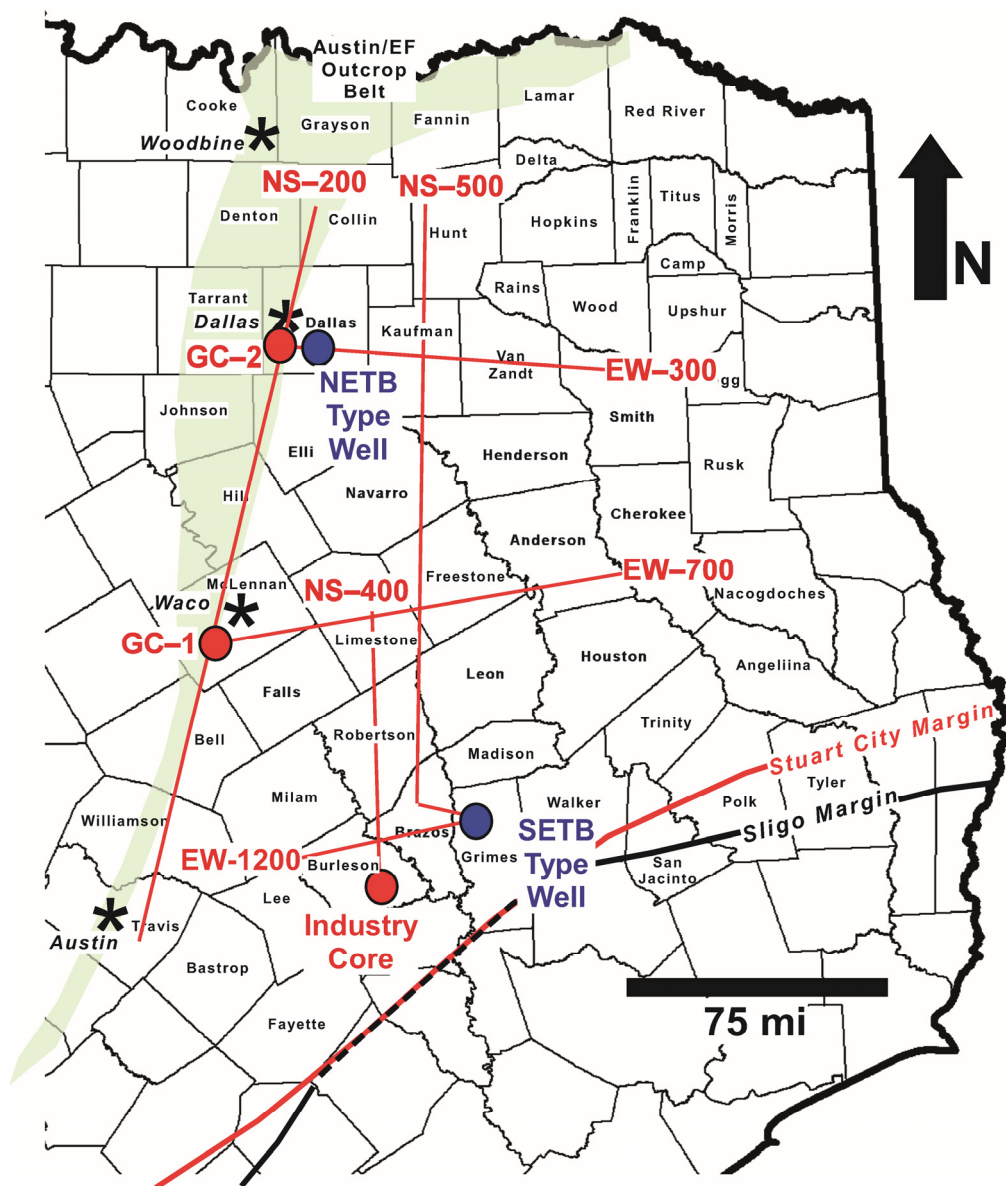


Figure 8. Detailed map of the East Texas Basin illustrating (1) outcrop belt along the western margin of the basin, (2) location of the GC-1, GC-2, and industry core, (3) type wells in the northern East Texas Basin and southern East Texas Basin, and (4) the location of the well-log cross-sections included in this paper.

tense. This ammonite is of interest (Fig. 3) because (1) its first occurrence marks the base of the middle Cenomanian on geologic time scale; and (2) it is the first (oldest) ammonite found in the Gulf Coast, as well as in the southern portions of the Cretaceous Western Interior Seaway, thus marking the time of the initial incursion of the Tethyan Seas into southern portions of the Cretaceous Western Interior Seaway (Fig. 3). Overlying the Tarrant Beds in the Dallas area is the Britton Formation, which was described as being more mudstone-prone than the basal Tarrant in its basal portions, and becoming more interbedded with sandstones in its upper two thirds (Adkins, 1932; Brown and Pierce, 1962). Finally, the uppermost Arcadia Park Formation was defined based on being more mudstone-prone than the underlying Britton Formation (Adkins, 1932; Brown and Pierce, 1962). For context, in a research borehole in the Dallas area, Brown and Pierce (1962) reported that the Eagle Ford Group was 474 ft (144 m) thick, with the Tarrant, Britton, and Arcadia Park formations being respectively 20 ft (6 m), 334 ft (101 m), and 120 ft (36.6 m) in thickness. In this borehole, they also noted a more bentonite-rich, 82 ft (25 m) thick Lower Britton, and a bentonite-poor, and more sandstone-prone, 252 ft (76.8 m) thick Upper Britton. In the adjacent outcrops, Kennedy (1988) assigned the thick,

more sandstone-prone, Upper Britton strata to the late Cenomanian *Sciponoceras gracie* ammonite zone, which as mentioned previously (Fig. 4), is restricted to the basal zone I of the OAE2, at the base Turonian stratotype in Pueblo, Colorado.

In contrast to the Dallas area, Adkins and Lozo (1951) divided the Eagle Ford Group along the outcrop belt from Waco to Austin (Fig. 6) into a lower, more carbonate- and bentonite-rich, Lake Waco Formation and an upper, more carbonate- and bentonite-poor South Bosque Formation. In a Mobil Research borehole in the Waco area (Fig. 8), Brown and Pierce (1962) reported that the Eagle Ford Group was 199 ft (60.1 m) thick with basal Lake Waco Formation being 79 ft (24.1 m) thick and the upper South Bosque Formation being 120 ft (36.6 m) thick. In this region, Adkins and Lozo (1951) divided the basal Lake Waco Formation into three members, named from the base up the (1) Bluebonnet, (2) Cloice, and (3) Bouldin (Fig. 6). Within this framework, the middle Cloice Member was interpreted as being more mudstone-prone and bentonite-rich, and the other two members were described as intervals dominated by interbedded mudstones and limestones. Adkins and Lozo (1951), also observed, that within their study area from Hill County to the north to Travis County to the south, the Woodbine Group changed from a more

sandstone-prone (Dexter) to mudstone-prone (Pepper) facies, as well as thins dramatically toward the southwest. They also stated that the mudstone-prone Pepper facies could not be mapped in outcrop "...south or west of the south boundary of Travis County" (Fig. 8).

In South Texas (Fig. 6), where the Woodbine equivalent deposits are thin or absent strata between the Buda Formation (below) and the Austin Group (above) are mapped as the Eagle Ford Group (Donovan et al., 2012, 2016). In this region, a more organic-rich, (unconformity-bounded) Lower Eagle Ford Formation (LEF) and more carbonate-rich (unconformity-bounded) Upper Eagle Ford Formation (UEF) were also defined and mapped (Donovan et al., 2012, 2016). The same LEF and UEF chronostratigraphic and lithostratigraphic framework into the outcrops of West Texas by Donovan et al. (2012). In both South Texas and West Texas, the base of the UEF, coincides with the onset of the positive carbon isotope ($\delta^{13}\text{C}$) excursion associated with the OAE2 (Donovan et al., 2016). This $\delta^{13}\text{C}$ excursion provides a useful chronostratigraphic marker to help define latest Cenomanian strata, as well as the base of the UEF across Texas (Fig. 6).

The LEF/UEF surface-based sequence stratigraphic framework was carried into the outcrops and shallow subsurface along the west flank of the East Texas Basin (Donovan et al., 2015). Within this framework (Fig. 6), the base of the UEF occurs within the upper portions of the Lake Waco Formation in the Waco area, and within the Britton Formation (Fig. 6) in the Dallas area. Similar to South Texas, two members (sequences) within the LEF and two members (sequences) within the UEF were originally defined (Fig. 6). These members (sequences) from the base up are: Lower Member of the LEF (LM:LEF); Upper Member of the LEF (UM:LEF); Lower Member of the UEF (LM:UEF); and Upper Member of the UEF (UM:UEF). More recently, Donovan et al. (2019), based on new data from a USGS core in the Dallas area (Fig. 6) proposed a more Ca- and TOC-enriched Middle Member of the UEF (MM:UEF).

In summary, along the outcrop belt of the East Texas Basin, organic- and Ca-rich, middle to late Cenomanian-aged LEF strata, overlie argillaceous-rich, TOC- and Ca-poor, early Cenomanian-aged strata of the Woodbine Group.

PREVIOUS WORK: SOUTHERN EAST TEXAS BASIN

In the southern portions of the East Texas Basin strata equivalent to the Woodbine and Eagle Ford groups were initially studied by Oliver (1971), Turner and Conger (1981, 1984), and Berg, 1986. These efforts recognized an older Freestone delta and younger Harris delta system (Fig. 5). In terms of separating these units, Turner and Conger (1981, 1984) identified a regional "top resistivity marker" (Fig. 5), which they used to define the base of the "Harris delta," and thus top of the underlying (older) "Freestone delta."

While these workers all suggested that the younger "Harris delta" might be age equivalent, in part, to the Eagle Ford Group along the outcrop belts to the west, in terms of terminology (Fig. 5) they followed a more lithostratigraphic approach, by designating the sandstones between the Buda Formation and the Austin Group, as the Dexter Formation of the Woodbine Group, which in turn made the underlying mudstone-prone strata, the Pepper Formation of the Woodbine Group.

More recently, Adams and Carr (2010), reinterpreted Turner and Conger's (1981, 1984) "high resistivity" zone as the Maness Shale (Fig. 5). For context, the Maness Shale was originally defined as an early Cenomanian (pre-Woodbine) shale, belonging to the underlying Washita Group (Bailey et al., 1945; Lozo, 1951). A Maness interpretation for these high-resistivity mudstones (Fig. 5) was also followed by Hentz et al. (2014), as well as Denne et al. (2016).

In terms of the paradigm of the "Eaglebine" in the southern East Texas Basin, whether the basal "resistivity mudstones," are assigned to the Pepper Formation, or older, Maness Formation, the net result is the same (Fig. 5). Both of these interpretations create a lithostratigraphic juxtaposition for the age and relative position of the "high-resistivity" interpreted organic-rich, mudstones as mapped along the outcrop belt to the west, and southern East Texas Basin to the southeast. Along the outcrop belt, Ca- and TOC-rich, middle to late Cenomanian, high-resistivity LEF mudstones unconformably overlie the Woodbine Group (Fig. 7). In the southern East Texas Basin (Fig. 5), similar high resistivity (TOC-rich facies), are interpreted as being older than the Eagle Ford Group, and are placed at either (1) in the Pepper Formation of the Woodbine Group (Oliver, 1971; Turner and Conger, 1981, 1984) or (2) beneath the Woodbine Group, as the Maness Formation of the Washita Group (Adams and Carr, 2010; Hentz et al., 2014; Denne et al., 2016).

In contrast to a Pepper Shale, or Maness Shale, interpretations for the "Eaglebine resistivity zone" in the southern East Texas Basin, a recent XRF study utilizing industry cores by Meyer et al. (2021) revealed that the strata typically assigned to the Maness actually consist of a vertical facies succession of four very distinct petrophysical and geochemical zones (Fig. 9), herein termed units 1, 2, and 3 from the base up. Unit 1 (Fig. 9) is characterized by (1) low GR and elevated resistivity, (2) high Ca, and (3) low TOC and Al. Unit 2 (Fig. 9) is characterized by (1) moderate GR and low resistivity, (2) low Ca and TOC, and (3) high Al, Si, and Ti. Unit 3 (Fig. 9) is characterized by (1) elevated GR and resistivity, (2) elevated Ca and TOC, and (3) lower Al-, Si-, and Ti-content, especially in the basal portions (3a subzone). Based on these findings (Fig. 9), Meyer et al. (2021) assigned unit 1, to Buda Formation (False Buda); the middle unit 2, to the Pepper Shale Formation of Woodbine Group, and the upper unit 3, to the LEF. In terms of the overlying low-resistivity "Harris delta" mudstones within the "Eaglebine" Meyer et al. (2021), included them as a separate unit, herein referred to as unit 4, and assigned it to UEF (Fig. 9).

PURPOSE AND METHODS

Three distinctly different paradigms presently exist as the for stratigraphic assignment for the "Eaglebine" succession in the southern East Texas Basin (Fig. 5). The first paradigm (Fig. 5) assigns the entire "Eaglebine" to Woodbine Group (Oliver, 1971; Turner and Conger, 1981, 1984; Berg, 1986). The second paradigm (Adams and Carr, 2010; Hentz et al., 2014; Denne et al., 2016) assigns the basal "high-resistivity" zone of the "Lower Eaglebine" to the Maness Shale, and the overlying "Upper Eaglebine" low-resistivity mudstones to the Pepper Shale of Woodbine Group (Fig. 5). The third paradigm (Meyer et al., 2021) assigns the "Eaglebine" to a variety of different stratigraphic units (Fig. 5), which from the base up are the Buda Formation (unit 1), the Pepper Shale (unit 2), the LEF (unit 3), and the UEF (unit 4). In this third paradigm (Fig. 5), the bulk of the "Eaglebine" is actually interpreted to be coeval to the Eagle Ford, not the Pepper Shale (Woodbine Group), or older Maness Formation.

In order to evaluate these three different interpretations for the "Eaglebine," as well as to better understand the chronostratigraphic relationships between the Woodbine and Eagle Ford groups as defined along the outcrop belt, and their coeval equivalents in the southern East Texas Basin, a detailed sequence stratigraphic framework was conducted using geochemical data from cores, tied to a grid of well-log cross-sections (Fig. 8). Key to this approach was defining and mapping key sequence stratigraphic surfaces: sequence boundaries (sb), transgressive surfaces (ts), and maximum flooding surfaces (mfs) within the Woodbine and Eagle Ford groups along the more mudstone-prone western margin of the basin, near the outcrop belt, and

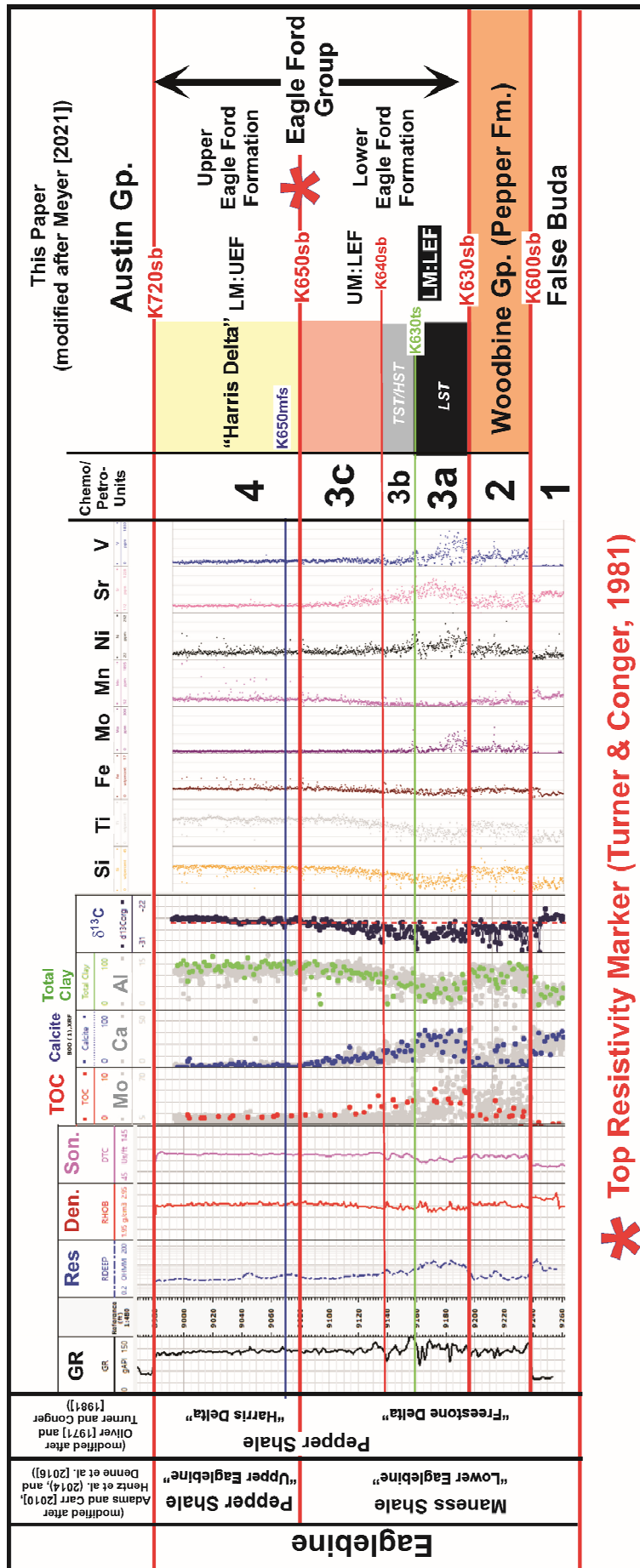


Figure 9. Geochemical and petrophysical data of the industry core in Burleson County, illustrating the previous lithostratigraphic interpretation for the "Eaglebine" succession in the southern East Texas Basin, and the sequence stratigraphic interpretation based on chemostratigraphic and petrophysical data from this core, and regional correlations. In this study 4 distinct unconformity bounded units (sequences), labeled 1 to 4 from the base up, were interpreted respectively as the False Buda (unit 1), Pepper Formation (unit 2), LEF (unit 3), and UEF (unit 4). Please note the location of the classic "top resistivity marker, traditionally used to separate strata of the "Freestone delta" (below) from the "Harris delta" (above). In this study, this surface coincides with the K650sb at the base of the UEF. Click [here](#) for a high-resolution, large-format version of this image.

correlating these surfaces and sequences, into the southern East Texas Basin. This contrasts with previous work (Hentz et al., 2014), which correlated into the southern East Texas Basin, from the eastern, more sand-prone (nonmarine), portions of the basin, where sequence surface identification is more problematic, and the Eagle Ford Group is commonly missing due to regional truncation beneath the base Austin unconformity (Halbouty, 1991). In order to define key surfaces, systems tracts, and sequences; geochemical work (x-ray fluorescence [XRF], TOC, and $\delta^{13}\text{C}_{\text{org}}$ isotope analysis) on key cores along the outcrop belt (USGS GC-1 and GC-2), as well as a key industry core in the southern East Texas Basin, was included as part of this study (Fig. 8). In these wells, the petrophysical and TOC data was provided by the operators, while the XRF and $\delta^{13}\text{C}_{\text{org}}$ analysis was conducted by researchers at Texas A&M University.

Trace element concentrations determined by XRF chemostratigraphy was a critical aspect of this study. These elemental data (Table 1) provides information on (1) mineral proxies, (2) depositional processes, (3) paleo oxic/redox conditions, (4) organic matter concentrations, and (5) mudstone compositions for regional correlations. For example, Ca, Si, and Al were used as proxies for carbonate, quartz, and clay input respectively in this study. Al, Si, and Ti were interpreted to indicate detrital input in depositional processes (Calvert and Pedersen, 1993). Fe, Mo, Mn, and V provide information on palaeoceanographic oxic/redox conditions (Algeo and Rowe, 2012), whereas potential source rock organic matter preservation can be determined by Mo and Va (Tribovillard et al., 2006). It was also hoped that the XRF chemostratigraphic data, could be used with TOC, as well as $\delta^{13}\text{C}$, data to better define chronostratigraphic units suitable for regional correlations.

Interpreted sequence boundaries (SB) were based in defining surfaces that (1) displayed truncation of underlying stratal markers on regional well-log cross-sections and/or (2) abrupt facies, geochemical, and/or petrophysical changes. Transgressive surfaces (ts) were defined by onlap below interpreted depositional shelf breaks, whereas maximum flooding surfaces (mfs) were defined by (1) high-GR zones separating more bell-shaped GR patterns (below) from funnel-shaped GR patterns (above) and (2) interpreted stratal downlap on the regional well-log cross-section.

Cross-sections were hung, and correlated, on multiple datums (K600sb, base Woodbine; K650mfs, within the LM:UEF; K670sb, base MM:UEF; and K720sb, base Austin) in order to gain different perspectives on stratal terminations, as well as angular discordance of strata.

A key aspect of this work, was to construct and interpret well-log cross-sections, that contained as many recent wells, with GR curves, as possible. To accomplish this, an important well-log source was the Texas Water Development Board's BRACS database, which provided abundant shallow oil and gas wells, as well as modern water wells, with GR curves. This database provided well-log data that greatly facilitated the surface to subsurface correlations ties in this study. Many previous studies (Oliver, 1971; Turner and Conger, 1981, 1984; Adams and Carr, 2010) had constructed well-log cross-sections which utilized older wells with only spontaneous potential (SP) and resistivity curves.

As illustrated on our type well for the northern part of the study area (Fig. 10), GR logs were critical throughout the study area for defining and placing the (K630) sequence boundary at the base of the Eagle Ford Group, since Eagle Ford mudstones consistently have higher background GR values, then mudstones of the underlying Woodbine Group.

Table 1. Trace element concentrations determined by XRF chemostratigraphy was a critical aspect of this study (modified after McCreary [2022]). These elemental data provides information on (1) mineral proxies, (2) depositional processes, (3) paleo oxic/redox conditions, (4) organic matter concentrations, and (5) mudstone compositions for regional correlations.

Element	Proxy	References
Al & K	Clay & Feldspar	Pearce & Jarvis (1992); Tribovillard et al. (2006)
Ca	Calcareous Input	Banner (1995); Tribovillard et al. (2006)
Si	Quartz (Terrigenous & Biogenic)	Pearce & Jarvis (1992); Sageman and Lyons (2004)
Ti	Terrigenous Input	Calvert and Pederson (1992); Zabel et al. (2001); Sageman and Lyons (2004)
Ni	Organic Matter/Micronutrients in the Water Column	Tribovillard et al. (2006)
Fe	Redox Sensitivity	Tribovillard et al. (2006)
S	Redox Sensitivity	Tribovillard et al. (2006)
P	Phosphate Accumulation/ Upwelling	Tribovillard et al. (2006)
Mn	Redox Sensitivity (Oxic Bottom Water)	Calvert and Pederson (1992); Sageman and Lyons (2004); Tribovillard et al. (2006); Brumsack (2006)
Sr	Carbonate Source & Diagenetic Influence	Pomerol (1976); Scholle (1977); Renard (1979); Banner (1995); Tribovillard et al. (2006)
V	Redox Sensitivity (Bottom Water Anoxia)	Helz et al. (1996); Sageman and Lyons (2004); Tribovillard et al. (2006); Algeo and Rowe (2012)
Ba	Paleoproductivity	Robin et al. (2003); Griffith and Paytan (2012); Liguori et al. (2016)

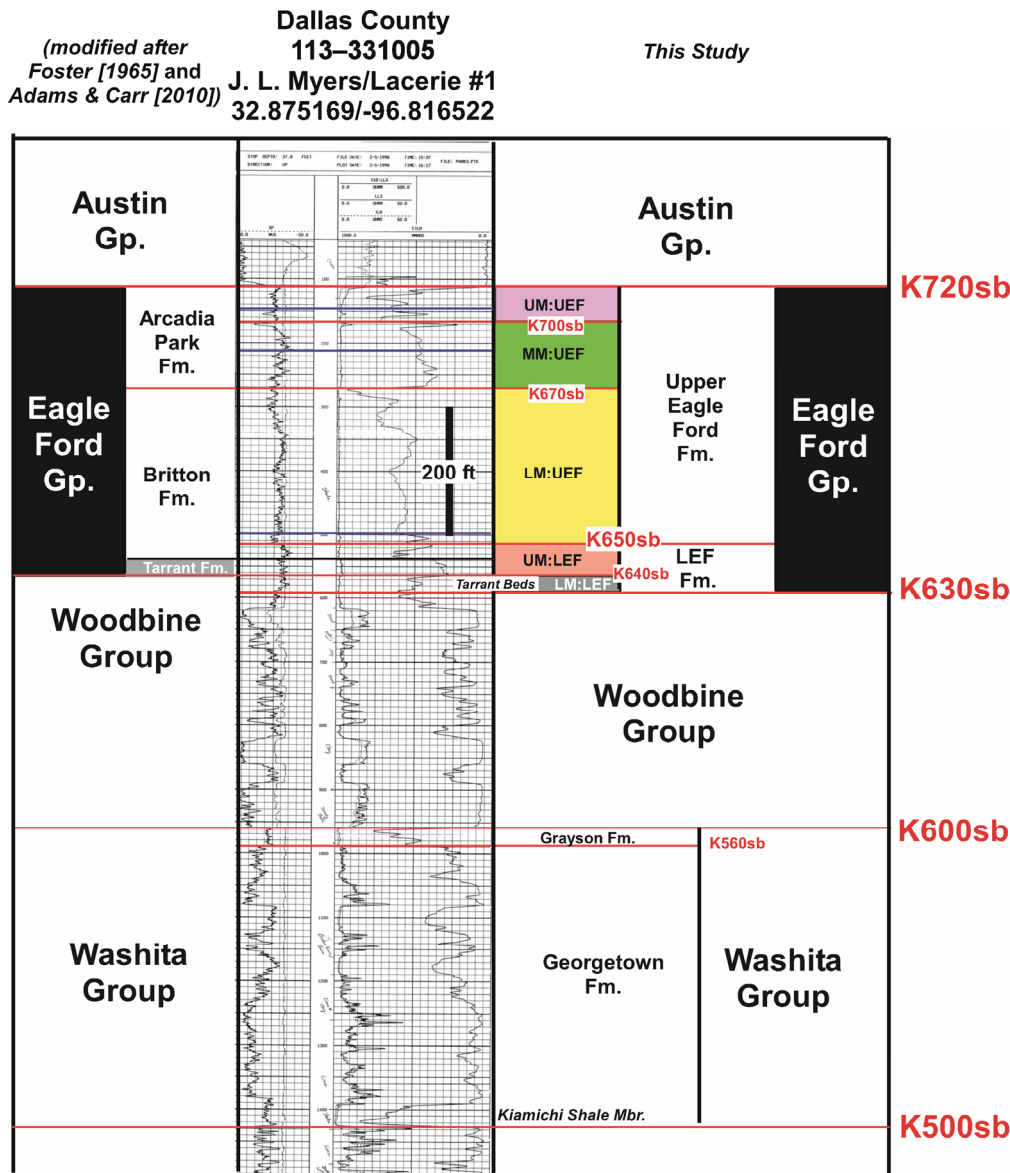


Figure 10. Type Eagle Ford well for the Northern East Texas Basin. This modern water well from the Texas Water Commission’s BRAC’s database, has a GR log, which nicely illustrates the GR drop that define the K630sb at the base of the Eagle Ford Group. The surfaces and sequences defined within the Eagle Ford Group in this study, are also illustrated on this figure. Click [here](#) for a high-resolution, large-format version of this image.

In this paper, sequence stratigraphic surfaces are numbered 0 to 999 from the base up for each geologic period. In the Cretaceous, the surfaces are preceded by the prefix K, for Cretaceous and the suffix sb (sequence boundary), mfs (maximum flooding surface), or ts (transgressive surface), in order to differentiate stratal types. For this study (Figs. 3 and 6), key surfaces include the (1) K600sb at the base of the Woodbine Group, (2) K630sb at the base of the Eagle Ford Group, and (3) K720sb at the base of the Austin Group. Another key boundary to note is the K650sb, which defines the base of the UEF. As mentioned previously, this boundary also corresponds the base (onset) of the positive $\delta^{13}\text{C}$ excursion associated with the OAE2. Finally, stratification (bedding) follows the classification of Campbell (1967).

RESULTS

USGS GC-2

The USGS GC-2 borehole is located near the type locality of the Eagle Ford Group, in Eagle Ford Texas (Fig. 8) just south of Texas. The well cored an approximate 750 ft (227 m) interval that spanned the basal Austin Group through the uppermost 118 ft (40 m) of the Woodbine Group. Unfortunately, a complete set

of borehole logs cover only the uppermost 510 ft (155.4 m) of the well, but core GR data extends to the base of the core (Fig. 11). The petrophysical and geochemical data, as well as the provincial lithostratigraphy, adjacent outcrop biostratigraphy, and sequence stratigraphic framework from this study, are plotted on Figure 11. In this well, the Eagle Ford Group is 464 ft (141.4 m) thick, and as mentioned previously, the uppermost 118 ft (40 m) of the Woodbine was also collected. For context, in the nearby northern East Texas Basin type well in Dallas County (Fig. 10), the Eagle Ford Group is 480 ft (166.3 m) thick, and the complete underlying Woodbine Group, is 370 ft (113 m) thick. The base of Eagle Ford Group (Fig. 11) is placed at the base of the classic Tarrant Formation in the GC-2. In this core, the base of the Tarrant Formation consists of a 4 ft (1.2 m) thick limestone, that has distinct rip-up clasts at its base. In the adjacent outcrops, the same basal Tarrant limestone bed contains the ammonite *Conlinoceras tarrantense*. As mentioned previously, this ammonite (Fig. 3) is important because (1) its first occurrence marks the base of the middle Cenomanian and (2) it is the first (oldest) Upper Cretaceous ammonite found in both Gulf Coast and Cretaceous Western Interior Seaway, marking the time that the Boreal sea waters first encroached into the southern portions of the Cretaceous

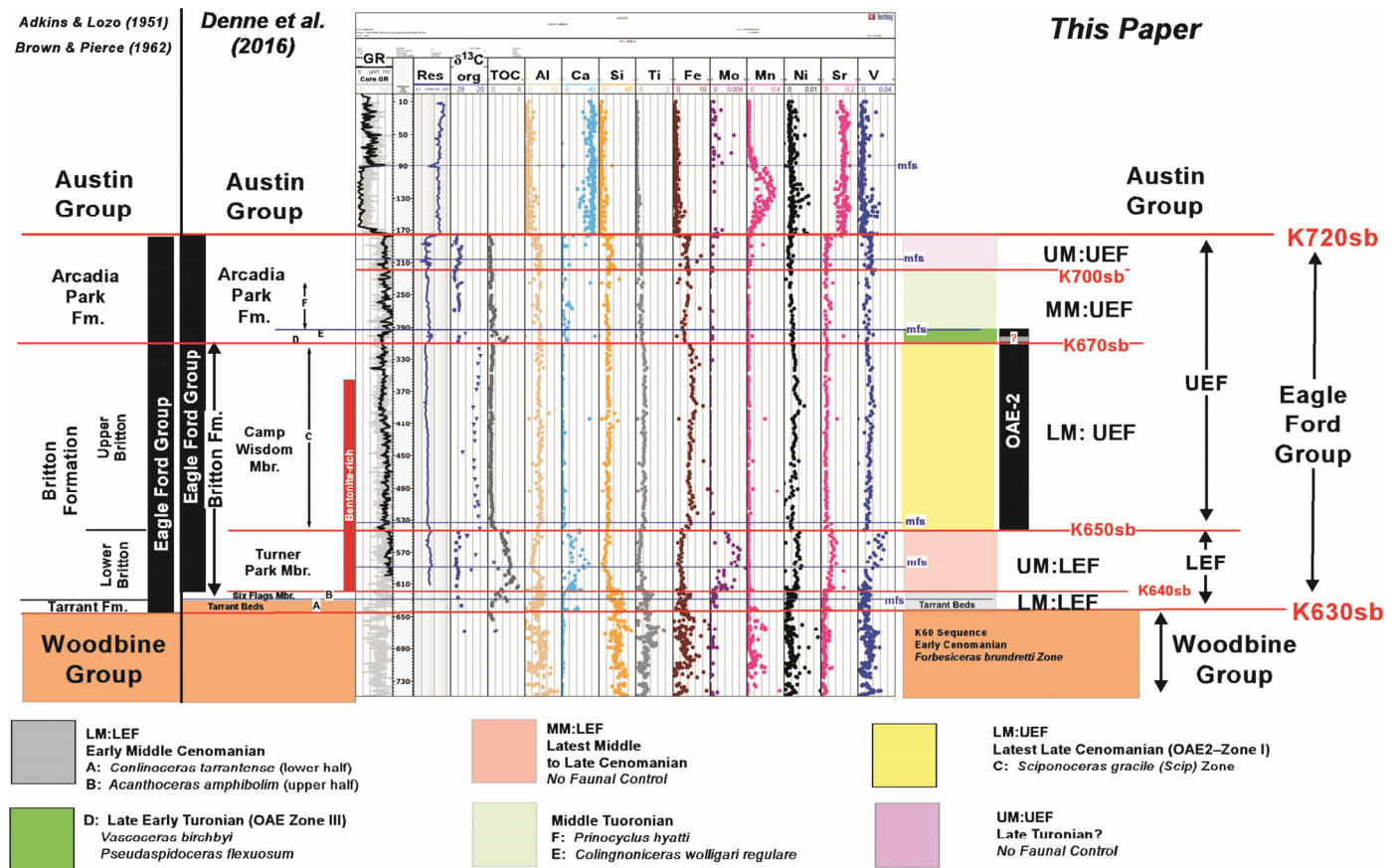


Figure 11. Petrophysical and geochemical data of the USGS GC-2 core near Dallas, as well as the ammonite data of Kennedy (1988) from the adjacent outcrops. Please note (1) Ca- and TOC-poor Woodbine: Ca- and TOC-rich LEF; Ca- and TOC-poor UEF, and (4) 230 ft (70 m) thick positive $\delta^{13}C$ excursion in the LM:UEF, which based on the adjacent outcrops is confined to the basal *Sciponoceras gracile* ammonite zone at the base of the OAE2 (zone I). Click [here](#) for a high-resolution, large-format version of this image.

Western Interior Seaway in the Upper Cretaceous. In this core, the basal limestone bed in the Tarrant Formation (Fig. 11), separates Ca-, Mo-, and TOC-poor, non-fossiliferous mottled greenish gray Woodbine mudstones and sandstones (below), from fossiliferous, medium to dark gray, Ca-, TOC-, Mo-enriched mudstones interbedded with thin sandstones, as well as limestones, of the Eagle Ford Group (above). Fortunately, this distinct lithologic contact also coincides with a distinct GR increase, that can be readily seen in the core GR plot in this well (Fig. 11), as well in the other wells across the study area, such as the northern East Texas Basin type (Fig. 10), and southern East Texas Basin type well (Fig. 5). Based on the geochemical, lithologic, and important biostratigraphic changes that occurs across this contact, an unconformity, the K600sb is placed at the base of the Eagle Ford Group in the GC-2 (Fig. 11).

In terms of the LEF in this core, it is 98 ft (29.9 m) thick, and can be characterized overall as a high-GR/resistivity interval, that is rich in Ca, TOC, and Mo (Fig. 11). This contrasts with underlying Woodbine Group that contains mudstones which (1) have lower GR and resistivity, (2) are rich in Al, and (3) are poor in Ca, Mo, and TOC. Following the work of Donovan et al. (2015), the LEF in the GC-2 can readily be divided (Fig. 11) into a lower/older, bentonite-poor LM:LEF, as well as an upper/younger, bentonite-rich UM:LEF. An unconformity, the K640sb, is placed at the base of the LM:LEF due to the change from bentonite-poor to bentonite-rich strata, which suggest two distinctly different chronostratigraphic units (Fig. 11).

The base of the UEF is denoted by a distinct GR decrease that also corresponds to (1) a decrease in TOC, Mo, Ni, Sr, Va, and Ca; (2) an increase in Al, Fe, and Ti; (3) a resistivity decrease, and (4) the onset of a positive $\delta^{13}C$ excursion interpreted as the OAE2 (Fig. 11). In the adjacent outcrops in the Dallas area (Fig. 11), Kennedy (1988) noted that the first occurrence of the ammonite *Sciponoceras gracile*, which denotes zone I of the OAE2 in Pueblo (Fig. 4), also coincides with the base of the Upper Britton (UEF). Lithologically, in the core, this contact coincides with an abrupt change from dark gray, organic- and bentonite-rich calcareous mudstones (below) to light gray organic-poor, argillaceous-rich, mudstones that are interbedded with thin sandstones (above). Based on the abrupt petrophysical, geochemical, and biostratigraphic changes that occur across this boundary, an unconformity, the K650sb, is placed at the base of the UEF (Fig. 11).

The LM:UEF, colored yellow on Figure 11, is a 230 ft (70 m) interval that coincides with the main positive $\delta^{13}C$ isotope excursion interpreted as the OAE2. Kennedy's (1988) ammonite work on the adjacent outcrops revealed that this thick stratigraphic unit is confined to the *Sciponoceras gracile* ammonite zone, which is restricted to the basal 6.6 ft (2 m) of the OAE2 at the type locality in Pueblo, Colorado (Fig. 4). Clearly, an important learning from this core, is that there was a major deltaic depocenter located in the Dallas area at the onset of the OAE2 (Fig. 11).

The overlying, MM:UEF, which is colored green on Figure 11, is a 93 ft (28.3 m) Ca- and TOC-enriched interval with ele-

vated resistivity, as well as GR readings. The petrophysical (high resistivity) characteristics of this unit make it useful for differentiating the MM:UEF from the underlying LM:UEF, as well as overlying UM:UEF, on individual wells (Figs. 10 and 11), as well as on regional well-log cross-sections. A distinct 2 ft (0.6 m) fossiliferous limestone bed, which is the adjacent outcrops is called the Kemp Ranch Limestone (Kennedy, 1988), occurs about 10 ft (3 m) above the base of this unit.

The base of the MM:UEF, coincides with the base of the provincial Arcadia Park Formation, as well as the end of the positive $\delta^{13}\text{C}$ excursion in this core (Fig. 11). Lithologically, this boundary coincides with an abrupt change from blueish-gray, massive mudstones (below), to brownish gray, laminated mudstones with scattered thin limestone beds (above). In the adjacent outcrops (Fig. 11), Kennedy (1988) observed ammonites of the Late Cretaceous *Sciponceras gracile* zone (OAE zone I) directly below this contact, and ammonites of the early Turonian *Watinoceras ammonite* zone (*Pseudaspidoceras flexuosum* and *Vascoceras birchbyi*), OAE zone II directly above. Thus compared to the type “base Turonian” section at Rock Creek, Colorado (Fig. 4) ammonites of the latest Cretaceous and earliest Turonian (OAE zone II), are missing across this contact (Fig. 11). Based on this interpreted biostratigraphic hiatus, Kennedy (1988) placed an unconformity at this contact. In this study, based on the lithological and geochemical changes that occur across this contact in the core (Fig. 11), as well as the biostratigraphic break, associated with this contact in the adjacent outcrops, an unconformity (K670sb), is placed at the base of the MM:UEF.

The UM:UEF, which is colored lavender on Figure 11, is a 40 ft (12.2 m), Al- and Si-enriched, TOC- and Ca-poor, mudstone-dominated succession, that overall has higher GR and lower resistivity values than the underlying MM:UEF. In core, the base of the UM:UEF coincides with an abrupt change from dark greenish-gray mudstones (below) to medium greenish gray mudstones interbedded with very thin to thin sandstone beds. Based on the abrupt lithologic, geochemical, and petrophysical changes that occur across this contact, an unconformity, the K700sb is placed at the base of the UM:UEF (Fig. 11). Finally, the base of the Austin Group (Fig. 11), shows an abrupt drop in GR, Al, Si, Ti, Fe, and V, as well as concurrent increase in resistivity, Ca, Mn, Ni, and Sr. In core these petrophysical and geochemical changes coincide with a change from dark gray mudstones interbedded with thin sandstones (below) to highly bioturbated light gray wackestones interbedded with darker gray calcareous mudstones (above). Based on the abrupt lithologic, petrophysical, and geochemical changes across this contact, an unconformity, the K720sb, is placed at the Austin Group (Fig. 11).

In summary, key learnings from the GC-2 core (Fig. 11) are (1) Ca- and TOC-rich LEF mudstones overlie Ca- and TOC-poor, Al- and Ti-rich Woodbine strata, and are in turn overlain by Ca- and TOC-poor, Al- and Ti-rich strata of the LM:UEF; (2) the thickness of the positive $\delta^{13}\text{C}$ signature in the GC-2 core indicates that a major depocenter existed in the Dallas area at the onset of the OAE2; and (3) a significant biostratigraphic hiatus/unconformity (K670sb) exists at the base of the MM:UEF in the Dallas area.

Subsurface: Northern East Texas Basin

Well-log cross-section EW-300 (Fig. 8) is a regional line that provides a subsurface perspective across the northern East Texas Basin. This well-log cross-section (Fig. 12) goes from Dallas County to the west to Smith County to the east, a distance of about 85 mi (137 km). The GC-2 well (Fig. 11) is located on western end of the line, while the type well for the northern East Texas Basin (Fig. 10), is located next to the GC-2. EW-300 (Fig. 12) is datumed on the K720sb, which is the unconformity at the

base of the Austin Group. This cross-section follows the color codes for the sequences identified in the GC-2 core (Fig. 11), however to simplify things, the LEF is simply colored gray. On this (Fig. 12), as well as on the other cross-sections, the Woodbine Group is colored orange, the False Buda Formation (aqua), and the Buda Formation (medium blue).

Starting from the base up (Fig. 12), the interpreted K600sb, or base Woodbine Group unconformity, sequentially truncates the False Buda Formation, and then the Buda Formation from east to west. The interpreted K630sb, or base Eagle Ford unconformity, sequentially truncates underlying Woodbine strata (orange) from east to west. The K650sb, at the base of the UEF (LM:UEF), truncates the LEF to the east (Fig. 12). Thus, in eastern Van Zandt and Smith counties, the LM:UEF is unconformably juxtaposed on the Woodbine Group. The three members of the UEF, unlike the underlying Washita and Woodbine groups, extend fairly continuously across this cross-section (Fig. 12). Finally, the K800sb at the base of the overlying Taylor Group appears to incise into the top of the Austin Group with apparent reciprocal fill of overlying basal Taylor strata.

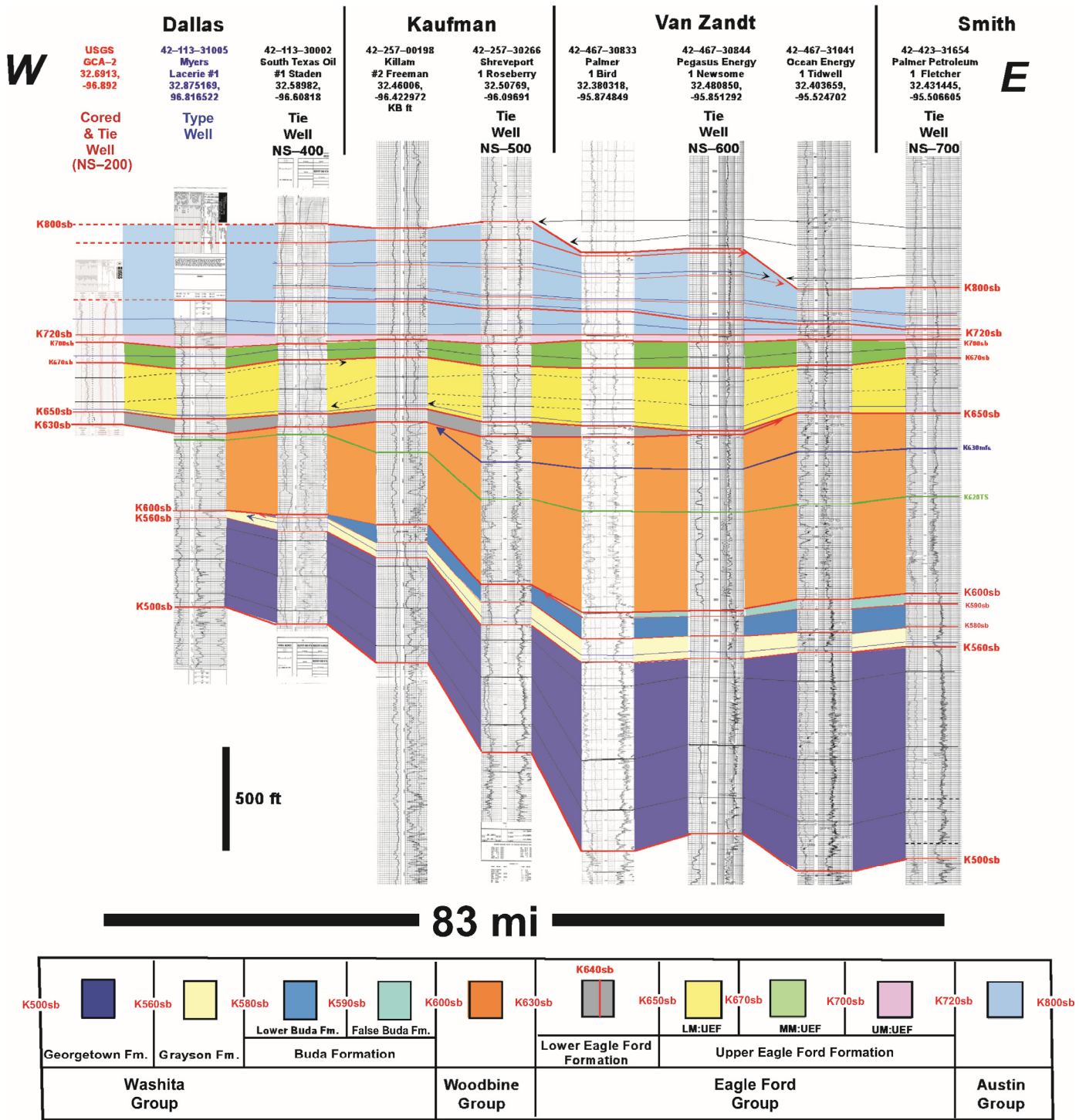
In summary, a key learnings from well-log cross-section EW-300 (Fig. 12), are that the (1) base Woodbine unconformity (K600sb) truncates underlying “Upper Washita” strata to the west, (2) base Eagle Ford unconformity (K630sb), also truncates Woodbine strata to the west, (3) base UEF unconformity truncates the LEF to the east, and (4) unless truncated by the K650sb, the Ca- and TOC-rich LEF deposits, separate Al- and Ti-rich, but Ca- and TOC-poor Woodbine strata below, from Al- and Ti-rich, but Ca- and TOC-poor strata of the LM:UEF (above).

Subsurface: Dallas to Austin

Well-log cross-section NS-200 (Fig. 8) is a regional line that provides a subsurface perspective of along the western margin of the East Texas Basin, close to the outcrop belt. This cross-section (Fig. 13) goes from Dallas County to the north to Travis County to the south, a distance of about 225 mi (362 km). The GC-2 well (Fig. 11) is located near the northern end of the line, while the GC-1 well (Fig. 7), is located near the central portions of this line. NS-200 (Fig. 13) is datumed on the K700sb, which is the unconformity at the base of the MM:UEF.

Starting from the base up (Fig. 13), the interpreted K600sb, or base Woodbine Group unconformity, sequentially truncates the Buda Formation from south to north. Thus, along most of this well-log traverse, the Woodbine Group is unconformably juxtaposed the Grayson Formation (Fig. 13). The interpreted K630sb, or base Eagle Ford unconformity, sequentially truncates underlying Woodbine strata from north to south (Fig. 13). This results in drastic thinning of the Woodbine Group, and the preservation of only the lowermost mudstone-prone strata of the lowermost Pepper Formation to the south (Fig. 13). On this line (Fig. 13), the K650sb at the base of the UEF, appears to have little effect on the thickness variations of the underlying LEF (gray). In sharp contrast, the LM:UEF (yellow) thins drastically from north to south, and is totally absent south of Bell County, due to interpreted truncation beneath the K670sb (Fig. 13). In general across NS-200 (Fig. 13), the MM:UEF (green), thin to the south due to truncation beneath the K700sb, while the UM:UEF (lavender) also thins to the south, especially south of Bell County, due to truncation interpreted beneath the K720sb, base Austin Group unconformity.

In summary, key learnings from well-log cross-section NS-200 (Fig. 13) are (1) the Buda is truncated to the north by the K600sb, (2) the LM:UEF thins and is eventually totally truncated, to the south, beneath the K670sb, and (3) high-resistivity (organic-rich) LEF mudstones overlie low-resistivity Woodbine mudstones.



Datum: K720sb (Base Austin Group)

Figure 12. Regional cross-section EW-300 from western Dallas County (W) to western Smith County (E), datumed on the K720sb at the base of the Austin Group. On this line (1) the K600sb at the base of the Woodbine Group truncates the False Buda and then the Buda formations to the west, (2) the K630sb at the base of the Eagle Ford Group thins the underlying Woodbine Group to the west, and (3) the K650sb at the base of the UEF truncates the LEF to the east. Thus on the eastern end of the line the UM:UEF is unconformably juxtaposed on the Woodbine Group. Click [here](#) for a high-resolution, large-format version of this image.

USGS: GC-1

The USGS GC-1 borehole located near Waco, Texas (Fig. 8) cored the uppermost Georgetown through the basal portions of the Austin Group. The petrophysical, geochemical, and lithologic data, as well as the provincial lithostratigraphy, and sequence

stratigraphic interpretation, from this for the upper portions of this core, are plotted on Figure 7. Unlike the Dallas area type well (Fig. 10), where the Woodbine Group was sandstone-dominated, and 370 ft (113 m) thick, in the GC-1 core (Fig. 7) the Woodbine Group is mudstone-dominated, and only 43.5 ft (13.25 m) thick. Similarly, while the Eagle Ford Group was 464

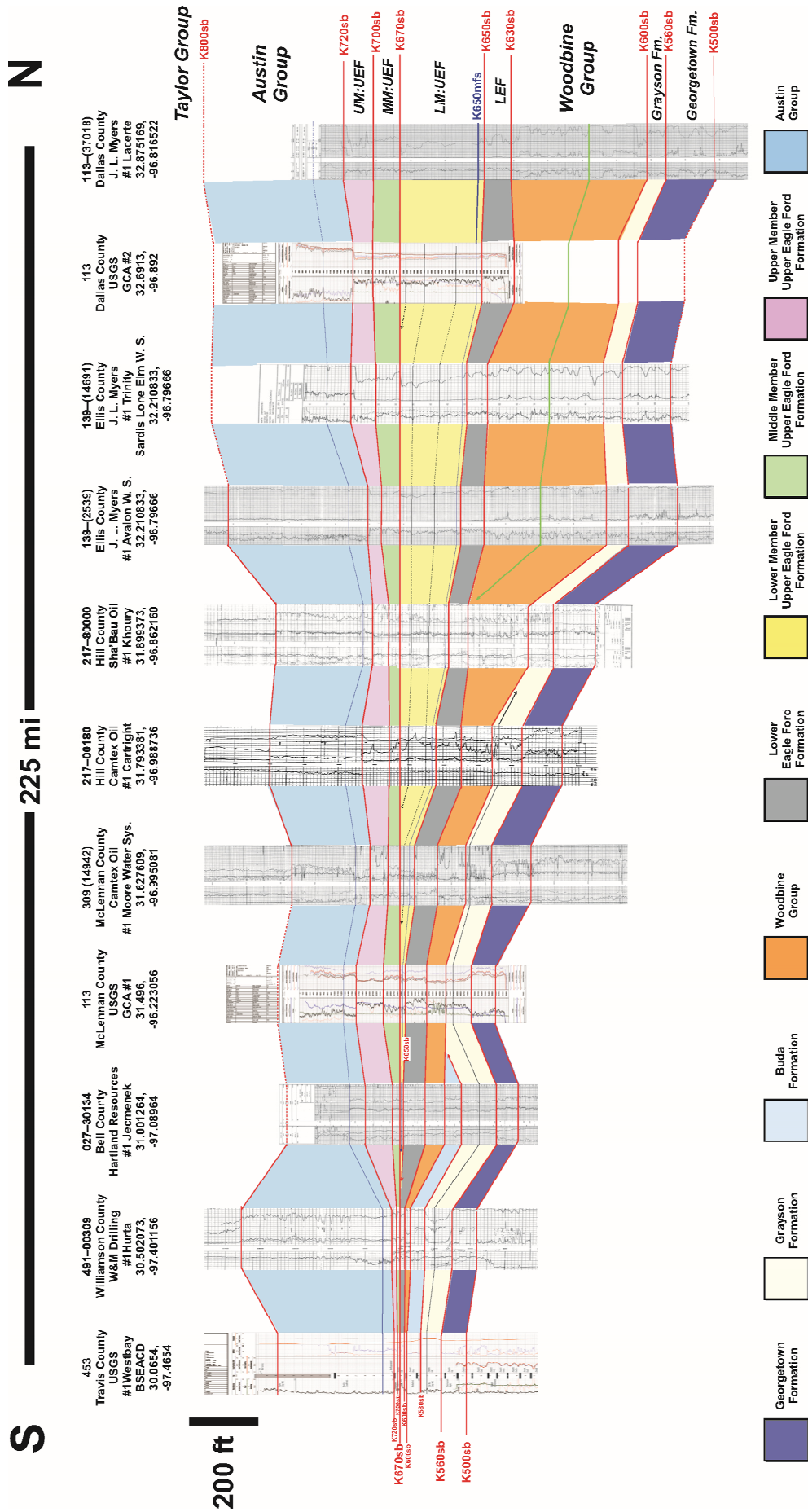


Figure 13. Regional well-log cross-section, that parallels the outcrop belt along the western flank of the East Texas Basin from Dallas to Austin, and is datumed on the K670sb at the base of the MM:UEF. On this line the K670sb thins, and eventually truncates the LM:UEF to the south. Thus on the southern end of this line, the MM:UEF is unconformably juxtaposed on the LEF. Click [here](#) for a high-resolution, large-format version of this image.

ft (141.4 m) thick in the GC-2 core (Fig. 11), in the GC-1 core (Fig. 7), the Eagle Ford Group is just 199 ft (60.7 m) thick.

In terms of the base of the Woodbine Group in the GC-1 core, (Fig. 7), like the GC-2 (Fig. 11), the Woodbine is juxtaposed on the Grayson Formation, and the False Buda as well as the underlying Buda Formation proper are absent. The Grayson/Woodbine contact (Fig. 7) is marked a distinct (upward) resistivity drop, that corresponds to a change from massive greenish-gray calcareous mudstones of the Grayson Formation (below) to black Al-rich and Ca-poor mudstones of the Pepper Formation (above). Due to the sharp lithologic, geochemical, and petrophysical changes at this contact, as well as the juxtaposition of the Woodbine Group on the Grayson Formation, the K600sb, is placed at the base of the Woodbine Group in the GC-1 (Fig. 7). The overlying Woodbine Group consists of the mudstone-prone Pepper Formation (Fig. 7), which in this core, consists of a massive mudstone that is rich in Al, but poor in Ca and TOC over its entire 42.5 ft (13.3 m) thickness.

The Woodbine/Eagle Ford contact (Fig. 7) is also characterized by the same distinct GR increase that defines the base of the Eagle Ford Formation across the entire study area. Geochemically (Fig. 7), this contact coincides with a change from Ca-, Mo-, Ni-, and TOC-poor, as well as Al- and Si-rich, strata (below) to Al- and Si-poor, as well as Ca-, Mo-, Ni-, and TOC-rich, strata (above). Overall the LEF, which is 61.5 ft (18.7 m) thick, consists of high resistivity/GR interval, that is Al and Si poor, as well as Ca, Mo, Ni, and TOC rich (Fig. 7). Similar to the GC-2 core (Fig. 11), the LEF in the GC-1 can be subdivided into a bentonite-poor LM:LEF, and bentonite-rich UM:LEF. The K640sb is placed at the base of the UM:LEF, based on the chronostratigraphic significance to the onset of bentonite-rich deposition within the LEF.

The base of the UEF in the GC-1 (Fig. 7), corresponds to (1) a drop in Mo and Ni content, (2) a drop in GR values, and (3) the onset of the positive $\delta^{13}\text{C}$ excursion associated with the OAE2 in the overlying LM:UEF. Lithologically, these geochemical changes coincide with a change from dark gray mudstones, with abundant thin bentonite and very thin limestone interbeds (below), to medium greenish gray mudstones and medium-bedded limestones (above). Due to the abrupt lithologic and geochemical changes that occur at the LEF/UEF contact, as well as the onset of the positive $\delta^{13}\text{C}$ excursion at the base of the UEF, the K6500sb is also placed at the base of the UEF in this core (Fig. 7). In terms of the LM:UEF, unlike the GC-2 core in Dallas, where the where the positive $\delta^{13}\text{C}$ excursion associated with the OAE2 was 230 ft (70 m) thick (Fig. 11), in the GC-1 core, the positive $\delta^{13}\text{C}$ excursion is only 10 ft (3 m) thick (Fig. 7). In the GC-1 core, the 10 ft (3 m) thick, LM:UEF is a Ca-rich, TOC-, Mo-, and Ni-poor low GR interval, that displays higher resistivity at its base, and lower resistivity towards its top (Fig. 7).

The LM:UEF, in the GC-1 (Fig. 7) is overlain by the MM:UEF, which is a 51 ft (15.5 m) thick interval with elevated Ca, Ni, and TOC, as well as elevated resistivity. Similar to the GC-2 (Fig. 11), the base of the MM:UEF in the GC-1 (Fig. 7), also coincides with the end of the positive $\delta^{13}\text{C}$ excursion, interpreted as the OAE2. Lithologically, this contact coincides with a change from medium greenish-gray mudstones, interstratified with medium-bedded limestones (below), to dark gray mudstones interstratified with very thin limestone beds (above). Based on (1) the abrupt lithologic and geochemical changes that occur at the base of the MM:UEF, (2) the abrupt termination of the positive $\delta^{13}\text{C}$ isotope excursion at the base of the MM:UEF, and (3) the thickness (10 ft [3 m]) of the positive $\delta^{13}\text{C}$ excursion in the GC-1; the K670sb is also placed at the base of the MM:UEF in the GC-1 (Fig. 7).

The MM:UEF in the GC-1 (Fig. 7) is overlain by the UM:UEF, which is a 67 ft (20.4 m) sequence characterized by (1) low GR and resistivity, (2) low Ca, Ni, and TOC, and

(3) slightly-elevated Si, Al, Fe, and Mo. The base of the UM:UEF (Fig. 7) is characterized by a sharp contact with the MM:UEF that coincides with (1) drop in GR and resistivity values, (2) drop in TOC, Ca, and Ni content, (3) slight increase in Al, Si, Fe, and Mo content, and (4) a lithologic change from medium greenish gray mudstones with scattered very thin limestone interbeds (below) to massive dark gray mudstones (above). Based on the abrupt changes in petrophysical, geochemical, and lithologic characteristics at the base of the UM:UEF, an unconformity, the K700sb, is placed at this contact (Fig. 7). Finally the base of the Austin Group, or top of the UM:UEF (Fig. 7), is also denoted by a sharp contact characterized by (1) distinct GR decrease and resistivity increase, (2) increase in Ca, Mn, Ni, and Sr content, (3) decrease in Al, Si, and Fe content, and (4) a lithologic change from massive medium gray mudstones (below) to highly burrowed, white limestones/wackestones (above). Based on the abrupt changes in petrophysical, geochemical, and lithologic characteristics at the base of the Austin Group, an unconformity, the K720sb, is placed at this contact (Fig. 7).

In summary, key learnings from the GC-1 core (Fig. 7) are (1) both the Woodbine and Eagle Ford Group are thinner in the Waco area compared to the Dallas area, (2) the Woodbine Group in the Waco area is dominated by the basal mudstone-prone Pepper Formation, (3) Ca- and TOC-rich LEF mudstones overlie Ca- and TOC-poor, Al- and Si-rich Woodbine strata, (4) the positive $\delta^{13}\text{C}$ excursion is present in the GC-1, but only 10 ft (3 m) thick, and (5) the thickness variations of the LM:UEF, and the associated positive $\delta^{13}\text{C}$ excision, are likely the result of truncation by the overlying K670sb at the base of the MM:UEF.

Central East Texas Basin

Well-log cross-section EW-700 (Fig. 8) is a regional line from McClennan County to the west, to Cherokee County to the east, a distance of about 85 mi (137 km). This cross-section is datumed on the K650mfs, near the base of the UEF, and the USGS GC-1 well is located near the western end of this line (Fig. 14).

On EW-700 (Fig. 14), the K600sb, or base Woodbine Group unconformity, sequentially truncates the False Buda Formation, and then underlying the Buda Formation toward the outcrop belt to the west (Fig. 14). The Woodbine Group also thins the west, due to interpreted truncation by the overlying K630sb, or base Eagle Ford unconformity (Fig. 14). The LEF is present on the western portion of this line, but thins, and is then absent east of central Anderson County, due to truncation interpreted beneath the 650sb, at the base the UEF (Fig. 14). The LM:UEF (yellow) thins to the west due to interpreted truncation by the overlying K670sb, at the base of the MM:UEF (Fig. 14). From west to east on line EW-700 (Fig. 14), the UM:UEF, MM:UEF, and LM:UEF are sequentially truncated by the K720sb, at the base of the Austin Group. The Austin Group also thins to the east, due to truncation interpreted at the K800sb at the base of the Taylor Group (tan) on this line (Fig. 14).

In summary, EW-700 (Fig. 14) illustrates (1) truncation to the west beneath the K600sb, at the base of the Woodbine Group, as well as the K670sb, at the base of the MM:UEF; (2) truncation to the east, beneath the K650sb, at the base of the UEF, and the K720sb; and (3) unless truncated by the K650sb, high-GR/resistivity LEF mudstones, overlies low-resistivity mudstones of the Woodbine Group, and are overlain by low-resistivity mudstones of the LM:UEF.

Central to Southern East Texas Basin

NS-400 (Fig. 8) is a sub-regional north/south well-log cross-section, that goes from Limestone County to the north, to Burleson County to the south, a distance of about 85 mi (137 km). This cross-section is datumed on the K600sb, or base Woodbine

Group unconformity (Fig. 15). The cored industry well is located near the southern end of the line in Burleson County (Fig. 15).

On NS-400, the LEF is subdivided into three parts, colored black, gray, and red from the base up (Fig. 15). For reference, the black and gray colored intervals represent the lower and upper portions of the LM:UEF, while the red colored interval represents the overlying (younger) UM:LEF. The lower portion of the LM:LEF, colored black, on Figure 15, is very distinctive high gamma ray/resistivity interval in the southern East Texas Basin, that is useful for sub-regional correlations and mapping. This basal zone within the LM:UEF is also the primary exploitation target for the Ca- and TOC-rich, "Eaglebine" source rock play in the southern East Texas Basin (Meyer et al., 2021), so knowing its presence, distribution, and thickness variations are critical for understanding its play fairway, and associated risks.

Starting from the base of the section on NS-200 (Fig. 15), the False Buda Formation is truncated to the north beneath the K600sb (base Woodbine) unconformity. In terms of the overlying Woodbine Group, it thins to the south, most noticeably just downdip of the interpreted K630 depositional shelf break (red dot) along the K630sb (Fig. 15). Within the overlying LEF (Fig. 15), (1) the basal black unit within the LM:UEF onlaps downdip of the interpreted K630 depositional shelf break, (2) the overlying gray unit within the LM:UEF thins, but extends over the interpreted K630 depositional shelf break to the north, and (3) the uppermost red unit (UM:UEF) extends across the cross-section. Based on these relationships the onlapping lower (black) unit within the LM:LEF is interpreted as a lowstand, while the overlying upper (gray) unit within the LM:UEF is interpreted as the transgressive to highstand systems tract of the LM:LEF (Fig. 15).

Overall the UEF (Fig. 15) thins to the south due to truncation beneath the K720sb at the base of the Austin Group, as does the overlying Austin Group due to truncation beneath the K800sb at the base of the overlying Taylor Group. The UEF is divided into the LM:UEF, MM:UEF, and UM:UEF, which are respectively colored yellow, green, and lavender on Figure 15. Within the LM:UEF (yellow), internal stratal correlations suggest downlap onto the K650mfs, and northerly offlapping clinoforms (Fig. 15). The MM:UEF (green), is restricted to the northern end of the line, as is the UM:UEF (lavender); however, the UM:UEF extends further to the south (Fig. 15). Due to truncation by the K720sb, at the base of the Austin Group, only the LM:UEF is present within the UEF on the southern half of the line (Fig. 15).

In summary, on NS-200 (Fig. 15), the (1) False Buda Formation thins and is eventually truncated to the north beneath the K600sb, at the base of the Woodbine Group, (2) Woodbine Group thins to the south, most noticeably outboard of the interpreted depositional shelf break of the K630sb along the Woodbine/Eagle Ford contact, (3) LEF thins to the north due to onlap of interpreted lowstand deposits beneath the 630 depositional shelf break, (4) UEF thins to the south, primarily due to truncation beneath the K720sb at the base of the overlying Austin Group, and (5) Austin Group thins to the south due to truncation beneath the K800sb at the base of the overlying Taylor Group.

Southern East Texas Basin Cored Well

The generalized location of the cored industry well in Burleson County is noted on Figure 8. The core, which is approximately 250 ft (76.2 m) thick, spans most of the traditional "Eaglebine" succession in this portion of the basin (Fig. 9). Geochemical and petrophysical data from this core (Fig. 9) was used to define a vertical succession of four distinct chemo-/petrofacies, labeled units 1 to 4 from the base up. Unit 3 (Fig. 9) is further subdivided into three additional subunits, labeled 3a to 3c from the base up, to gain additional stratigraphic fidelity within that unit. Units 1 to 4 (Fig. 9) each have abrupt petrophysical and geochemical boundaries with their adjacent units, suggesting that these contacts are also depositional sequence boundaries. This

interpretation is also supported by the correlations into the cored well on cross-section NS-400 (Fig. 15) where all four units tie directly to the depositional sequences interpreted on Cross Section NS400.

The top 15 ft (4.6 m) of unit 1 (Fig. 9), was penetrated in this core. In the cored interval, unit 1 can be characterized as a high-resistivity and low-GR mudstone, that is rich in Ca, but poor in Al, Si, Ti, and TOC. Based on ties to NS-200 (Fig. 15), unit 1 is interpreted as the False Buda Formation.

Unit 2 (Fig. 9) is a 42 ft (12.8 m) thick interval, that can be characterized as a low-resistivity mudstone, with moderate GR values, that is enriched in Al, Si, and Ti, but poor in TOC and Ca. Based on ties to NS-200 (Fig. 15), unit 2 correlated to the Pepper Formation (Woodbine Group). The base of unit 2 (Fig. 9), which is interpreted as the K600sb, coincides with an abrupt change from low-GR, high-resistivity, Ca-rich, as well as Al-, Ti-, and Si-poor, mudstones of the False Buda Formation (below) to Ca-poor, but Al-, Ti-, and Si-rich mudstone of the Pepper Formation (above).

Unit 3 (Fig. 9) is a 104 ft (31.7 m) interval, that can be characterized as a mudstone with elevated resistivity and GR values, that is also TOC and Ca enriched. Based on correlations on NS-200 (Fig. 15), unit 3 correlates to the LEF (Fig. 9). The base of unit 3 (Fig. 9), which is interpreted as the K630sb, coincides with an abrupt change from Ca- and TOC-poor, but Al-, Ti-, and Si-rich mudstones of the Pepper Formation (below), to Ca- and TOC-enriched mudstones of the LEF (above).

As mentioned previously, unit 3 can be subdivided into three subunits, labeled 3a to 3c from the bottom up (Fig. 9). Subunit 3a are the most Ca- and TOC-rich, highest-resistivity mudstones, that have the lowest Al, Ti, and Si content within unit 3 (Fig. 9). Based on correlations on NS-200 (Fig. 15), unit 3a correlates to the interpreted lowstand systems tract of the LM:LEF.

The base of subunit 3b (Fig. 9), coincides with distinct decreases in resistivity, Mo, Ca, Ni, Sr, and V. Overall subunit 3b (Fig. 9) is a slightly lower-resistivity zone, compared to subunit 3a, that is characterized by an upward decrease in Ca, Mo, Ni, Sr, and V, as well as a concurrent upward increase in Si, Ti, and Al. Based on correlations on NS-200 (Fig. 15), unit 3b correlates to the interpreted transgressive and highstand systems tract of the LM:LEF.

The base of unit 3c (Fig. 9) is denoted by a distinct GR increase and resistivity decrease, that geochemically coincides with an abrupt decrease in Ca content, and increase in Al content. Overall subunit 3c (Fig. 9) is characterized by an upward decrease in resistivity, as well as Ca, Ni, and Sr, and V content, and a concurrent upward increase in Si, Ti, and Al content. Based on correlations on NS-200 (Fig. 15), unit 3c correlates to the interpreted UM:LEF.

Unit 4 (Fig. 9) is 110 ft (33.5 m) interval, of which, the basal 90 ft (27.4 m) was cored. It can be characterized as a low resistivity mudstone that is rich in Al, Si, and Ti, but poor in TOC and Ca.

The base of unit 4 (Fig. 9) coincides with the classic top resistivity marker (Turner and Conger, 1981, 1984), which is used to define the traditional base of the (Woodbine) Harris delta. Geochemically this surface, which coincides with a change from TOC- and Ca-enriched mudstones (below) to TOC- and Ca-poor, as well as Al-, Si-, and Ti-rich, mudstones (above), is interpreted as the K650sb, or base of the UEF. Interestingly, the base of unit 4 (Fig. 9) also coincides with the onset of a more blocky, less irregular, and slightly elevated positive $\delta^{13}\text{C}$ excursion. This blocky, slightly positive $\delta^{13}\text{C}$ excursion, based on the regional correlations (Figs. 12-15), likely represents a more TOC-starved manifestation of the positive $\delta^{13}\text{C}$ excursion associated with the OAE2. Based on correlations on NS-200 (Fig. 15), unit 4 correlates to the interpreted LM:LEF.

In summary, the petrophysical and geochemical data from the industry core (Fig. 9), tied to NS-200 (Fig. 15), indicate that

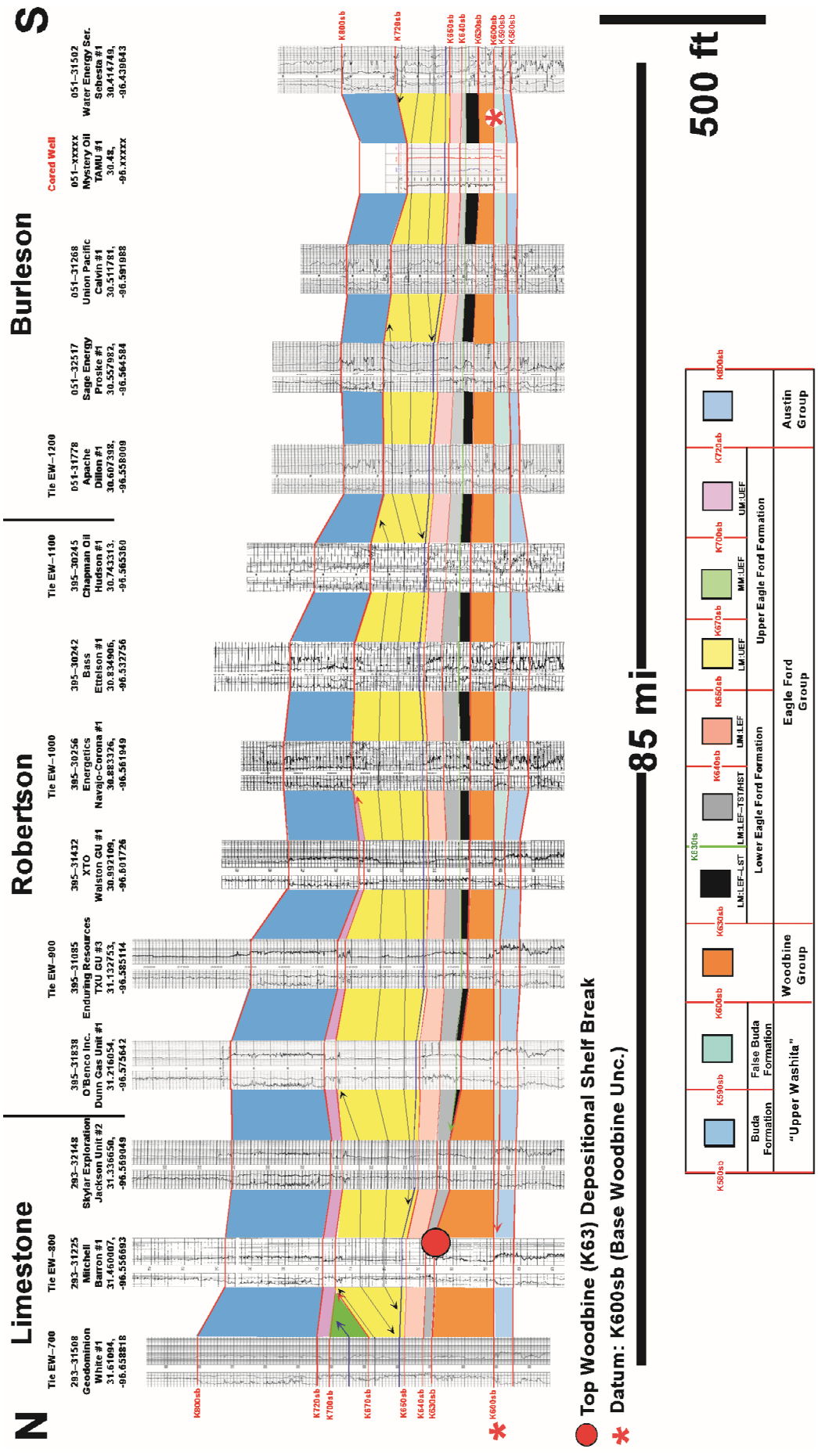


Figure 15. Regional cross-section NS-400 from Limestone County (N) to southern Burleson County (S) datumed on the K600sbm. On this line, the K600sb truncates the False Buda Formation to the north, (2) the Woodbine Group thins outboard of the interpreted K630 depositional shelf break (red dot) to the south, and (3) the K630 lowstand systems tract (black) overlies the K630sb toward the K630 depositional shelf break to the north. Please note the location of the cored industry well near the end of the line. Click [here](#) for a high-resolution, large-format version of this image.

classic “Eaglebine” succession is the southern East Texas Basin can geochemically and petrophysically be divided into four distinct units, or depositional sequences, and that these sequences represent from the base up, the False Buda Formation (unit 1), the Pepper Mudstone of the Woodbine Group (unit 2), LEF (unit 3), and UEF (unit 4). Most importantly, however, this core (Fig. 9) documents that Ca- and TOC-rich, high-resistivity LEF mudstones overlie low-resistivity, Ca- and TOC-poor, as well as Al-, Si-, and Ti-rich, mudstones of the Pepper Shale/Woodbine Group (below), and are overlain by similar low-resistivity, Ca- and TOC-poor, as well as Al-, Si-, and Ti-rich, mudstones of the LM:UEF (above).

Southern East Texas Basin

Regional cross-section EW-1200 (Fig. 8) traverses from Burleson County to the west to Grimes County to the east, a distance of approximately 45 mi (72 km). It is datumed on the K600sb at the base of the Woodbine Group (Fig. 16). This cross-section ties with cross-sections NS-400 (Fig. 15) in eastern Burleson County, and NS-500 (Fig. 17) in western Grimes County. The tie well with NS-500 (Fig. 15) is also the Type well (Casco #1 Sanders) for the southern East Texas Basin (Fig. 5).

On this line, the Georgetown Formation, Grayson Formation, Buda Formation, False Buda Formation, Pepper Shale (Woodbine Group), and LEF remain fairly uniform in thickness across the line (Fig. 16). In sharp contrast (Fig. 16), the LM:UEF (yellow), thins to the west likely by a combination of interpreted depositional pinch-out and/or truncation beneath the K720sb (base Austin unconformity). The overlying Austin Group, thins across the central portion of this line, due to interpreted incision by the K800sb at the base of the overlying Taylor Group (Fig. 16). The overlying Taylor Group (tan) displays a reciprocal thickness variations to the underlying Austin Group, with interpreted basal onlap onto the inherited topography at the top of the underlying Austin Group (Fig. 16).

In summary, EW-900 (Fig. 16) illustrates how the correlations on various regional well-log cross-sections (Figs. 12–17); tie to the type well in Grimes County (Fig. 5), based on the ties to the industry core in Burleson County (Fig. 9). Similar to the other lines, high-resistivity LEF mudstones, overlie low-resistivity mudstones of the Pepper Shale (Woodbine Group), and are overlain by low-resistivity mudstones of the LM:UEF.

Type Well: Southern East Texas Basin

As outlined on Figure 5, in previous studies, the classic high-resistivity zone within the “Lower Eaglebine” was either assigned to the Freestone delta of the Woodbine Group (Oliver, 1971; Turner and Conger, 1981, 1984), or the pre-Woodbine Maness Shale (Adams and Carr, 2010; Hentz et al., 2014; Denne et al., 2016); while the overlying low-resistivity “Eaglebine” mudstones were assigned to the Harris delta of the Woodbine Group.

Data from the GC-1 (Fig. 7), GC-2 (Fig. 11), and industry core (Fig. 9), as well the correlations on the various regional lines (Figs. 12–17), used in this study, however, reveal that “Lower Eaglebine” (Fig. 5) actually consists of three petrophysically an geochemically distinct depositional sequences, and that these sequences correlate from the base up to the: False Buda Formation (unit 1), Pepper Shale of the Woodbine Group (unit 2), and the LEF (unit 3). Furthermore, within this sequence stratigraphic framework, the low resistivity “Upper Eaglebine,” or classic “Harris delta,” actually correlates to the LM:UEF.

In summary, the bulk of the “Eaglebine” in the type well (Fig. 5) is actually the Eagle Ford Group, with the majority of the classic high-resistivity “Lower Eaglebine” equating to the LEF, not the Woodbine Group, or pre-Woodbine Maness Formation.

In the type well (Fig. 5), the Woodbine Group, is actually represented by a relatively thin, approximately 32 ft (9.8 m) thick, low-resistivity argillaceous mudstone, that represents distal basinal deposits of the Pepper Shale (Freestone delta). In the type well (Fig. 5), similar to the industry core in Burleson County (Fig. 9), high-resistivity LEF mudstones, which are interpreted to be rich in Ca and TOC, overlie low-resistivity mudstones of the Pepper Formation, which are interpreted to be poor in Ca and TOC, and are in turn overlain by low-resistivity mudstones of the LM:UEF, which are also interpreted to be poor in Ca and TOC.

Regional N–S Summary Line

NS-500 (Fig. 8) is a regional well-log cross-section which extends from Hunt County to the north to Grimes County, to the south, a distance of about 200 mi (322 km). This line nicely summarizes the stratal relationships for the Washita, Woodbine, Eagle Ford, Austin, and Taylor groups, across the long, north-south, axis of the East Texas Basin (Fig. 17).

On NS-500, the K600sb at the base of the Woodbine Group (Fig. 17) sequentially truncates the False Buda Formation, and then the underlying Buda Formation to the north. Thus on the northern end of the line (Fig. 17) the Woodbine Formation is unconformably juxtaposed on the Grayson Formation.

The overlying Woodbine Group (Fig. 17), thins incrementally to the south, due to angular discordance beneath the depositional shelf profile of the K630sb, at the base of the Eagle Ford Group, and then thins dramatically south of the interpreted depositional shelf break of the K630sb in northern Robertson County. Thus downdip of the interpreted K630 depositional shelf break, only mudstone-prone, basinal deposits of the Pepper Shale (Woodbine Group) are present (Fig. 17). Overlying the depositional basin profile of the K630sb in the southern part of the East Texas Basin (Fig. 17) is a distinctive high GR/resistivity (high TOC/Ca) zone at the base of the LEF (colored black). This unit (Fig. 17) onlaps to the north, downdip of the interpreted K630 shelf break, is interpreted as the lowstand system tract of the LM:LEF.

The K650sb, or base UEF unconformity, truncates the underlying LEF strata (gray) to the north in Hunt County (Fig. 17). The overlying LM:UEF (yellow) extends across the cross-section (Fig. 17). The regional correlation of the LM:UEF (yellow) illustrates that (1) the thick clastic depocenter present in the Dallas area, during the onset of the OAE2 in the latest Cenomanian, is coeval to the classic Harris delta in the southern East Texas Basin, (2) the classic top resistivity marker in the southern East Texas Basin is the K650sb at the base of the UEF, (3) stratal markers within the LM:UEF appear to downlap to the north, and (4) thickness variations in the LM:UEF in the northern portions of the East Texas Basin are due to truncation beneath the K670sb at the base of the MM:UEF (Fig. 17).

Both the MM:UEF (green) and UM:UEF (lavender) are restricted to the northern portions of the East Texas Basin (Fig. 17). The MM:UEF (green) thins and eventually truncated to the south beneath the K700sb at the base of the UM:UEF, while the UM:UEF is truncated to the south by the K720sb at the base Austin Group (Fig. 17). Thus in the southern portions of the East Texas Basin the Austin Group is unconformably juxtaposed on the LM:UEF, forming a toplap (sub-unconformity) play for UEF deltaic reservoirs in that part of the basin.

In summary, similar to other well-log cross-section (Figs. 12–16), unless the LEF is truncated by K650sb at the base of the UEF, across this line high-resistivity (Ca- and TOC-rich) LEF mudstones are encased between low-resistivity (Al-rich, but TOC- and Ca-poor) mudstones of the Woodbine Group (below) and the UEF (above).

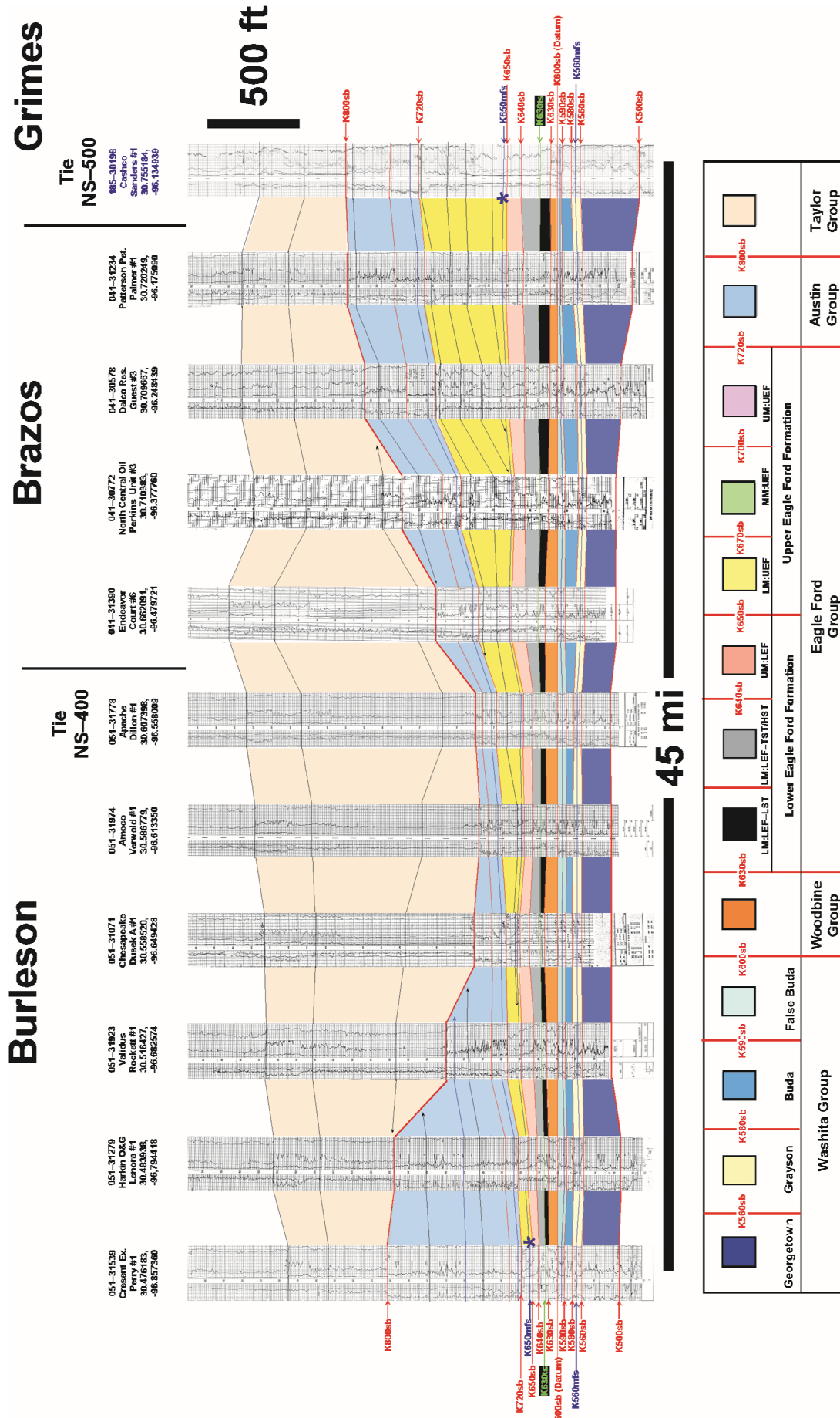


Figure 16. Western portion of well-log cross-section 880, which is datumed on the K600sb, the base of the Woodbine Group. This cross-section illustrates that the LEF (black, gray, red), overlies basal mudstones of the Woodbine Group (orange), and is overlain by the LM:UEF (yellow). Please note (1) scale bar, (2) thinning of the LM:UEF to the west due to depositional thinning and truncation beneath the K720, base Austin unconformity, (3) incision at the top of the Austin (light blue), by the K800sb, base Taylor unconformity, and (4) reciprocal thickness of overlying Taylor Group (tan). Click [here](#) for a high-resolution, large-format version of this image.

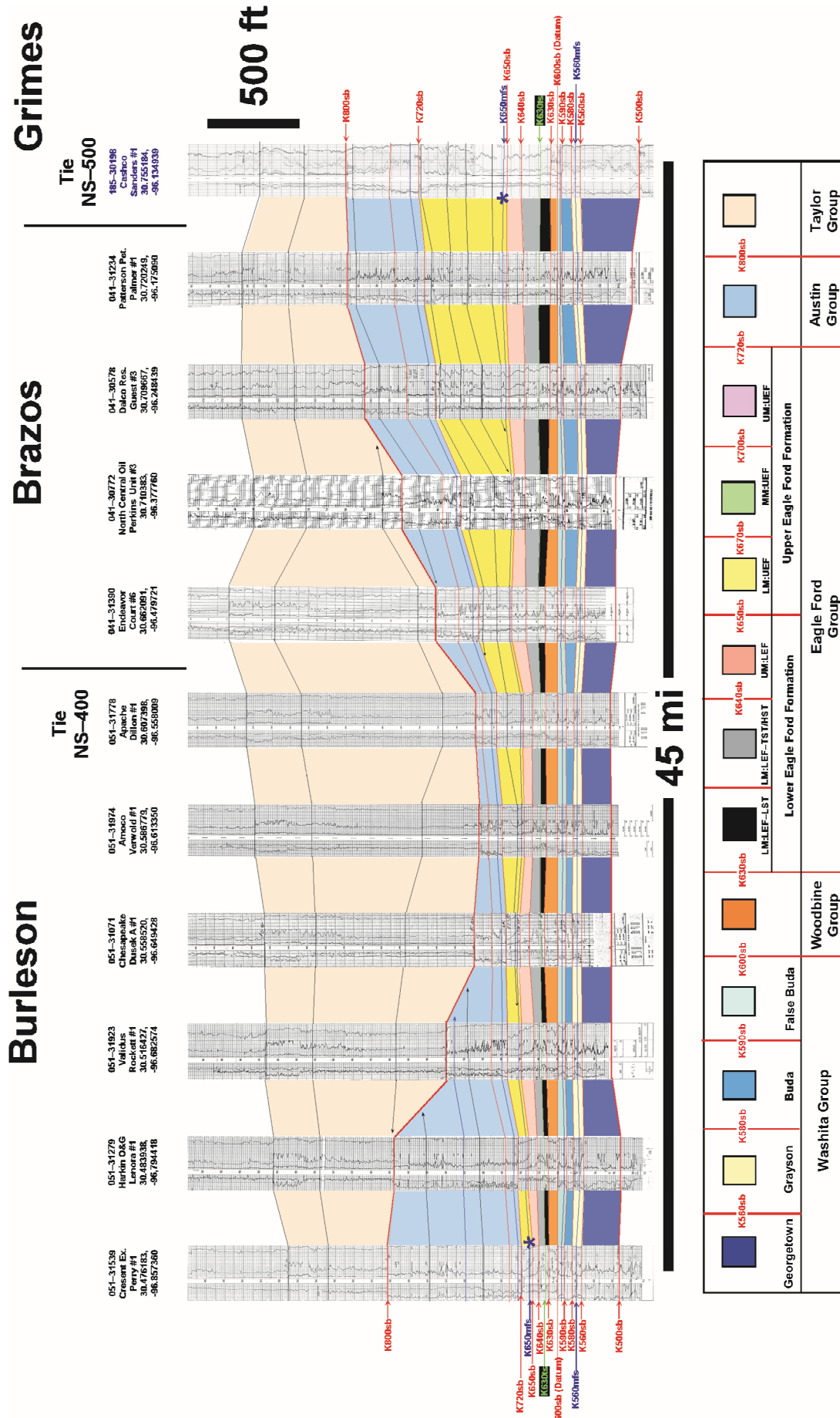


Figure 16. Western portion of well-log cross-section 880, which is datumed on the K600sb, the base of the Woodbine Group. This cross-section illustrates that the LEF (black, gray, red), overlies basal mudstones of the Woodbine Group (orange), and is overlain by the LM:UEF (yellow). Please note (1) scale bar, (2) thinning of the LM:UEF to the west due to depositional thinning and truncation beneath the K720, base Austin unconformity, (3) incision at the top of the Austin (light blue), by the K800sb, base Taylor unconformity, and (4) reciprocal thickness of overlying Taylor Group (tan). Click [here](#) for a high-resolution, large-format version of this image.

DISCUSSION

Overview

Based on the learnings from the GC-1 (Fig. 7), GC-2 (Fig. 11), the industry core (Fig. 9), as well as the regional well-log cross-sections presented (Figs. 12–17), the following generalizations can be made about the sequences and sequence boundaries identified in this study.

False Buda Formation (K590 Sequence)

In this study, the strata commonly referred to as the False Buda in the subsurface of the southern East Texas Basin (Hentz et al., 2014) is defined as the False Buda Formation, and interpreted as the K590 depositional sequence. While only the top 15 ft (4.6 m) of the False Buda Formation was present at the base of the industry in Burleson County (Fig. 9), the petrophysical characteristics of the basal contact of the False Buda Formation with the underlying Buda Formation, are nicely illustrated in the type well for the southern East Texas Basin (Fig. 5). In this well, the Buda/False Buda contact is marked by a distinct GR increase and resistivity decrease at the base of the False Buda Formation (Fig. 5). This contact is interpreted as the K590sb.

As outlined in the discussion of the industry core, the mudstones in the False Buda Formation are rich in Ca, but poor in Al, Si, Ti, and TOC (Fig. 9). Petrophysically, as illustrated on Figure 5, the GR profile within the False Buda Formation increases, and then decreases upward, whereas the resistivity decreases then increases upward (Fig. 5). The maximum-GR and minimum-resistivity values in this interval, is interpreted as the K590mfs.

Woodbine Group (K600 Composite Sequence)

An abrupt petrophysical and geochemical contact occurs at the base of the Woodbine Group. In the southern East Texas Basin this contact typically separates low-GR and high-resistivity mudstones of the False Buda Formation, which are rich in Ca, as well as poor in Al, Si, Ti, and TOC, from moderate-GR and low-resistivity mudstones of the Pepper Shale (Woodbine Group), which are poor in Ca and TOC, as well as rich in Al, Si, and Ti (Fig. 9). Regionally, however this contact, interpreted as K600sb (Fig. 17) sequentially truncates the underlying False Buda Formation, and then the Buda Formation, to the north and northwest. Thus in the northern and northwestern portions of the East Texas Basin (Fig. 17), the Woodbine Group is unconformably juxtaposed on the Grayson Formation.

Overall, the Woodbine Group (Fig. 17), thins incrementally to the south, due to angular discordance beneath the depositional shelf profile of the overlying K630sb, at the base of the Eagle Ford Group, and then thins dramatically, south of the interpreted depositional shelf break of the K630sb. Downdip of the interpreted K630 depositional shelf break, only mudstone-prone, basinal deposits of the Pepper Shale (Woodbine Group) are present (Figs. 17 and 18B).

LEF (K630 Composite Sequence)

Throughout the study area, an abrupt petrophysical and geochemical contact also occurs at the base of the LEF. Throughout the study area, this contact separates (1) moderate-GR and low-resistivity mudstones of the Woodbine Group, which are poor in TOC and Ca, as well as rich in Al, Si, and Ti (below), from (2) high-GR/resistivity mudstones of the LEF, which are rich in TOC and Ca, as well as poor in Al, Si, and Ti (above). Regionally, the Woodbine/Eagle Ford contact, interpreted as K630sb (1) incrementally truncates the upper portions of Woodbine Group to the south due to angular discordance beneath the depositional shelf profile of the K630sb and (2) displays Woodbine thinning, as well as reciprocal LEF thickening and onlap,

seaward of the interpreted K630 depositional shelf break (Fig. 17).

The LEF in the southern East Texas Basin is a high-GR/resistivity mudstone that is enriched in Ca and TOC (Figs. 5 and 8). Previous studies had incorrectly assigned these high-resistivity mudstones to the Pepper Formation of the Woodbine Group (Oliver, 1971; Turner and Conger, 1981, 1984), or to the Maness Shale (Adams and Carr, 2010; Hentz et al., 2014; Denne et al., 2016). Following the work of Donovan et al. (2015), the LEF in the East Texas Basin is divided into two sequences, an organic-rich, bentonite-free LM:UEF, and an organic- and bentonite-rich UM:LEF. The K640sb separates the two units. In the southern East Texas Basin, the LM:LEF can be divided into a lower zone, interpreted as a lowstand systems tract, which onlaps below the interpreted K630 depositional shelf break, and an upper zone, interpreted as transgressive to highstand deposits, which extends updip of the interpreted K630 depositional shelf break (Figs. 15 and 18C).

UEF (K650 Composite Sequence)

An abrupt petrophysical and geochemical contact also occurs at the base of the UEF across the study area. Typically, this contact separates (1) high-GR/resistivity mudstones of the LEF (below), which are rich in Ca and TOC, from (2) low-GR/resistivity mudstones of the LM:UEF (above), which are poor in Ca and TOC, as well as enriched in Al, Si, Ti, and $\delta^{13}\text{C}$. Regionally, this contact, interpreted as the K650sb, truncates the LEF to the north and east (Fig. 18C). Thus in the northern and eastern portions of the East Texas Basin (Fig. 18C), the LM:UEF is unconformably juxtaposed on the Woodbine Group.

The UEF consists of three unconformity-bounded depositional sequences, referred to as the LM:UEF, MM:UEF, and the UM:UEF, respectively. Whereas the lowermost LM:UEF extends across the study area, the MM:UEF and UM:UEF are restricted to the northern portions of the basin (Fig. 17), mainly due to truncation beneath the K720sb at the base of the Austin Group.

The LM:UEF is poor in Ca and TOC, as well as enriched in Al, Si, and Ti, and the main positive $\delta^{13}\text{C}$ excursion associated with the OAE2, which starts at the base, and ends at the top, of this unit (Figs. 7, 9, and 11). Regional correlation of the LM:UEF in this study revealed that (1) the classic top resistivity marker in the southern East Texas Basin is the K650sb and (2) the thick clastic depocenter present in the Dallas area, during the onset of the OAE2 in the latest Cenomanian, is coeval to the classic Harris delta in the southern East Texas Basin. Between Dallas and Waco, this unit thins from 230 ft (70 m) thick in the GC-2 (Fig. 11), to 10 ft (3 m) thick in the GC-1 (Fig. 7), due to truncation interpreted at the base of the K670sb at the base of the overlying MM:UEF (Fig. 13).

The K670sb at the base of the MM:UEF is denoted by a distinct geochemical, petrophysical, and biostratigraphic contact, that coincides with the base of the classic Arcadia Park Formation in the Dallas area (Fig. 11). This contact typically separates (1) Al-, Si-, Ti-, and TOC-poor mudstones of the LM:UEF (below), from (2) Ca- and TOC-enriched mudstones of the MM:UEF above. While a small part (zone III?) of the OAE2 may extend into the basal portions of the MM:UEF in the GC-2 (Fig. 11), the end of the most distinctive portion $\delta^{13}\text{C}$ excursion coincides with the placement of K670sb at the base of the MM:UEF.

Kennedy (1988) also interpreted an unconformity at this boundary in the Dallas outcrops based on missing ammonite zones across this contact (Fig. 11). Furthermore, as mentioned previously, thickness variations of the LM:UEF between Dallas and Waco (Fig. 13) are interpreted as due to truncation beneath this surface.

The MM:UEF is a Ca- and TOC-enriched interval with elevated resistivity, as well as GR. The petrophysical (high-resistivity) characteristics of this unit make it useful for differen-

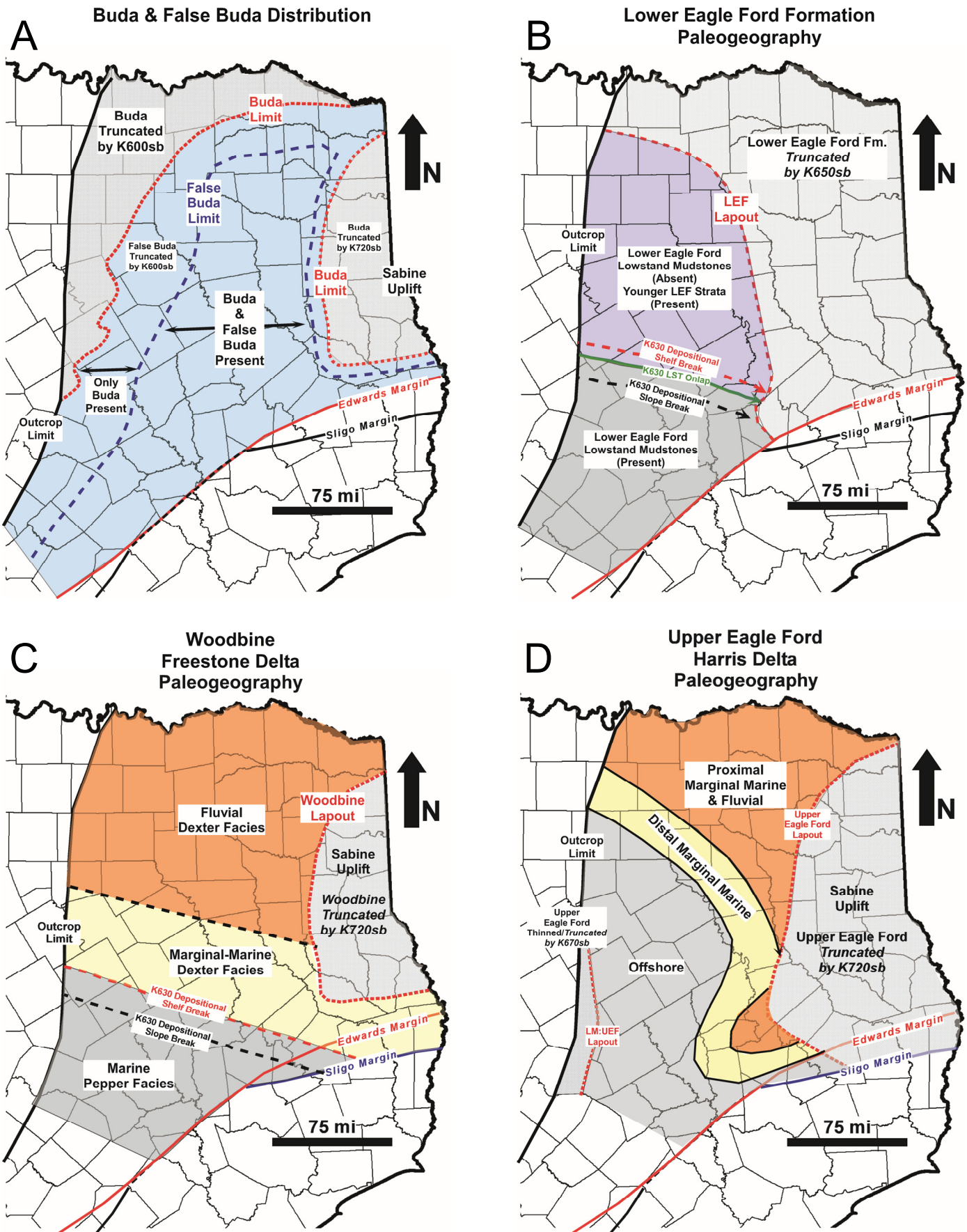


Figure 18. (A) Distribution map of the False Buda and Buda formations, (B) paleogeographic map of the Woodbine Group (Freestone delta), (C) paleogeographic map of the LEF, and (D) paleogeographic map of the LM:UEF (Harris delta).

tiating the MM:UEF from the underlying LM:UEF, as well as overlying UM:UEF, on individual wells (Figs. 10 and 11), as well as on regional well-log cross-sections.

Finally, the UM:UEF is a more Al- and Si-enriched, but TOC- and Ca-poor, mudstone-dominated succession, that overall has higher-GR and lower-resistivity values than the underlying MM:UEF (Figs. 7 and 11). The drop off in TOC, Ca, and resistivity values aids in the geochemical and petrophysical identification of the K700sb at the base of the UM:UEF (Figs. 7 and 11).

Paleogeographic Maps and Play Fairways

The distribution/paleogeographic maps of the Buda Formation, Woodbine Group, LEF, and LM:UEF (Figs. 18A–18D) provide a modern sequence stratigraphic framework to define the plays, and associated play fairways, for these units within the East Texas Basin.

The False Buda Formation (Fig. 18A) is geographically restricted to the central (deeper) portions of the East Texas Basin, while the older Buda Formation extends further towards the basin margins. Both units (Fig. 18A) are sequentially truncated to the (1) north and west by the K600sb at the base of the Woodbine Group and (2) east by the K720sb at the base of the Austin Group.

The Woodbine Group, as defined in this study (Fig. 18B), equates to the classic Freestone delta of Oliver (1971). The facies belts in this unit (Fig. 18B) trend northwest to southeast across the study area, but are truncated toward the Sabine Uplift to the east due to erosion beneath the K720sb at the base of the Austin Group. Interestingly, while the Sabine Uplift controls the present (post-depositional) distribution of the Woodbine Group, the facies patterns within it suggest that the Sabine Uplift had little impact on Woodbine paleogeography during deposition. Overall the updated paleogeographic map of the Woodbine Group (Fig. 18B) outlines the downdip play fairway limits for conventional, as well as unconventional, nonmarine and marginal marine, plays for this unit.

Figure 18C is a distribution map for the LEF. This map reveals that the LEF (Fig. 18C) is absent to the north and east in the East Texas Basin, due to post-depositional truncation by the K650sb at the base of the UEF. Thus the present distribution of LEF source rocks are aerially limited to western portions of the East Texas Basin (Fig. 18C). In terms of the unconventional source rock plays within the LEF, the TOC- and Ca-rich K630 lowstand deposits (dark gray) have an even more limited geographic distribution being restricted to the southwest portions of the East Texas Basin outboard (south) of the interpreted K630 depositional shelf break, and west of its erosional limit, dictated by truncation beneath the K650sb at the base of the UEF (Fig. 18C). Similar to the underlying Woodbine Group, the trend of the K630 depositional shelf break, as well as the distribution of the K630 lowstand (gray) suggests Sabine Uplift had little impact on Woodbine paleogeography during deposition.

Figure 18D illustrates the facies belts within the LM:UEF, which represents strata coeval to the classic Harris delta (Oliver, 1971; Turner and Conger, 1981, 1984). The map highlights the distribution for the sandstone-prone strata for this unit, and thus the associated unconventional and unconventional play fairways (Fig. 18D). This updated paleogeographic map indicates that sandstone-prone strata coeval to the Harris delta are far more extensive than previously mapped (Oliver, 1971; Turner and Conger, 1981, 1984). Of particular importance are potential top- and downdip facies change regions (yellow), which could be potential new tight rock plays or reservoirs utilized for CO₂ storage.

Finally, the paleogeographic map for the LM:UEF (Fig. 18D) illustrates a more bowing of the facies belts to the east, compared to older Woodbine Freestone delta (Fig. 18B). Thus

the facies belts within the LM:UEF suggest that the Sabine Uplift was active prior to, as well as during, deposition of the LM:UEF. This interpretation is also supported by the distribution of the LEF, which is truncated by the K650sb at the base of the UEF, across the Sabine Uplift (Fig. 18C).

OAE2 Learnings

Based on $\delta^{13}\text{C}$ data from the GC-2 core, and ammonite work on the adjacent outcrops by Kennedy (1988), it appears that the LM:UEF was deposited fairly rapidly, during a narrow few hundred-thousand-year window during the onset of the OAE2 (Fig. 11). In the East Texas Basin, the onset of the OAE2 coincides with a tectonically enhanced unconformity (K650sb), overlain by a major regional flooding surface (K650mfs), which in turn is overlain by a highstand denoted by major siliciclastic input. These East Texas Basin learnings may provide insights to evaluate sea-level variations, as well as siliciclastic input, during the onset of the OAE2, in other regions as well.

The biostratigraphic work by Kennedy (1988) in the Dallas area (Fig. 11) and the identification of the K670sb in this study indicate that a major angular unconformity exists near the end of the OAE2 in the East Texas Basin. This unconformity truncates the underlying LM:UEF from Dallas to Austin (Fig. 13), and explaining why the thickness of the LM:UEF, and the associated positive $\delta^{13}\text{C}$ excursion, varies from 230 ft (70 m) thick in the GC-2 (Fig. 11) in the Dallas area, to 10 ft (3 m) thick in the GC-1 (Fig. 7) in the Waco area. Thus one of the main learnings from the East Texas Basin in terms of the OAE2 is that (1) the OAE2 may not be a conformable succession and (2) the distribution, thickness, and duration of the positive $\delta^{13}\text{C}$ excursion associated with the OAE2 may related to unconformities.

CONCLUSIONS

Three distinctly different paradigms presently exist for the stratigraphic assignment of the “Eaglebine” succession in the southern East Texas Basin (Fig. 5). The first paradigm (Fig. 5) assigns the entire “Eaglebine” succession to Woodbine Group (Oliver, 1971; Turner and Conger, 1981, 1984; Berg, 1986). The second paradigm (Adams and Carr, 2010; Hentz et al., 2014; Denne et al., 2016) assigns the basal “high-resistivity” mudstone of the “Lower Eaglebine” to the Maness Shale, and the overlying “Upper Eaglebine” low-resistivity mudstones to the Pepper Shale of Woodbine Group (Fig. 5). The third paradigm (Meyer et al., 2021) assigns the bulk of the “high-resistivity” “Lower Eaglebine” (unit 3) to the LEF, and the “low-resistivity” “Upper Eaglebine” (unit 4) to the UEF (Fig. 5). Within this third paradigm a thin <50 ft (15 m) thick, low-resistivity mudstone (unit 2) within the “Lower Eaglebine” is interpreted as distal Al-, Si-, and Ti-rich basinal deposits of the Woodbine Group.

Using a grid of regional well-log cross-sections, tied to the outcrop belt, and incorporating geochemical and petrophysical data from two USGS, and one industry core, a regional sequence stratigraphic framework for the Woodbine and Eagle Ford groups was defined and correlated across the East Texas Basin for the first time. This framework, when carried into the southern East Texas Basin, supports the interpretation proposed by Meyer et al. (2021).

The classic “Eaglebine” succession in the southern East Texas Basin can be divided using petrophysical, geochemical, and sequence stratigraphic methods, into four units or sequences, which from the base up equate to the False Buda Formation (sequence 1), the Pepper Shale of Woodbine Group (sequence 2), the LEF (sequence 3), and UEF (unit 2). Based on this sequence stratigraphic framework, the actual “high-resistivity (Ca- and TOC-rich) mudstones (sequence 3), within the “Lower Eaglebine” are not the Maness Shale of the Washita Group, or the Pepper Shale of the Woodbine Group, but the LEF.

Throughout the study area, unless the LEF is truncated by the K650sb at the base of the LM:UEF, high-resistivity (Ca- and TOC-rich) LEF strata, unconformably overlie low-resistivity (Ca- and TOC-poor) mudstones of the Woodbine Group, and are in turn unconformably overlain by low resistivity (Ca- and TOC-poor) mudstones of the LM:UEF.

Within the East Texas Basin, the Woodbine Group thins incrementally from north to south due to angular discordance beneath the depositional shelf profile of the K630sb, at the base of the Eagle Ford Group, and then thins dramatically south of the interpreted depositional shelf break of the K630sb. Thus downdip of the interpreted K630 depositional shelf break, only mudstone-prone, basinal deposits of the Pepper Shale (Woodbine Group) are present. Overlying the depositional basin profile of the K630sb in the southern part of the East Texas Basin are distinctive high-GR/resistivity (high-TOC/Ca) mudstones at the base of the LEF. These strata onlap to the north, downdip of the interpreted K630 shelf break, and are interpreted as the lowstand system tract of the LM:LEF.

Regional sequence stratigraphic correlations in this study revealed that the classic top “low-resistivity marker” in the southern East Texas Basin coincides with the K650sb at the base of the LEF. Thus the overlying low resistivity “Upper Eaglebine” mudstones in the southern East Texas Basin, traditionally assigned to the “Harris delta,” are actually the LM:UEF. Within this framework, the clastic depocenter identified in the Dallas area at the onset of the OAE2 in this study, is coeval with the classic “Harris delta” in the southern East Texas Basin.

Paleogeographic maps of the Woodbine Group and LEF, strongly suggest that the Sabine Uplift was not active during Woodbine and LEF times. However, the post depositional erosional patterns of the LEF in the East Texas Basin, along with the facies patterns within the LM:UEF in the East Texas Basin strongly suggest that the Sabine Uplift was active during the formation of the K650sb at the base of the UEF, as well as during the deposition of the LM:UEF.

In the East Texas Basin, the onset of the OAE2 coincides with an unconformity (K650sb), overlain by a major regional flooding surface (K650mfs), which in turn is overlain by a highstand denoted by major siliciclastic input. These East Texas Basin findings may provide insights to evaluate sea-level variations, as well as siliciclastic input, during the onset of the OAE2, in other regions.

Finally, the end of the main positive $\delta^{13}\text{C}$ excursion in the East Texas Basin coincides with a major angular unconformity (K670sb) that thins and eventually truncates the LM:UEF between Dallas and Austin. Thus key learnings from the East Texas Basin, in terms of the OAE2, are that (1) the OAE2 may have internal hiatuses, and not be a conformable succession and (2) the distribution, thickness, and duration of the positive $\delta^{13}\text{C}$ excursion associated with the OAE2 may be related to unconformities.

ACKNOWLEDGMENTS

This paper summarizes completed theses (Meyer, 2018; Gifford, 2021; Evans, 2022), as well as work in progress (Johnson; Dangtran), of research conducted by the Unconventional Reservoirs Outcrop Characterization (UROC) Consortium Research Group at TAMU. The goal of this group is to conduct state-of-the-art sequence stratigraphic studies in order to define plays and play fairways within a chronostratigraphic framework, in order to better explain and predict the distribution, thickness variations, and sweet spots for conventional and unconventional plays within the Woodbine and Eagle Ford groups within the East Texas Basin. More detailed maps of the various facies and plays within these units can be found in the various theses.

The authors would like to thank the USGS Gulf Coast Assessment Team, as well as Apache Corporation, for access to their core, geophysical, and geochemical data, for the wells used

in this study. Over the years, UROC consortium members including Chevron, University Lands, Shell, Exxon Mobil, EOG, Oasis, and Conoco Phillips supported this research. Student research scholarships from HGS and SIPES also supported individual student research.

REFERENCES CITED

- Adams, R. L., and J. P. Carr, 2010, Regional depositional systems of the Woodbine, Eagle Ford, and Tuscaloosa of the U.S. Gulf Coast: Gulf Coast Association of Geological Societies Transactions, v. 60, p. 3–27.
- Adkins, W. S., 1932, The Mesozoic systems in Texas, in E. H. Sellards, W. S. Adkins, and F. B. Plummer, eds., The geology of Texas: University of Texas Bulletin 3232, p. 239–518.
- Adkins, W. S., and F. E. Lozo, 1951, Stratigraphy of the Woodbine and Eagle Ford, Waco area, Texas, in F. E. Lozo, ed., The Woodbine and adjacent strata of the Waco area of Central Texas, a symposium for the 1951 field trip sponsored by the East Texas Geological Society: Southern Methodist University Press Fondren Science Series 2, p. 101–163.
- Algeo, T. J., and H. Rowe, 2012, Paleoceanographic applications of trace-meta concentration data: Chemical Geology, v. 224/225, p. 6–18.
- Banner, J. L., 1995, Application of the trace-element and isotope geochemistry of strontium to studies of carbonate diagenesis. Sedimentology, v. 42, p. 805–824.
- Bailey, T. L., F. G. Evans, and W. S. Adkins, 1945, Revision of stratigraphy of part of Cretaceous in Tyler Basin, northeast Texas: American Association of Petroleum Geologists Bulletin, v. 29, p. 170–166.
- Berg, R. R., 1986, Reservoir sandstones: Prentice-Hall, Inc., 480 p.
- Brown, C. W., and R. L. Pierce, 1962, Palynologic correlations in Cretaceous Eagle Ford Group, northeast Texas: American Association of Petroleum Geologists Bulletin, v. 46, p. 2133–2147.
- Brumsack, H. J., 2006, The trace metal content of recent organic carbon-rich sediments: Implications for Cretaceous black shale formation: Palaeogeography, Palaeoclimatology, Palaeoecology, v. 232, p. 334–361.
- Calvert, S. E., and T. F. Pedersen, 1993, Geochemistry of Recent oxic and anoxic marine sediments: Implications for the geological record, in R. J. Parkes, P. Westbroek and J. W. de Leeuw, eds., Marine sediments, burial, pore water chemistry, microbiology and diagenesis: Marine Geology, v. 113, p. 67–88.
- Campbell, C. V., 1967, Lamina, laminaset, and bedset: Sedimentology, v. 8, p. 7–26.
- Cobban, W. A., and G. R. Scott, 1972, Stratigraphy and ammonite fauna of the Graneros Shale and Greenhorn Limestone near Pueblo, Colorado: U.S. Geological Survey Professional Paper 645, 108 p.
- Cobban, W. A., 1985, Ammonite record from Bridge Creek Member of Greenhorn Limestone at Pueblo Reservoir State Recreation Area, Colorado, in L. M. Pratt, E. G. Kauffman, and F. B. Zelt, eds., Fine-grained deposits and biofacies of the Cretaceous Western Interior Seaway: Evidence of cyclic sedimentary processes: Society of Economic Paleontologists and Mineralogists Field Trip Guidebook 4, p. 135–138.
- Cobban, W. A., 1993, Diversity and distribution of Late Cretaceous ammonites, Western Interior, United States, in W. G. E. Caldwell and E. G. Kauffman, eds., Evolution of the Western Interior Basin: Geological Association of Canada Special Paper 39, p. 435–451.
- Denne, R., J. Breyer, A. Callender, R. Hinote, M. Karimnia, T. Kosanke, Z. Kita, J. Lees, H. Rowe, J. Spaw, and N. Tur, 2016, Biostratigraphic and geochemical constraints on the stratigraphy and depositional environments of the Eagle Ford and Woodbine groups of Texas, in J. A. Breyer, ed., The Eagle Ford Shale: A renaissance in U.S. oil production: American Association of Petroleum Geologists Memoir 110, p. 1–86.
- Donovan, A. D., T. S. Staerker, A. Pramudito, W. Li, M. J. Corbett, C. M. Lowery, A. M. Romero, and R. D. Gardner, 2012, The Eagle Ford outcrops of West Texas: A laboratory for under-

- standing heterogeneities within unconventional mudstone reservoirs: Gulf Coast Association of Geological Societies Journal, v.1, p. 162–185.
- Donovan, A. D., R. D. Gardner, A. Pramudito, T. S. Staerker, M. P. Wehner, M. J. Corbett, J. J. Lundquist, A. M. Romero, L. C. Henry, J. R. Rotzien, and K. S. Boling, 2015, Chronostratigraphic relationships of the Woodbine and Eagle Ford groups across Texas: Gulf Coast Association of Geological Societies Journal, v. 4, p.67–87.
- Donovan, A. D., T. S. Staerker, R. Gardner, M. C. Pope, A. Pramudito, and M. Wehner, 2016, Chapter 9: Findings from the Eagle Ford outcrops of West Texas and implications to the subsurface of South Texas, in J. A. Breyer, ed., The Eagle Ford Shale: A renaissance in U.S. oil production: American Association of Petroleum Geologists Memoir 110, p. 301–336.
- Donovan, A. D., S. Gifford, A. Pramudito, M. Meyer, M. C. Pope, and S. Paxton, 2019, Unraveling the secrets of the Eaglebine: American Association of Petroleum Geologists/Society of Exploration Geophysicists Second International Meeting for Applied Geoscience and Energy, p. 836–849.
- Evans, L. N., 2022, Sequence stratigraphy of the middle Cretaceous Woodbine and Eagle Ford groups in the northwest East Texas Basin: M.S. Thesis, Texas A&M University, 57 p.
- Freeman, V. L., 1968, Geology of the Comstock–Indian Wells area, Val Verde, Terrell, and Brewster counties, Texas: U.S. Geological Survey Professional Paper 694-K, 26 p.
- Forkner, R. M., J. Dahl, A. Fildani, S. M. Barbanti, L. A. Yurchenko, and J. M. Moldowan, 2021, Anatomy of an extinction revealed by molecular fossils spanning OAE2: Scientific Reports, v. 11, Article 13621.
- Gifford, S., 2021, The sequence stratigraphy of the Woodbine and Eagle Ford groups in the East Texas Basin (USA): A new chronostratigraphic framework to properly identify and map their associated plays and play fairways: M.S. Thesis, Texas A&M University, 117 p.
- Griffith, E., and A. Paytan, 2012, Barite in the ocean—Occurrence, geochemistry and palaeoceanographic applications: Sedimentology, v. 59, p. 1817–1835.
- Halbouty, M. T., 1991, East Texas Field, U.S.A., in N. H. Foster and E. A. Beaumont, eds., Stratigraphic traps II: American Association of Petroleum Geologists Special Publication 24, p. 189–206.
- Hentz, T. F., W. A. Ambrose, and D. C. Smith, 2014, Eaglebine play of the southwestern East Texas Basin: Stratigraphic and depositional framework of the Upper Cretaceous (Cenomanian–Turonian) Woodbine and Eagle Ford groups: American Association of Petroleum Geologists Bulletin, v. 98, p. 2551–2580.
- Hill, R. T., 1887, The topography and geology of the Cross Timbers and surrounding regions in North Texas: American Journal of Science, v. 3, no. 33, p. 291–303.
- Hill, R. T., 1902, Geography and geology of the Black and Grand prairies, Texas: U.S. Geological Survey Annual Report 21, pt. 7, 666p
- Jackson, M. P. A., and S. J. Seni, 1983, Geometry and evolution of salt structures in a marginal rift basin of the Gulf of Mexico, East Texas: Geology, v. 11, p. 131–135.
- Jackson, M. L., and S. E. Laubach, 1991, Structural history and origin of the Sabine Arch, East Texas and northwest Louisiana: Bureau of Economic Geology Geological Circular 91–3, 47 p.
- Kaufman, E. G., 1995, Global change leading to biodiversity crisis in a greenhouse world: The Cenomanian–Turonian (Cretaceous) mass extinction, in S. M. Stanley and T. Usselman, eds., The effects of past global change on life: National Academy Press National Academy of Sciences Studies in Geophysics, p. 47–71.
- Kennedy, W. J., 1988, Late Cenomanian and Turonian ammonite faunas from north-east and Central Texas: The Palaeontological Association Special Papers in Palaeontology 19, 131 p.
- Kennedy, W. J., and W. A. Cobban, 1990, Cenomanian ammonite faunas from the Woodbine Formation and lower part of the Eagle Ford Group, Texas: Paleontology, v. 33, p. 75–154.
- Liguori, B., M. Almeida, and C. Rezende, 2016, Barium and its importance as an indicator of paleoproductivity: *Academia Brasileira De Ciências*, v. 88, p. 2093–2103.
- Lozo, F. E., 1951, Stratigraphic notes on the Maness (Comanche Cretaceous) Shale, in F. E. Lozo, ed., The Woodbine and adjacent strata of the Waco area of central Texas, a symposium for the 1951 field trip sponsored by the East Texas Geological Society: Southern Methodist University Press Fondren Science Series 2, p. 67–100.
- McCreary, M.E., 2022, Chemostratigraphic and sequence stratigraphic analysis of the Austin Group in the outcrops and subsurface of Texas: M.S. Thesis, Texas A&M University, 36 p.
- Meyer, M. J., A. D. Donovan, and M. C. Pope, 2021, Depositional environment and source rock quality of the Woodbine and Eagle Ford groups, southern East Texas (Brazos) Basin: An integrated geochemical, sequence stratigraphic, and petrographic approach: American Association of Petroleum Geologists Bulletin, v. 105, p. 809–843.
- Meyer, M. J., 2018, High-resolution chemostratigraphy of the Woodbine and Eagle Ford groups, Brazos Basin, Texas: M.S. Thesis, Texas A&M University, 68 p.
- Ogg, J., and L. A. Hinnov, 2012, Cretaceous, in J. G. Ogg et al., eds., Geologic time scale 2012: Elsevier, p. 793–853.
- Oliver, W. B., 1971, Depositional systems in the Woodbine Formation (Upper Cretaceous), northeast Texas: Bureau of Economic Geology Report of Investigations 73, 30 p.
- Pearce, M. A., I. Jarvis, B. A. Tocher, 2009, The Cenomanian–Turonian boundary event, OAE2 and palaeoenvironmental change in epicontinental seas: New insights from the dinocyst and geochemical record: Palaeogeography, Palaeoclimatology, Palaeoecology, v. 280, p. 207–234.
- Pearce, T., and I. Jarvis, 1992, Applications of geochemical data to modelling sediment dispersal patterns in distal turbidites—Late Quaternary of the Madeira abyssal plain: Journal of Sedimentary Petrology, v. 62, p. 1112–1129.
- Pratt, L. M. and C. N. Thelkeld, 1984, Stratigraphic significance of ¹³C/¹²C ratios in mid-Cretaceous rocks of the Western Interior of the U.S.A., in D. F. Sloll and D. J. Glass, eds., The Mesozoic of middle North America: Canadian Society of Petroleum Geologists Memoir 9, p. 305–312.
- Renard, M., 1979, *Aspect géochimique de la diagenèse des carbonates. Teneurs en strontium et en magnésium des carbonates: essai d'interprétation de l'inversion de la corrélation Sr/Mg observée dans les carbonates du domaine pélagique par rapport à ceux du domaine néritique: Bulletin de la Société Géologique de France*, Section 2, No. 4, p. 133–152.
- Sageman, B., and T. Lyons, 2004, Geochemistry of fine-grained sediments and sedimentary rocks, in F. Mackenzie, ed., Sediments, diagenesis, and sedimentary rock: Elsevier Treatise on Geochemistry 7, p. 115–158.
- Scholle, P., 1977, Chalk diagenesis and its relation to petroleum exploration—Oil from chalks, a modern miracle: American Association of Petroleum Geologists Bulletin, v. 61, p. 982–1009.
- Tribovillard, N., J. Thomas, T. Lyons, and R. Armelle, 2006, Trace metals as paleo-redox and paleo-productivity proxies—An update: Chemical Geology v. 232, p. 12–32.
- Turner, J. R., and S. J. Conger, 1981, Environment of deposition and reservoir properties of the Woodbine Sandstone at Kurten Field, Brazos County, Texas: Gulf Coast Association of Geological Societies Transactions, v. 31, p. 213–232.
- Turner, J. R., and S. J. Conger, 1984, Environment of deposition and reservoir properties of the Woodbine Sandstone at Kurten Field, Brazos Co., Texas, in R. W. Tillman and C. T. Siemers, eds., Siliciclastic shelf sediments: Society of Economic Paleontologists and Mineralogists Special Publication v.34, p. 215–249.
- Zabel, M., R. R. Schneider, T. Wagner, A. T. Adegbe, U. de Vries, and S. Kolonic, 2001, Late Quaternary climate changes in Central Africa as inferred from terrigenous input to the Niger Fan: Quaternary Research, v. 56, p. 207–217.
- Zelt, F. B., 1985, Paleooceanographic events and lithologic/geochemical facies of the Greenhorn Marine Cycle (Upper Cretaceous) examined using natural gamma-ray spectrometry, in L. M. Pratt, E. G. Kauffman, and F. B. Zelt, eds., Fine-grained deposits and biofacies of the Cretaceous Western Inter-

or Seaway: Evidence of cyclic sedimentary processes: Society of Economic Paleontologists and Mineralogists Fieldtrip Guidebook 4, p. 49–59.

Zuckerman, G., 2013, *The frackers*: Penguin Group, 404 p.

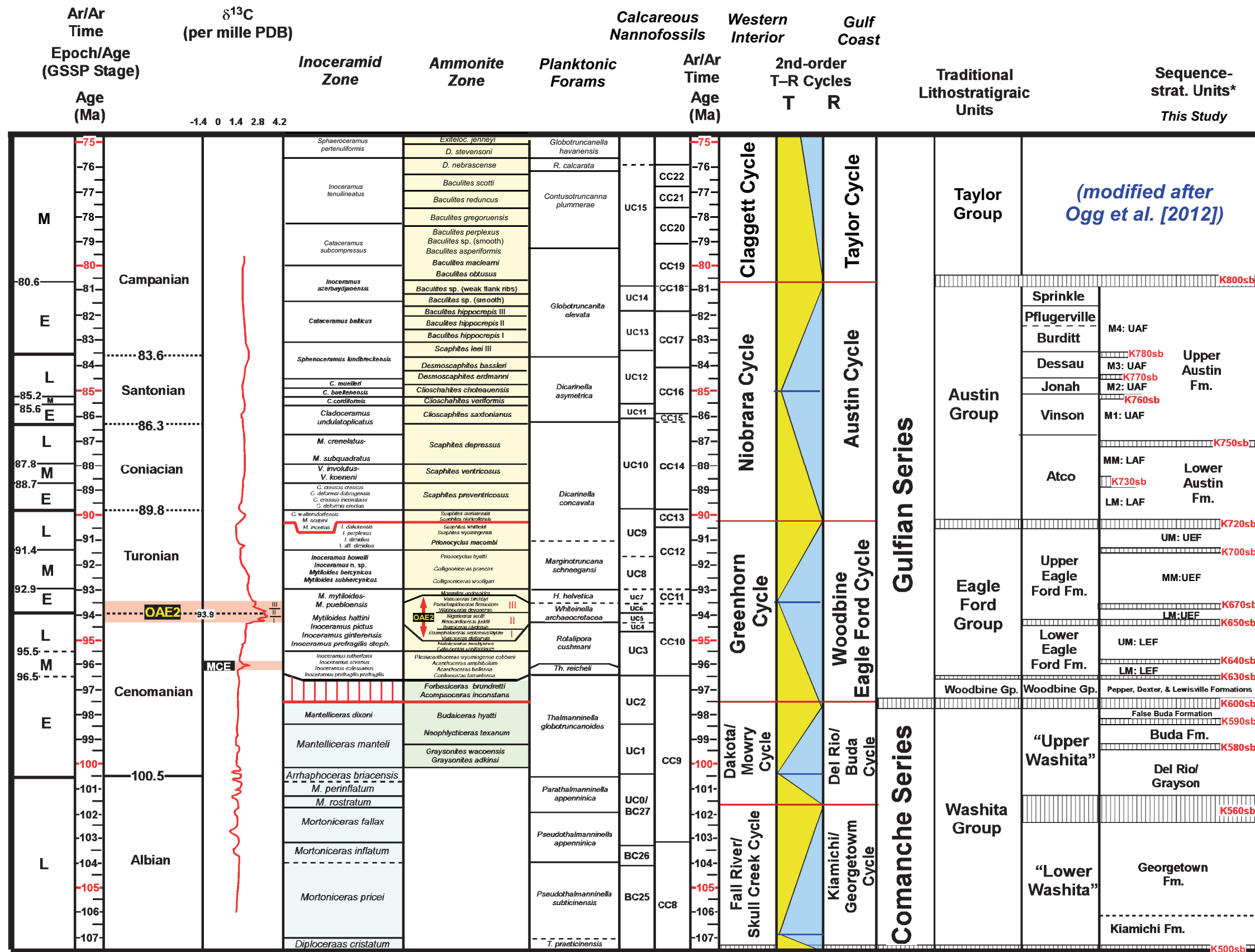


Figure 3

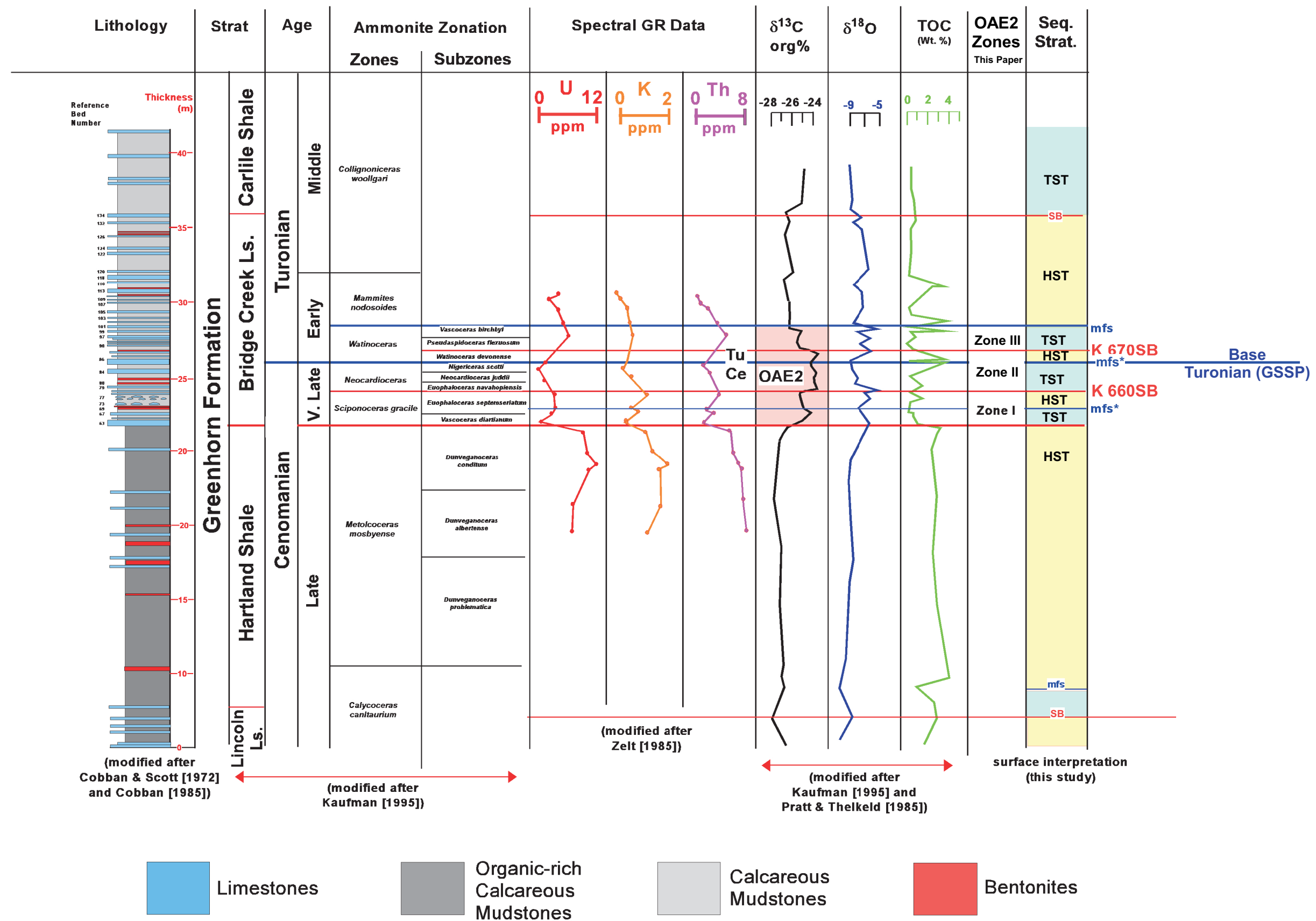


Figure 4

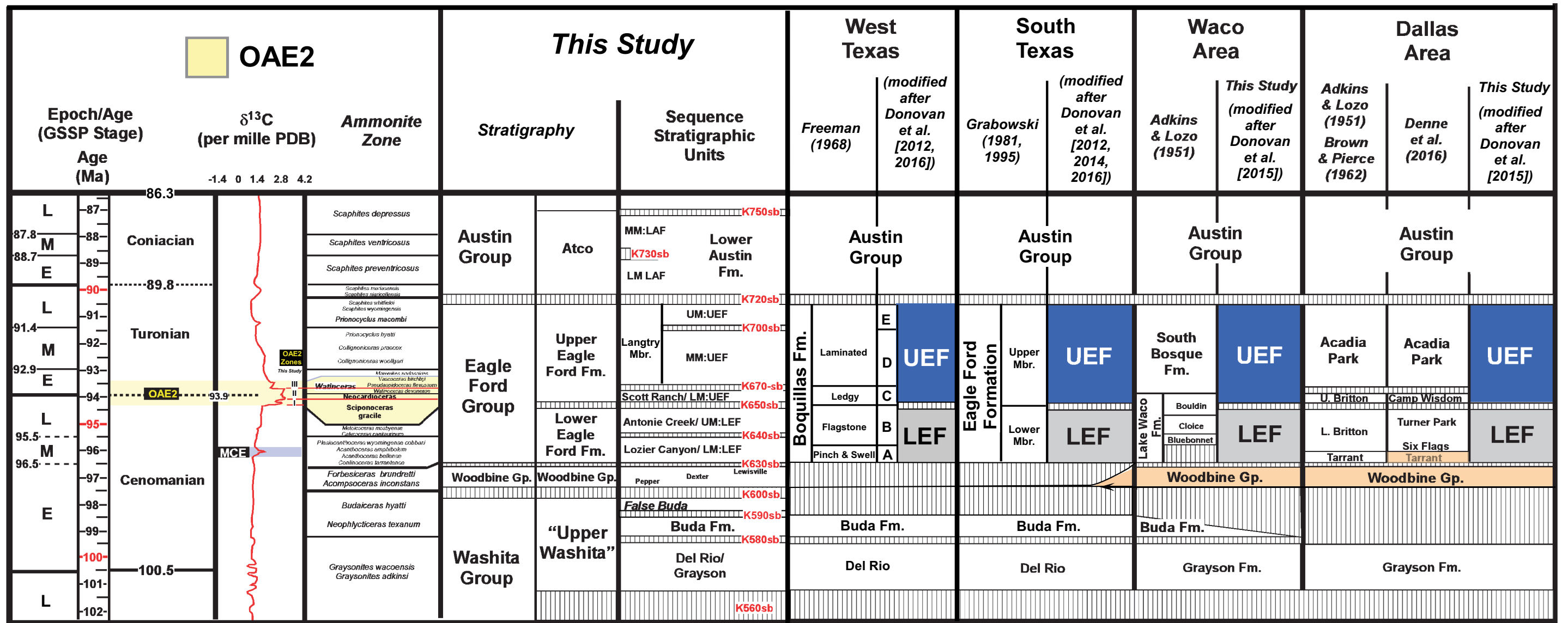


Figure 66

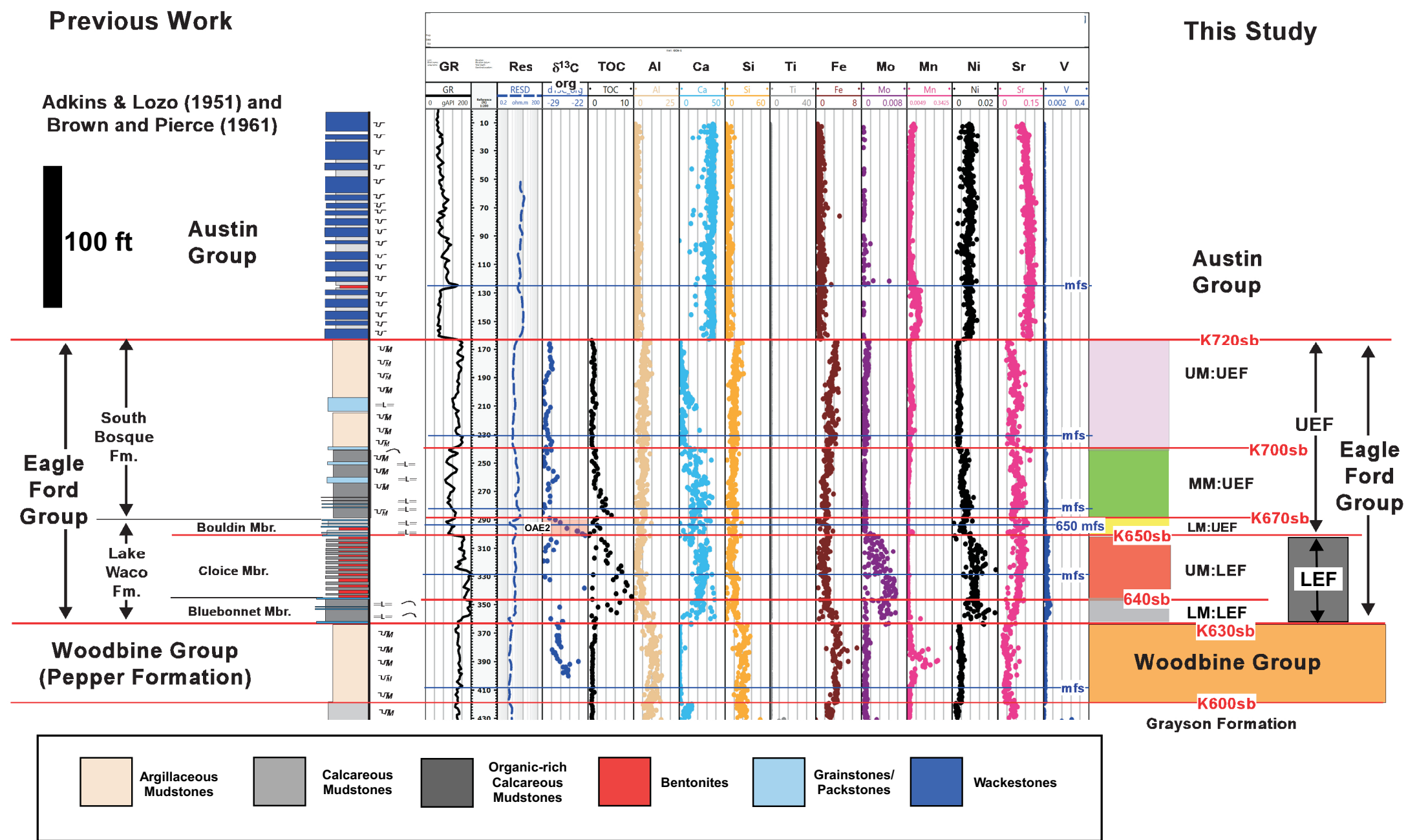


Figure 77

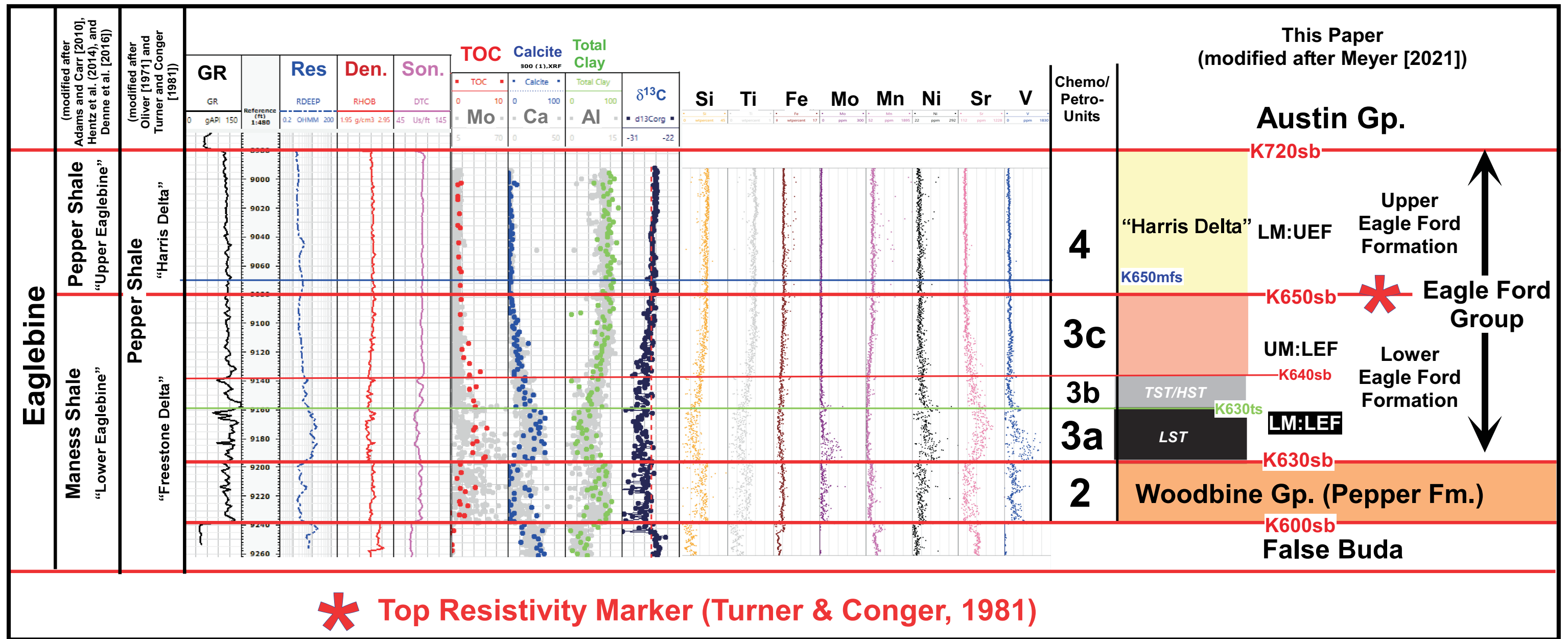


Figure 9

(modified after Foster [1965] and Adams & Carr [2010])

Dallas County
113-331005
J. L. Myers/Lacerie #1
32.875169/-96.816522

This Study

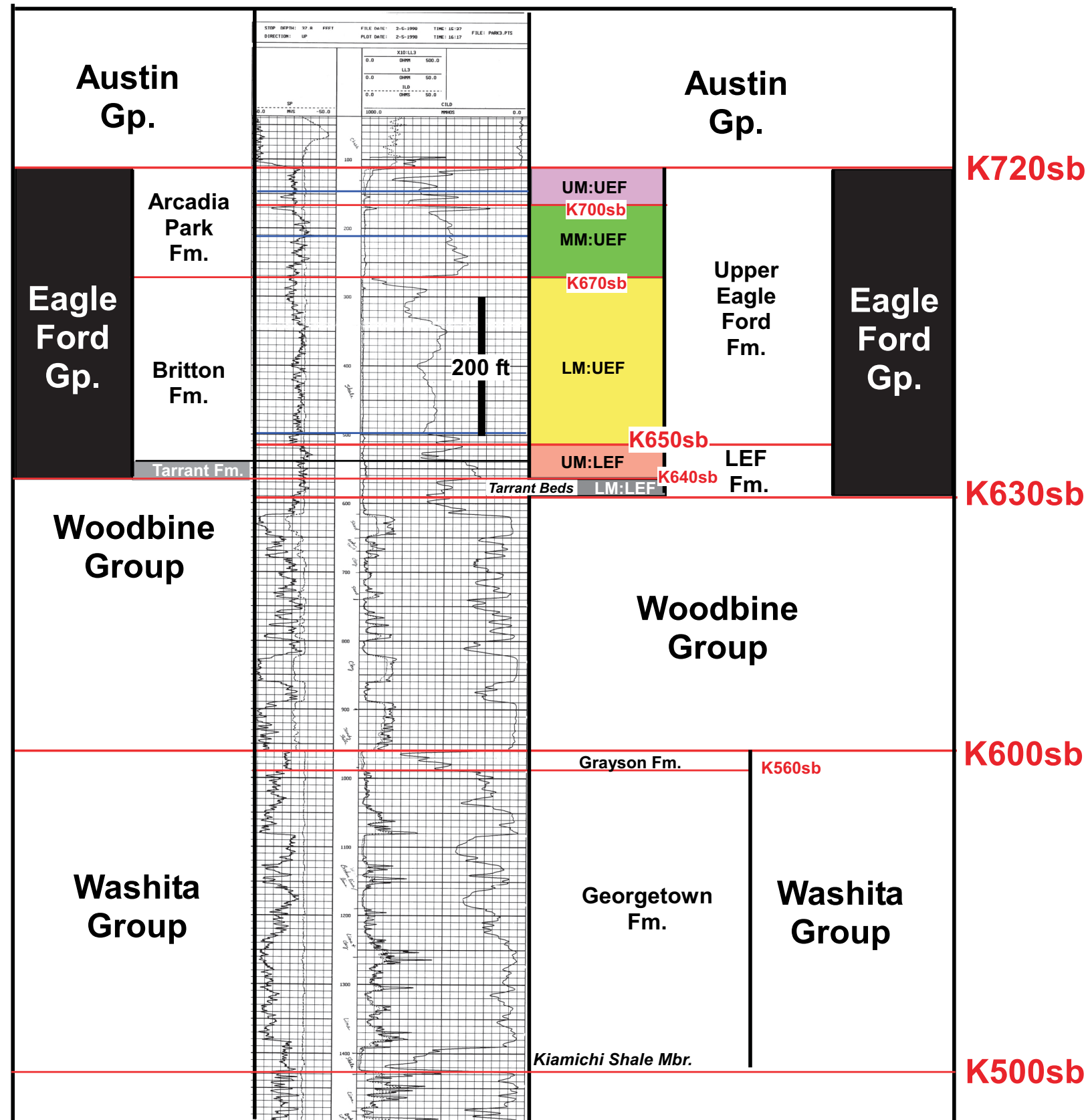
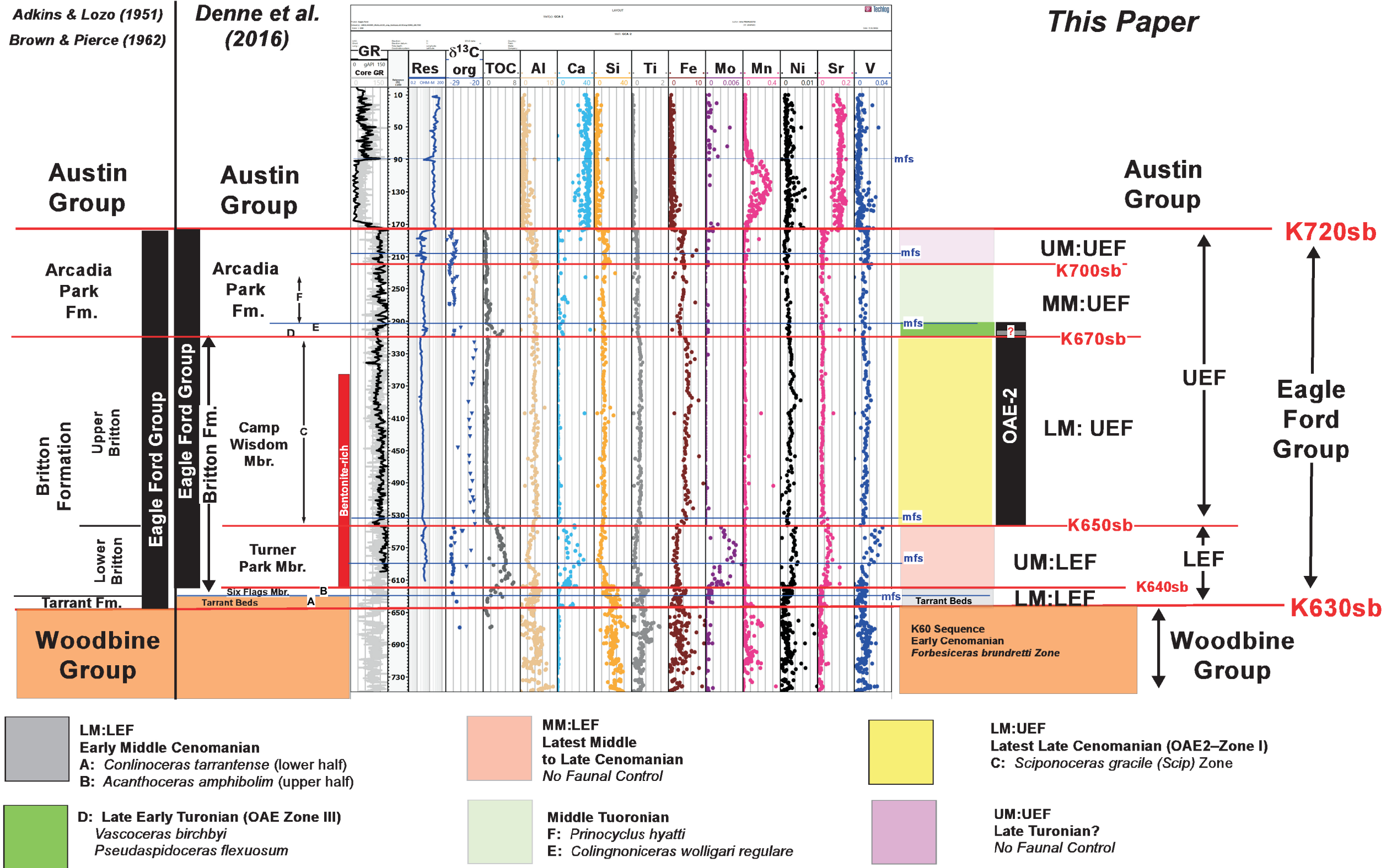


Figure 10



Ammonite biostratigraphy from adjacent outcrops (Kennedy, 1988)

Figure 11

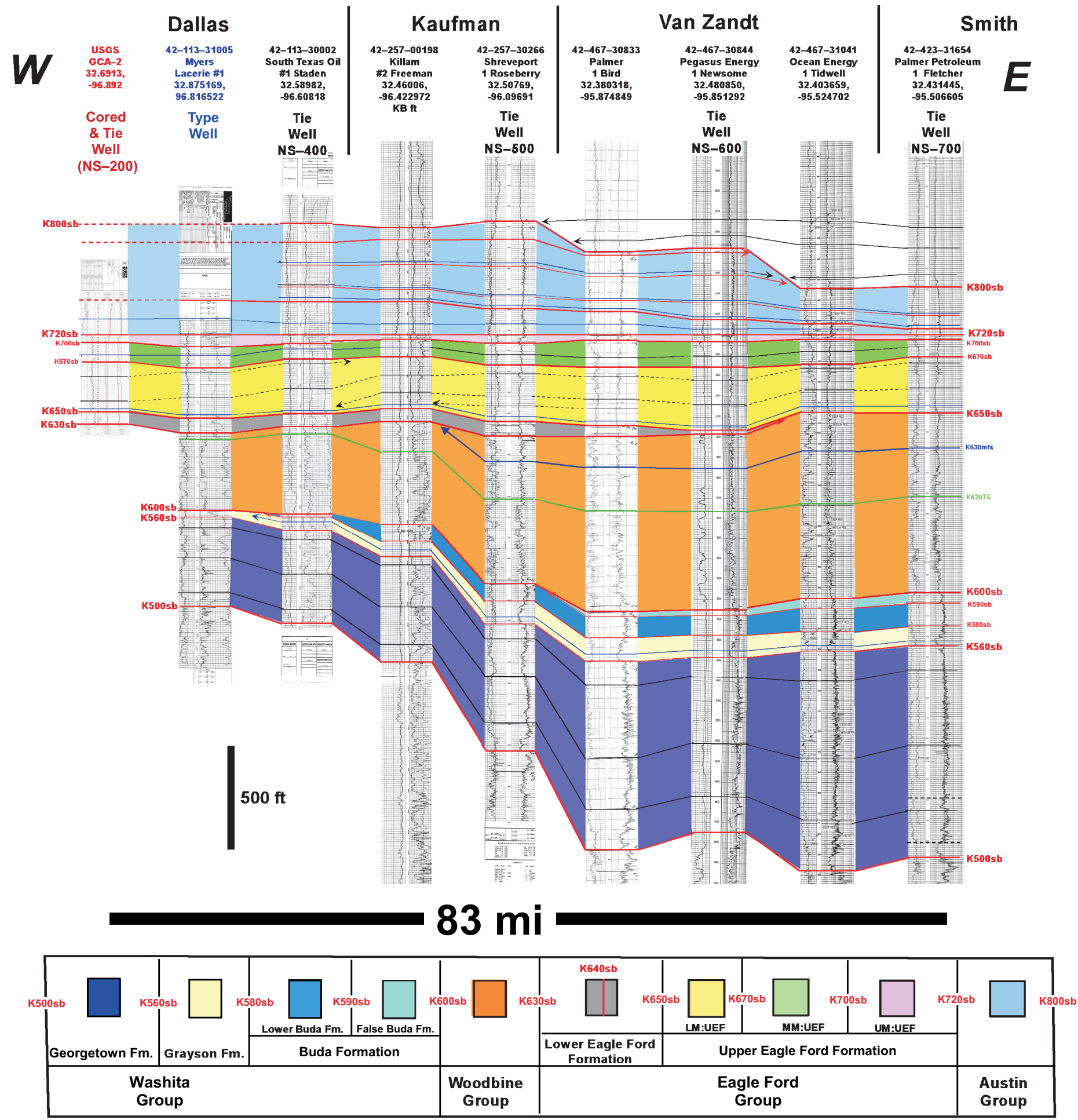


Figure 12

S 225 mi N

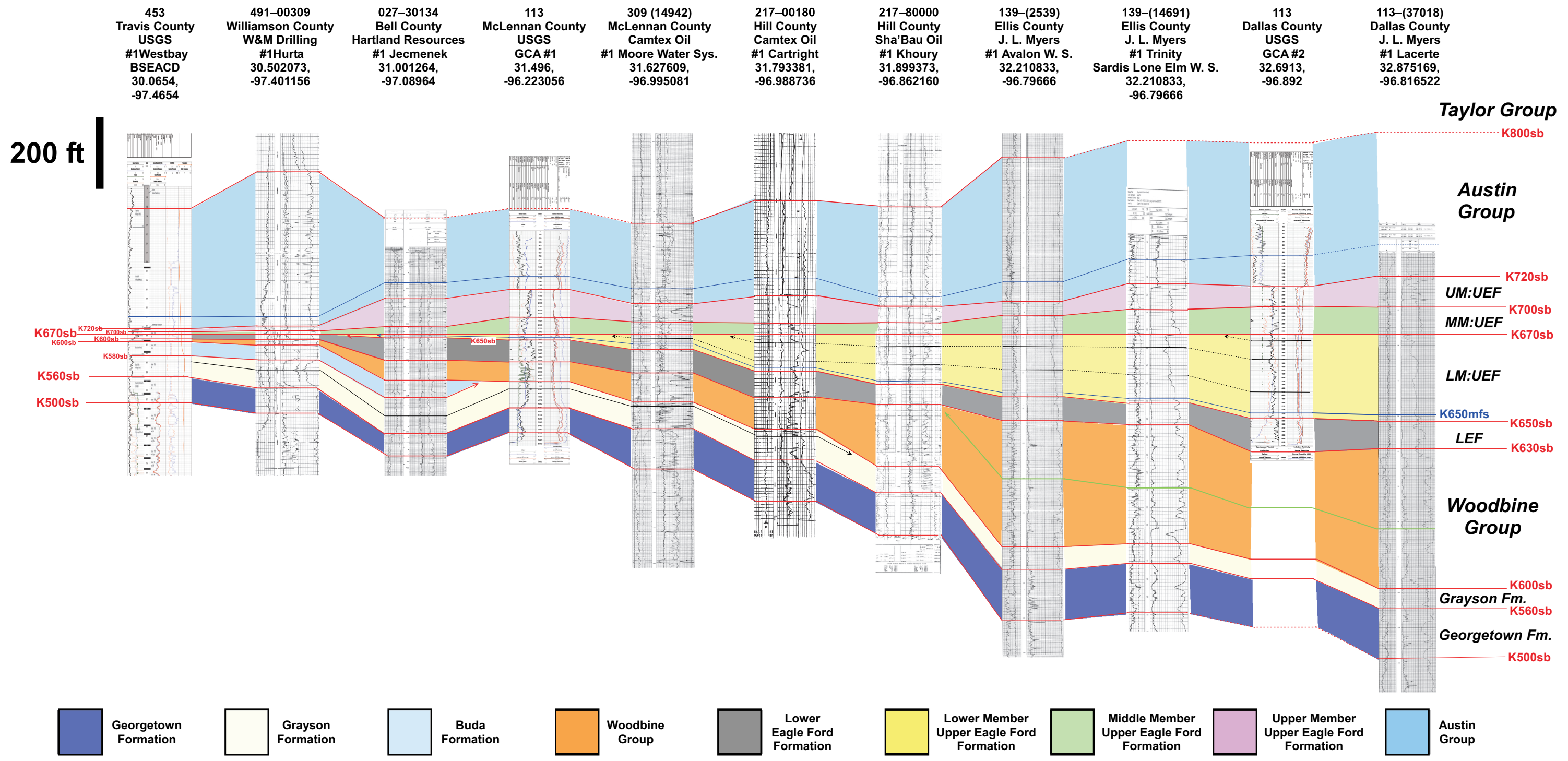


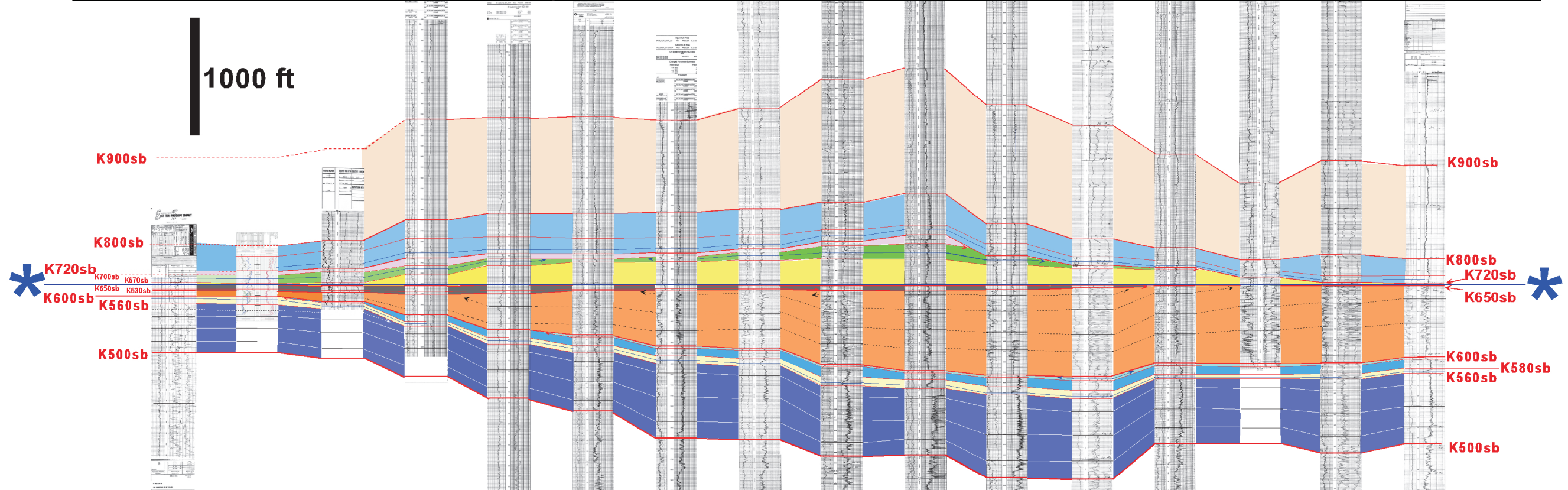
Figure 13

W

85 mi

E

McClennan			Limestone		Freestone			Anderson			Cherokee				
McClennan 42-309-00131 Beacon Hill Myrtle Trice #1 31.437250, -97.247664	McClennan USGS GC-1 31.466527, -96.813230	McClennan 42-309-00097 Neff 1-Smyht 31.535570, -96.813230	42-293-31508 Geodominion 1-White 31.61094, -96.658818	42-293-32122 Barrow Shaver 1-Samford 31.643961, -96.407869	42-161-31489 Sklar & Phillips 1-Vickers 31.71368, -96.333481	42-161-33559 Eagle O&G 1-Stewart A 31.783927, -96.208945	42-161-31840 Matador 1-Aultman 31.78882, -96.124302	42-161-31627 Anadarko 1-Hill B 31.78486, -96.018499	42-001-32407 Hunt 2-TDC 31.814679, -95.916649	42-001-32499 Petralis Energy Royall C-3R 31.764561, -95.844114	42-001-30612 Hughey 1-Boyling 31.777121, -95.605349	42-001-32284 Brown 1-Swanson 31.78061, -95.55582	42-001-32260 WJW Oper. 1-Daystar 31.78947, -95.46561	42-073-30633 Petro Corp 1 Temple Eastex A 31.720661, -95.31204	42-073-30467 Arkla 1-Black 31.712069, -95.283941
Tie NS-200	Tie NS-300	Tie NS-400	Tie NS-400	Tie NS-500	Tie NS-600	Tie NS-700	Tie NS-800	Tie NS-900	Tie NS-1000	Tie NS-1200					



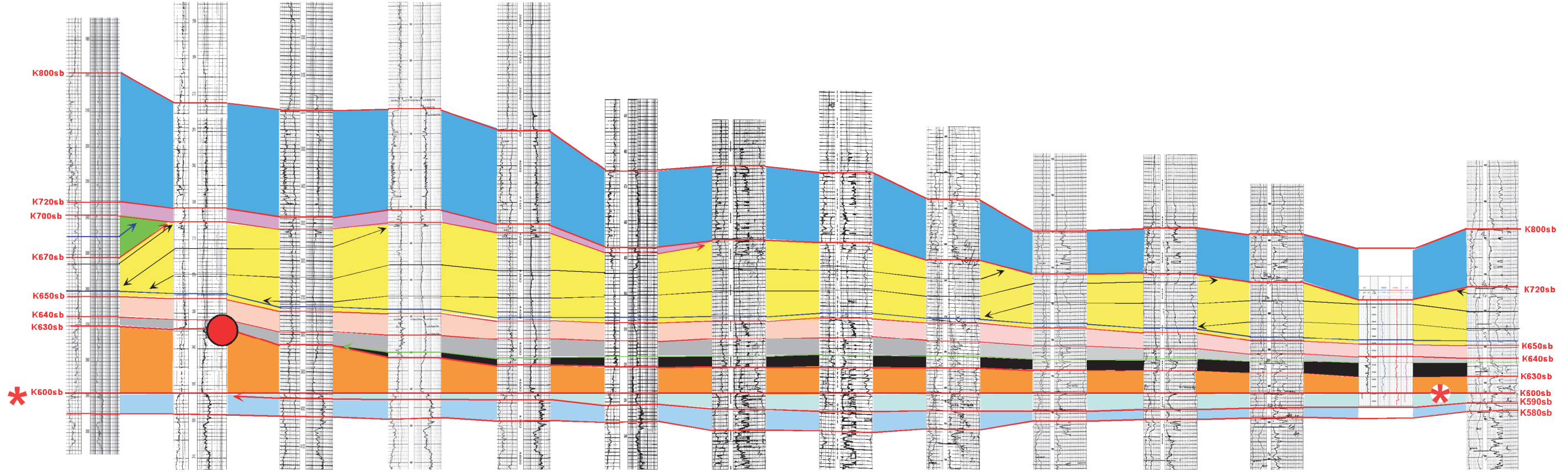
K560sb	K580sb	K590sb	K600sb	K630sb	K640sb	K650sb	K670sb	K700sb	K720sb	K800sb	K900sb
Georgetown Fm	Grayson Fm.	Buda Fm.	False Buda Fm.				LM:UEF	MM:UEF	UM:UEF		
Washita Group				Woodbine Group	Eagle Ford Group			Austin Group	Taylor Group		

* Datum: K650mfs (Top Res. Marker): Near Base Upper Eagle Ford Fm.

Figure 14

N **Limestone** **Robertson** **Burleson** **S**

Tie EW-700	Tie EW-800		Tie EW-900		Tie EW-1000		Tie EW-1100		Tie EW-1200		Cored Well		
293-31508 Geodominion White #1 31.61094, -96.658818	293-31225 Mitchell Barron #1 31.460007, -96.556693	293-32148 Skylar Exploration Jackson Unit #2 31.336650, -96.569049	395-31838 O'Benco Inc. Dunn Gas Unit #1 31.216054, -96.575642	395-31085 Enduring Resources TXU GU #3 31.132753, -96.585114	395-31432 XTO Walston GU #1 30.992109, -96.601726	395-30256 Energetics Navajo-Corona #1 30.883326, -96.561949	395-30242 Bass Ettelson #1 30.834906, -96.532756	395-30245 Chapman Oil Hudson #1 30.743313, -96.565360	051-31778 Apache Dillon #1 30.607398, -96.558009	051-32517 Sage Energy Proske #1 30.557982, -96.564584	051-31268 Union Pacific Calvin #1 30.511781, -96.591988	051-xxxxx Mystery Oil TAMU #1 30.48, -96.xxxxx	051-31502 Water Energy Ser. Sebesta #1 30.414749, -96.439643



- Top Woodbine (K63) Depositional Shelf Break
- * Datum: K600sb (Base Woodbine Unc.)

85 mi

K580sb		K590sb		K600sb		K630sb		K630ts		K640sb		K650sb		K670sb		K700sb		K720sb		K800sb
Buda Formation		False Buda Formation		Woodbine Group		LM:LEF-LST			LM:LEF-TST/HST			UM:LEF		LM:UEF		MM:UEF		UM:UEF		
"Upper Washita"				Woodbine Group		Lower Eagle Ford Formation						Upper Eagle Ford Formation				Austin Group				
				Woodbine Group		Eagle Ford Group						Austin Group								

500 ft

Figure 15

Burleson

Brazos

Grimes

Tie
NS-400

Tie
NS-500

051-31539
Crescent Ex.
Perry #1
30.476183,
-96.857360

051-31279
Harkin O&G
Lenora #1
30.483938,
-96.794418

051-31923
Validus
Rockett #1
30.516427,
-96.682574

051-31071
Chesapeake
Dusek A #1
30.558520,
-96.649428

051-31974
Amoco
Verwold #1
30.586779,
-96.613350

051-31778
Apache
Dillon #1
30.607398,
-96.558009

041-31390
Endeavor
Court #6
30.662091,
-96.479721

041-30772
North Central Oil
Perkins Unit #3
30.710383,
-96.377760

041-30578
Dalco Res.
Guest #3
30.709667,
-96.248439

041-31234
Patterson Pet.
Palmer #1
30.720249,
-96.175090

185-30198
Cashco
Sanders #1
30.755184,
-96.134939

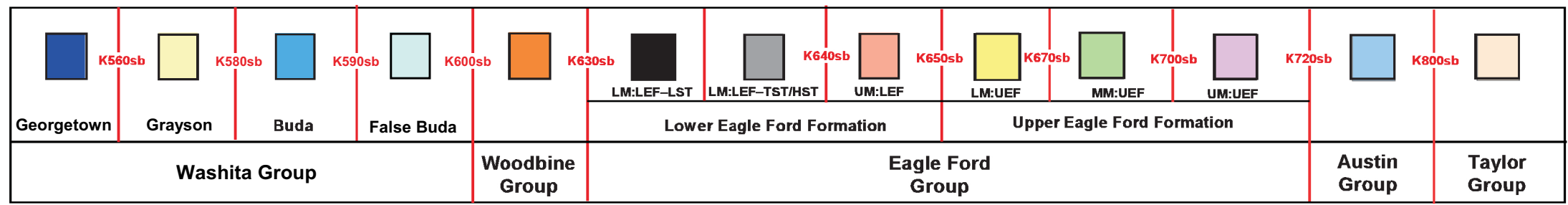
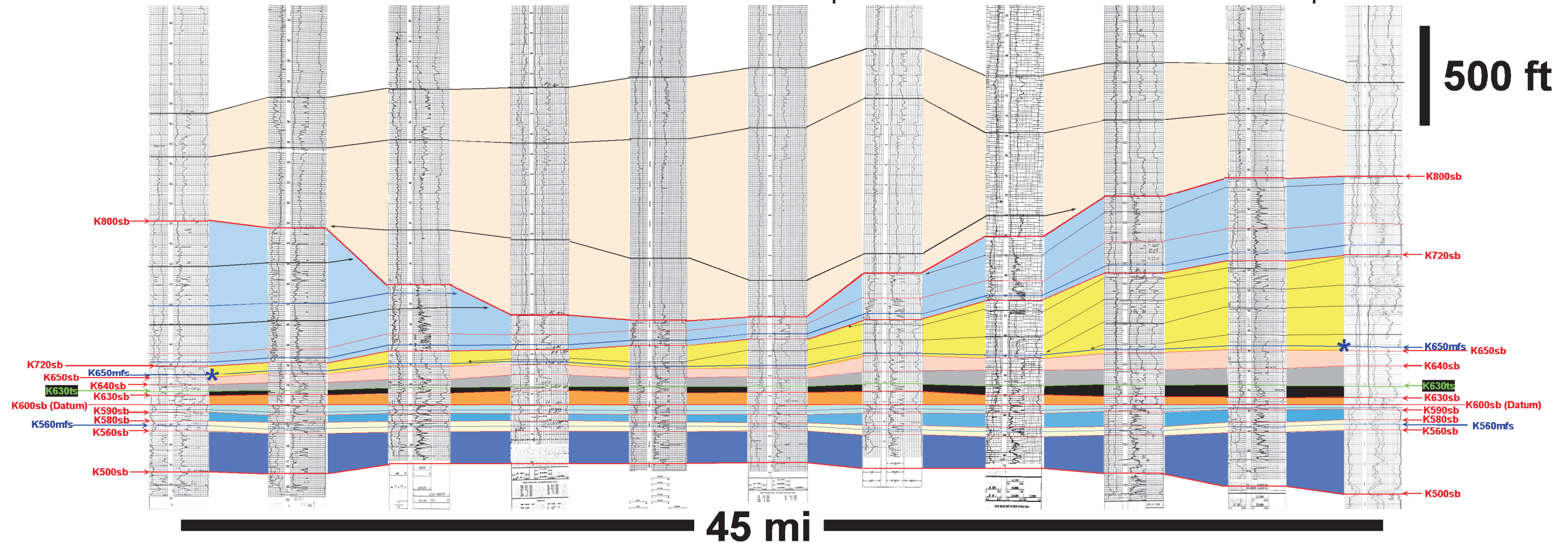
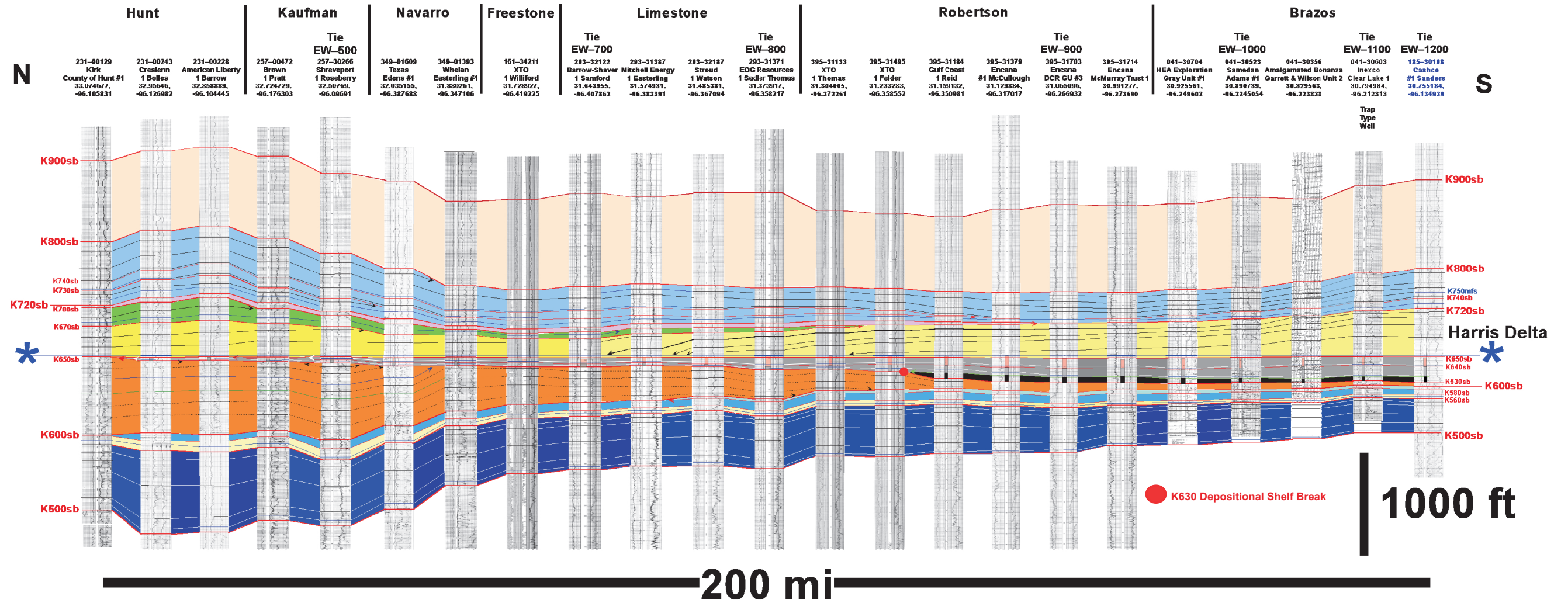













Figure 16



											
Georgetown Formation	Grayson Formation	Buda Formation	False Buda Formation		K630 LST	K640sb	LM:UEF	MM:UEF	UM:UEF		
Washita Group				Woodbine Group	Lower Eagle Ford Formation			Upper Eagle Ford Formation			
					Eagle Ford Group			Austin Group	Taylor Group		

* Datum: K650mfs (Top Res. Marker): Near Base Upper Eagle Ford Formation

Figure 17